The Systemic Pathogenesis of Enterovirus D68

Syriam Sooksawasdi Na Ayudhya

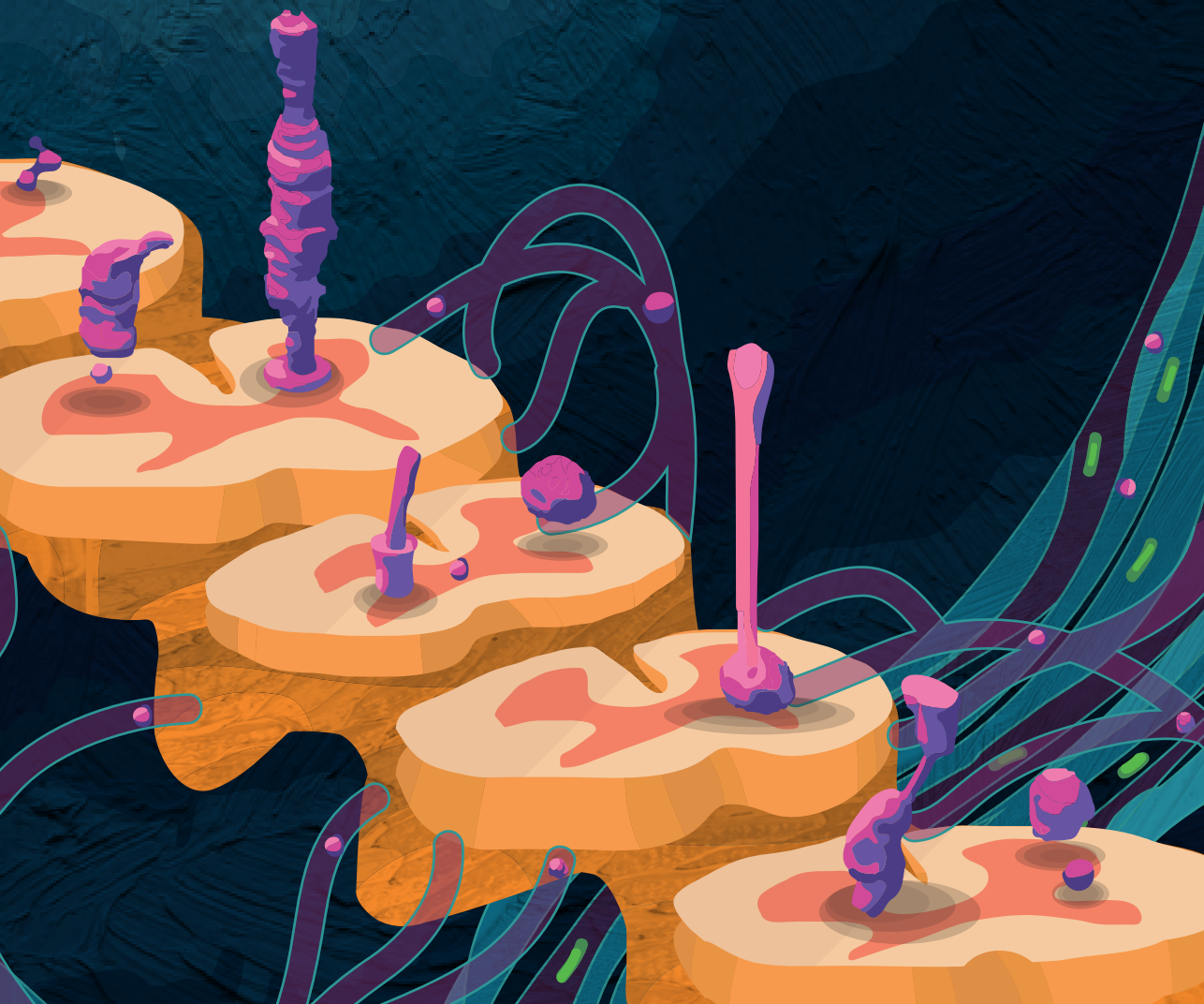

The Systemic Pathogenesis of Enterovirus D68

Syriam Sooksawasdi Na Ayudhya

The work described in this thesis was conducted at the Department of Viroscience, Erasmus University Medical Center, Rotterdam, The Netherlands.

Cover design: Yi-Chien Liao, Syriam Sooksawasdi Na Ayudhya
Lay-out design: Yi-Chien Liao (yichien1006@gmail.com)
Printing: Ridderprint (https://www.ridderprint.nl)
ISBN: 978-94-6483-453-6

The Systemic Pathogenesis of Enterovirus D68

De systemische pathogenese van enterovirus D68

Thesis

to obtain the degree of Doctor from the

Erasmus University Rotterdam

by command of the

rector magnificus

Prof. dr. A.L. Bredenoord

and in accordance with the decision of the Doctorate Board.

The public defence shall be held on

Wednesday, 15 November 2023 at 10.30 hours

by

Syriam Sooksawasdi Na Ayudhya
born in Chiang Mai, Thailand.

Erasmus University Rotterdam

Doctoral Committee:

Promotor:	Prof. dr. T. Kuiken
Other members:	Prof. dr. M.P.G. Koopmans Prof. dr. C. Tapparel Dr. M.J. Titulaer
Copromotor:	Dr. D.A.J. van Riel

“Science is like a map: it can tell us how to get to a given place, but it cannot tell us where to go”

Carl Hempel

Table of contents

Chapter 1
General introduction 9

Chapter 2
The potential role of human immune cells in the systemic dissemination of enterovirus D68 35

Chapter 3
Enhanced enterovirus D68 replication in neuroblastoma cells is associated with a cell culture adaptive amino acid substitution in VP1 63

Chapter 4
Comparative analysis of EV-D68 clinical isolates from before and after 2014 in human pluripotent stem cell-derived neural models 87

Chapter 5
Detection of intrathecal antibodies to diagnose enterovirus infections of the central nervous system 115

Chapter 6
General discussion 127

Chapter 7
Summary / Samenvatting 143

Chapter 8
Appendices 149
- About the author
- PhD Portfolio
- Publication lists

Chapter 9
Acknowledgements 155

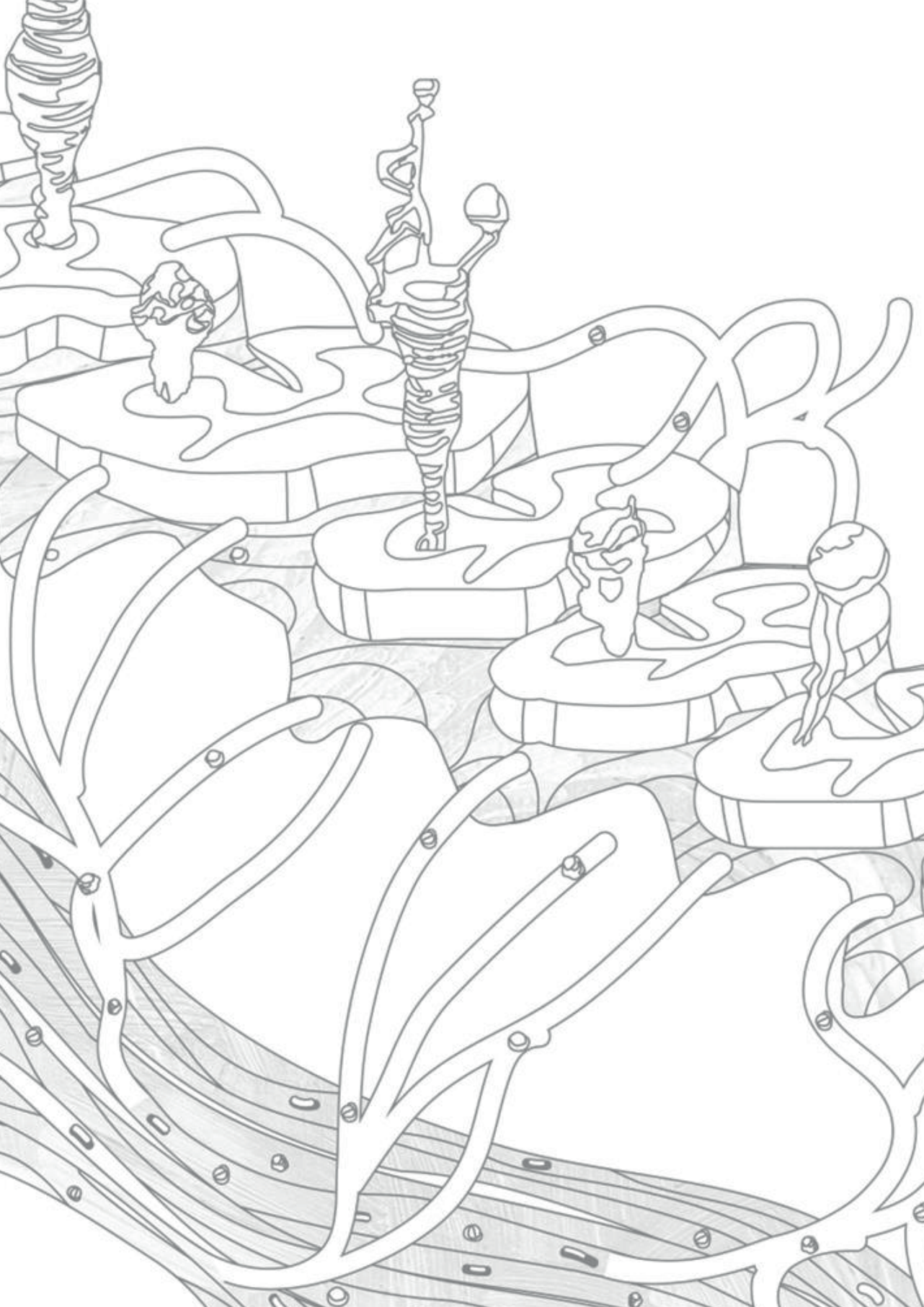

Chapter

1

General introduction

The pathogenesis and virulence of enterovirus-D68 infection

Syriam Sooksawasdi Na Ayudhya, Brigitta M. Laksono, Debby van Riel

Virulence. 2021 Dec;12(1):2060-2072.

General Introduction

Enterovirus-D68 (EV-D68) is a non-enveloped, positive-sense single-stranded RNA virus that belongs to the family *Picornaviridae*, genus Enterovirus. Most picornaviruses, such as poliovirus, hepatitis A virus and coxsackievirus, are transmitted through the oral-fecal route. Other members, however, such as rhinovirus and EV-D68, are respiratory viruses and transmitted through inhalation of infectious virus particles. EV-D68 infection generally results in mild upper respiratory symptoms, but it can also cause severe lower respiratory tract disease, leading to hospitalization, intubation and occasionally death. Children are an important risk group for severe diseases from EV-D68 infection, but reports have also shown that adults, especially those with underlying hematological malignancies or immune suppression, can also develop severe EV-D68-associated respiratory diseases (1-3). EV-D68 infection is also associated to a variety of central nervous system (CNS) complications, of which acute flaccid myelitis (AFM) is most commonly observed. Number of AFM cases has been increasing biennially since 2014 (4-7). However, since 2020 due to COVID-19 no increase in the number of AFM cases has been observed (8). EV-D68-associated AFM has overlapping clinical presentations with acute flaccid paralysis (AFP) caused by poliovirus, which has caused large, documented outbreaks worldwide since 1940 until the development of an effective vaccine in the 1962 (9, 10). However, some different clinical features, including paralysis of upper limbs and cranial nerve dysfunction, are more frequently reported in AFM patients infected with EV-D68 rather than poliovirus (11, 12).

The life cycle of EV-D68 is similar to other enteroviruses. Following attachment to a cell receptor, the virus is taken up into the host cell through endocytosis. The viral RNA is transferred across the endosomal membrane into the cytoplasm, where replication takes place. Upon replication, assembly and virion maturation, newly produced viruses are released from the host cells through the release of extracellular vesicles without inducing lysis or through induction of host cell lysis (13).

To date, EV-D68 has evolved into four phylogenetic clades: A, B, C and D, although the original division in three clades A, B and C with subclades A1 and A2 is also being used (Fig 1). Clade A is classically divided into subclades A1 and A2, although A2 is by some considered a different clade and named clade D1. Clade B is further divided into subclades B1, B2 and B3. The viral clades co-circulate, although clade C has not been detected approximately since 2010. In 2014, all isolates from the USA associated with AFM belonged to the subclade B1 (14). However, after 2014, the predominant circulating viruses belonged to subclade B3 (15) and, to a lesser extent, A2 (16).

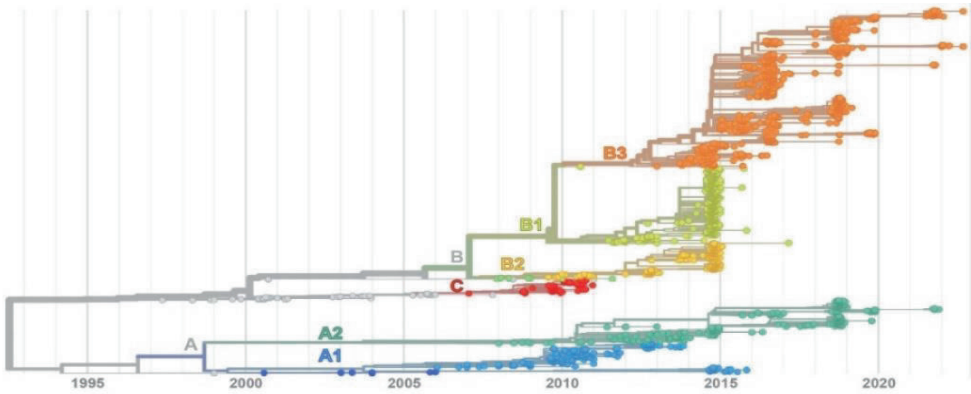

Fig 1. Phylogenetic analysis based on VP1 gene sequences of enterovirus D68 strains by the maximum likelihood method, with bootstrap values calculated from 1000 trees (17, 18) The figure is adapted from nextrain.org and updated on September 2022.

Unlike poliovirus, there is no vaccine available for EV-D68, despite its ability to cause neurological symptoms and acute paralysis, most especially in children. Moreover, because EV-D68 cases were only reported sporadically before 2014, and diagnostics for EV-D68 are not a standard practice in most laboratories, the burden of disease and trends are not fully understood. In order to be able to develop a preventive or intervention measures, knowledge on the pathogenesis of the virus infection is essential. Here, I present a concise overview on the current knowledge of the systemic pathogenesis of EV-D68 infections.

EV-D68 receptors and their distribution

Tissue and cell tropism are determined by many factors, of which cellular receptors on host cell surfaces are considered to be an important one. Several studies have identified functional EV-D68 receptors in vitro, but the association of these receptors with the tropism of EV-D68 in vivo has not been comprehensively studied. Both α2,6-linked sialic acids (SAs) and α2,3-linked SAs serve as an essential functional receptor for EV-D68 (19, 20). The prototype laboratory-adapted EV-D68 strain Fermon has a stronger affinity to α2,6-linked SAs than α2,3-linked SAs in vitro (20). Whether current circulating clinical isolates of EV-D68 have preferential affinity towards α2,6-linked SAs or α2,3-linked requires further investigation. In humans, α2,6-linked SAs are abundantly expressed on ciliated epithelial cells of the upper respiratory tract (URT; nasal cavity, nasopharynx and oropharynx) and lower respiratory tract (LRT; trachea, bronchi and bronchioles). In the LRT, α2,6-linked SAs are predominantly expressed on type I pneumocytes in the alveoli. In contrast, α2,3-linked SAs are predominantly expressed on club cells in the bronchioles and type II pneumocytes in the alveoli (21, 22) (Table 1). Human lung epithelial cell lines, including A549, also express SAs, which corresponds to the susceptibility of these cells to EV-D68 infection in vitro (23, 24). Haploid genetic

screening revealed that the laboratory-adapted Fermon strain is SA-dependent, whereas some clinical isolates from 2009 and 2010 from the Netherlands are SA-independent suggesting a potential role of other functional receptors for EV-D68 (19). SAs are also abundantly expressed beyond the respiratory tract but this has not been studied in the context of cellular tropism for EV-D68. In vitro, EV-D68 infection of neuroblastoma (SK-N-SH) cells with EV-D68 isolates from 2009 to 2016 from the Netherlands is in part associated with attachment to SAs (25).

In addition to SAs, heparan sulfate proteoglycans have been identified as a functional receptor for EV-D68 in vitro (26). Whether heparan sulfate is also a functional receptor in vivo remains to be determined, since it is associated with cell culture-adaptive mutations (25, 26). In human airway epithelial cells, heparan sulfate is mainly expressed on the basolateral side of respiratory epithelial cells, which suggest that heparan sulfate might not be an important receptor for infection in the human respiratory tract. However, heparan sulfate is abundantly expressed on cells outside the respiratory tracts, such as the cells of the CNS and muscle cells (27-29) (Table 1), and could therefore allow infection of EV-D68 outside the respiratory tract.

Intercellular adhesion molecule 5 (ICAM-5) has been identified as a functional receptor for SA- dependent and -independent EV-D68 virus strains in vitro (30). ICAM-5 expression was detected on human rhabdomyosarcoma (RD), human embryonic kidney (HEK) 293T and HeLa cells (30, 31). ICAM-5 expression in vivo is limited to the somatodendritic membrane of neurons of the telencephalon in the brain, so ICAM-5 is not expressed on cells in the brainstem and spinal cord (31, 32). All known cellular receptors for EV-D68 and expression in various human cell types are summarized in Table 1.

Overall, EV-D68 can recognize multiple receptors, of which expression may vary among tissues. This is likely an important factor for the broad tropism of EV-D68 in mammals, including respiratory epithelial cells, but possibly also muscle cells, lymphoid cells and even cells in the CNS. Differences in receptor recognition has been reported between EV-D68 isolates. However, it remains to be determined whether this has an impact on the tissue and cell tropism *in vivo* and the associated pathogenesis of EV-D68 infection.

Receptors	Tissue		
	Respiratory tract	**CNS**	**Lymphoid**
α2,3-linked SAs	goblet cells; club cells; type II pneumocytes; alveolar macrophages (21, 22)	neurons; astrocytes; glial cells (33)	monocytes; macrophages (34, 35)
α2,6-linked SAs	ciliated epithelial cells; goblet cells; type I pneumocytes (21, 22)	neurons; glial cells; astrocytes; oligodendrocytes (33, 36)	monocytes; macrophages; B cells (34-36)
ICAM-5	NA	dendrites/soma of neurons of the telencephalon (32, 37)	NA
Heparan sulfate	basal side of human respiratory epithelial cells* (27)	neurons*; astrocytes (27, 29)	monocytes; macrophages; immature DCs; mature DCs; B cells (38, 39)

Table 1 Cellular receptors for EV-D68 and their expression on different cells types of the respiratory tract, CNS and lymphoid system SAs: Sialic acids; CNS: central nervous system; DCs: dendritic cells; NA: not available; *: in vitro study

EV-D68 infection in the respiratory tract

Clinical observations

EV-D68 infection causes mild to severe respiratory diseases, especially in young children with a median age of 4 years old (40, 41). It is thought that during a mild or subclinical infection the virus mainly causes URT infections, which are associated with fever and coughing. However, complications include involvement of the LRT, causing dyspnea, wheezing pneumonia and hypoxia, which can lead to the need for ventilator support and intensive care admission (42). Previous history of asthma or recurrent wheezing appears to be an important risk factor for asthma exacerbation and the development of a pneumonia (40, 43, 44). However, patients with no high-risk underlying diseases with severe pneumonia caused by EV-D68 have been reported (41).

Although EV-D68 infections have mostly been reported in children, viral RNA has been detected in previously healthy adults (16, 45, 46). Mild to severe respiratory disease

has been observed in adults which are immunocompromised or have an underlying co-morbidity, including hematologic malignancy or undergoing hematopoietic cell transplant patients (1-3).

Pathogenesis

The pathogenesis of EV-D68 infection in the respiratory tract in humans is poorly studied. Few clinical studies have reported interstitial pneumonia with diffusion and patchy alveolar infiltration in lobes of the lungs characterized by computed tomography angiograms of the chest (46, 47). The fact that EV-D68 was detected in diagnostic samples from the URT and LRT suggests that the virus is able to replicate throughout the respiratory tract (Fig 2A) (1, 41). Although cellular receptors for EV-D68 are present in human URT and LRT cells (Table 1), the exact cell tropism during mild or severe respiratory disease in humans is unknown.

The cell tropism of EV-D68 in the URT has been studied in vitro in human nasal airway epithelial cells and in in vivo models. EV-D68 infected predominantly ciliated epithelial cells in human nasal airway cultures and infection resulted in cell lysis. The infection also resulted in the induction of several cytokines, such as IL-8, IP-10, interferon- (IFN-) λ1/λ3, interleukin- (IL-) 1β, IL-6, and granulocyte-macrophage colony-stimulating factor (GM-CSF) at 4 days post-inoculation (dpi) (48). In vivo, infectious viruses and viral RNA were detected in nasal washes from intranasally inoculated ferrets (Mustela putorius furo) and cotton rats (Sigmodon hispidus), indicating virus replication in the URT (49, 50). Unfortunately, the cell tropism of EV-D68 and the associated inflammatory response in the URT have not been studied in these in vivo models.

The pathogenesis of LRT disease caused by EV-D68 has been studied to a limited extend in animal models. From cotton rats that were intranasally inoculated with isolates from 2012 and 2014 or Fermon strain, infectious virus has been isolated from bronchoalveolar lavage (BAL) and lung tissues. Virus titers peaked at 24 hours post-inoculation (hpi) and rapidly dropped afterwards. In cotton rats inoculated with a clinical isolate of EV-D68, rapid antiviral responses in the LRT were detected within 4 to 48 hpi, including inflammatory cytokines (IL-6 and IFN-γ), chemokines (GRO, MCP-1, IP-10 and RANTES), IFN-β and two IFN-inducible proteins (Mx-1 and Mx-2). Histological changes in the lungs, characterized by mild peribronchiolitis and interstitial pneumonia, were observed at 48 hpi. Unfortunately, the tissue and cell tropism—by detection of virus antigen in vivo—was not determined (49). In ferrets intranasal inoculated with Fermon strain, viral RNA was detected in lung tissues at 3 dpi. Acute inflammatory responses in the lungs were detected at 7 and 14 dpi, and included the expression of IL-1, IL-5 and IL-8. Histological evidence for mild interstitial pneumonia was observed at 3 up to 7 dpi whereas no lesions were observed in trachea. Additionally, EV-D68 viral capsid protein VP1 antigen was detected in the connective tissues surrounding the alveoli with thickening of the alveolar wall. Double stainings for viral VP1 and cellular

SAs in the ferret lungs revealed that EV-D68 exclusively infected cells that expressed α2,6-linked SAs (50).

In vivo studies using mice—both BALB/c and IFN-α/β and -γ receptor-deficient mice—revealed that EV-D68 replication in the lungs peak within 24 hpi (51, 52). In IFN-α/β and -γ receptor-deficient mice, inflammatory cytokines and chemokines were detected in the lungs at 24 hpi, which included MCP-1 and IL-6, compared to sham-infected mice. Histopathological changes comprised of moderate interstitial pneumonia characterized by mononuclear inflammatory cell infiltration in the perivascular space and alveolar walls. In addition, EV-D68 viral capsid protein VP2 antigen was detected at 48 hpi in alveolar epithelial cells (51). Infection of BALB/c mice with clinical isolates from 2014 resulted in elevated lung pro-inflammatory cytokines and chemokines, including IL-17A and its target proteins CXCL1 and CXCL2, compared to sham-infected mice and rhinovirus-inoculated mice. EV-D68 viral capsid protein VP3 antigen was detected in the murine lungs at 24 hpi. In BAL fluid of these animals, there was an increase of neutrophils at 48 hpi. These findings suggest that EV-D68 induces neutrophilic airway inflammation facilitated by IL-17A, which may explain the development of asthma exacerbation following EV-D68 infection in humans (52).

Current findings suggest that EV-D68 is able to infect and replicate in the URT and LRT. In most individuals, infection is followed by the induction of innate immune responses, that limits virus replication and associated inflammation early after infection (16, 46). The mechanisms by which some individuals, especially children and immunocompromised adults, develop more severe disease is not fully understood (1). However, it is likely that the host immune responses, or the lack thereof, is an important determinant, together with the different mechanisms of EV-D68 for evading the host innate immune responses. Evasion strategies of EV-D68 have mainly been studied in vitro and thus will be important to study in vivo (53-55).

Altogether, to get more insight into the pathogenesis of EV-D68-induced respiratory disease, an animal model that mimics disease in humans is essential. Experimental infections in ferrets and cotton rats suggested that these animal models can be promising to study the pathogenesis of respiratory disease caused by EV-D68. However, the limited use of relevant EV-D68 clinical isolates and instead the use of laboratory-adapted virus strains might not fully represent the clinical presentations in humans. Therefore, ideally future in vivo studies should use contemporary strains to unravel the receptor usage and associated cell tropism, as well as the host and viral factors that impact immune response and associated pathogenesis.

Systemic dissemination of EV-D68

EV-D68 can be detected outside the respiratory tract, although the frequency is not well known. Viral RNA has been detected in EV-D68-associated AFM patient cerebrospinal fluid (CSF), sera or blood and stool samples (6, 7, 14, 45, 56, 57). The mechanisms of extra-respiratory spread are not completely understood, but will be discussed in this section.

Even though virus has been detected in the blood or serum of EV-D68 infected patients, the temporal kinetics of such an RNAemia and whether this only occurs during severe disease are unclear. Unfortunately, in most cases, only respiratory tract samples are tested for EV-D68 (Table 2). In animal models, viremia and RNAemia have also been detected. Infectious virus has been detected in the lungs, blood, muscle, spinal cord, liver, kidneys and spleen of intranasally inoculated interferon-deficient four-week-old mice (51, 58). Similarly, viral RNAs were also detected in several tissues of intraperitoneally inoculated one-day-old mice (59). Viral RNAs were also been detected in the blood of intranasally Fermon-inoculated ferrets at 3 dpi and Kunming strain-inoculated Chinese rhesus macaques (*Macaca mulatta*) at 9 days post-inoculation (50, 60).

The contribution of infected lymphoid cells and lymphoid tissues to a viremia is not fully understood. Other picornaviruses, such as poliovirus, have been found to replicate in CD11c+ macrophages or dendritic cells in the tonsil follicles (61), but whether EV-D68 is capable of replicating in the same or other immune cells in vivo remains to be determined. In vitro inoculation of human leukocytic cell lines with the Fermon strain have shown that infection of granulocytic (KG-1), monocytic (U-937), T (Jurkat and MOLT) and B (Raji) cell lines resulted in production of infectious progenies at 24 hpi (62). Unfortunately, these studies have not been performed with clinical isolates. Nonetheless, this finding suggests that infection of leukocytes may play a role in EV-D68 viremia and thereby contribute to the systemic spread of EV-D68 in vivo. An in vivo study in ferrets inoculated intranasally with the Fermon strain showed viral RNA in axillary lymph nodes at 5 and 7 dpi (50). Intramuscular inoculation of cotton rats with a clinical isolate showed the presence of negative stranded viral RNA, indicating replication, in the draining lymph nodes of the site of inoculation (49). Whether there was productive infection in the lymph nodes of the animals is unknown.

How EV-D68 enters the bloodstream is unknown. Possible routes are through the disruption of respiratory epithelial-endothelial barrier, via basolateral release of polarized respiratory epithelial cells or through direct infection of pulmonary endothelial cells. EV-D68 infection of primary human nasal epithelial cells grown in air-liquid interface led to high cytotoxicity, as measured by lactate dehydrogenase release into the basal medium, and loss of tissue integrity, as shown by decrease in transepithelial electrical resistance (48). Whether this disruption of epithelial integrity leads to spillover of virus particles into the bloodstream in vivo remains to be

determined. Since EV-D68 infection leads to cell lysis at late stages of infection, it might be challenging to determine if there is basolateral release of viral progeny prior to cell lysis using in vitro models. Nonetheless, studies have shown that enteroviruses can exit the infected host cell in autophagosomes before cell lysis and EV-D68 has also been suggested to reshape the autophagic pathway to promote virus replication and egress (13, 63). Whether EV-D68 infection of respiratory epithelial cells releases these autophagosome-like vesicles containing new virus progeny into the basolateral side remains to be determined. Infection of endothelial cells by EV-D68 has not been reported. Other picornaviruses have been shown to infect various endothelial cells in vitro, but this is not studied in vivo (64-71).

EV-D68-associated acute gastroenteritis has been reported, suggesting that the virus, despite being a respiratory virus, may also be able to infect the gastrointestinal tract like other enteroviruses (72). This enterotropism is supported by the fact that EV-D68 has been detected in stool samples in patients, but does not seem to occur regularly as many stool samples of EV-D68 infected patients do not contain viral RNA (Table 2) (56, 73-75). In vitro, the virus has been shown to infect human intestinal epithelial cell lines. Inoculation of human colorectal adenocarcinoma HT-29 and LS174T cell lines with the Fermon strain resulted in detection of viral RNA and intracellular VP1 in the cells, but dramatically low RNA level and virus titer in the supernatant as compared to inoculation with the enterotropic EV-A71 (76). Ferrets inoculated intranasally with the Fermon strain showed that viral RNA could be detected in feces at 3 dpi (50). Similar observation can be seen in Chinese rhesus macaques inoculated intranasally with the Kunming strain. Despite the appearance of mild clinical symptoms in these animals, viral RNA detection peaked at 3 dpi in feces (60). The low detection percentage in stool samples of EV-D68 infected patients, the inefficient replication efficiency in vitro, together with the early and transient detection of EV-D68 in stool samples of experimentally infected ferrets or macaques suggest that EV-D68 replication in the gastrointestinal tract is suboptimal.

Some patients with EV-D68 infection have been reported to show cardiac symptoms, such as myocarditis, pericarditis and acute cardiac failure (77). Several clinical cases have also reported the appearance of skin rash in EV-D68 patients (78-80). Whether the virus infects the cells of the heart, which leads to cardiac symptoms, or the dermis and epidermis, which leads to skin rash, remains to be determined. Intranasal or intraperitoneal inoculation of mice resulted in infection of limb muscles and development of muscle disease, suggesting that EV-D68 is capable of replicating in muscle cells in vivo (51, 81). Potential replication sites and affected tissues during the systemic dissemination of EV-D68 are summarized and illustrated in Fig 2B.

All in all, the frequency and mechanism of the systemic dissemination of EV-D68 remains poorly understood. However, as systemic spread of EV-D68 is an important factor in the pathogenesis of EV-D68, it is important to get more insight into the

frequency and temporal kinetics of systemic spread as well as its association with extra-respiratory complication. In addition, future studies should reveal if systemic spread is solely a spillover of virus produced in the respiratory tract into the circulation, or if virus is transported—either cell-free or cell-associated—to lymphoid tissues where virus is amplified and released into the circulation.

Studies	Total EV-D68-positive sample tested	Number of EV-D68-positive samples out of total EV-D68-positive sample tested				
		Respiratory tract	Whole blood	Serum or plasma	Stool	CSF
Imamura et al. (57)	30	30/30	NA	28/30	NA	NA
Greninger et al. (14)	12	12/12	1/12	NA	1/12	0/12
Esposito et al. (6)	1	1/1	NA	NA	NA	0/1
Chong et al.(56)	11*	7/11	1/11	1/11	2/11	1/11
Giombini et al. (2)	1*	1/1	0/1	NA	0/1	1/1
Cabrerizo et al. (82)	3*	3/3	0/3	NA	3/3	0/3
Sejvar et al. (83)	11	11/11	NA	NA	0/11	1/11
Pfeiffer et al. (84)	2	2/2	NA	0/2	0/2	0/2
Van Haren et al. (73)	9	9/9	NA	1/9	NA	NA
Kusabe et al.(45)	1	NA	NA	1/1	NA	0/1
Hu et al. (85)	9*	9/9	0/9	0/9	0/9	0/9
ElBadry et al. (86)	1	NA	NA	1/1	NA	NA

Table 2. Detection of EV-D68 in diagnostic samples including whole blood, serum or plasma, stool and CSF samples in human samples. CSF: cerebrospinal fluid; NA: not available. *: More than 1 sample were collected from a patient

EV-D68 infection in the central nervous system

Clinical observations

Various CNS complications are associated with EV-D68 infections, of which the development of AFM is reported most frequently. In addition, EV-D68 infection has been associated with cranial nerve dysfunction, encephalitis/meningoencephalitis and aseptic meningitis. Signs of CNS complications mostly occur following febrile upper respiratory symptoms, such as rhinorrhea, coughing and pharyngitis, and

gastrointestinal symptoms, such as vomiting and diarrhea. Diagnostics of EV-D68 associated CNS disease is difficult since virus is rarely detected in the CSF (Table 2). However, EV-D68 viral RNA can be detected most commonly in nasopharyngeal samples in the first week after onset of CNS complications, after which the rate of EV-D68 detection in respiratory samples declines through the course of infection (11, 73, 83, 87).

The development of EV-D68-associated AFM can progress rapidly in hours to days (73, 88). Early manifestations of AFM include headache, stiffness or pain in the back and neck or affected limb, followed by reduced or absent reflexes (11, 73). One to four limbs can be affected with asymmetric distribution. Generally, upper limbs are more commonly affected than lower limbs (11, 73, 83, 87). In severe cases, the diaphragm muscles may also be affected, resulting in ventilator support requirements (84, 87). Magnetic resonance imaging (MRI) predominantly showed lesions in the anterior horn of the spinal cord, especially in cervical regions (C2-C8) and upper thoracic regions (T1-T3). In addition, electrodiagnostic studies showed a motor neuropathy at C5-C8 level (87). Together, these clinical and diagnostic evidences support EV-D68-associated spinal motor neuron injury. Nearly all patients had notable muscle atrophy in the affected limbs within weeks to months after paralysis onset (11). Diffused muscle aches and limb pain for weeks to months after onset have occasionally been reported (73).

Other neurological complications have been associated with EV-D68 infections (73, 83). Cranial nerve dysfunction can be observed in AFM patients, which correlated with brainstem lesions in the cranial motor nuclei particularly within the pons, medulla and midbrain as observed by MRI (87, 89). Interestingly, a number of patients had cranial nerve dysfunction without clinical evidence for AFM (11, 88). Cranial nerve dysfunction is mostly characterized by facial weakness associated with the facial nerve (cranial nerve VII), diplopia associated with the abducens nerve (cranial nerve VI), or hypophonia, dysarthria and dysphagia associated with the glossopharyngeal nerve (cranial nerve IX) and the vagus nerve (cranial nerve X) (11, 83). Furthermore, some patients experience sensory deficit in paralyzed limbs or autonomic deficit associated with bowel and/or bladder dysfunction (73, 88).

EV-D68 infection is occasionally associated with encephalitis/meningoencephalitis or aseptic meningitis. Brainstem encephalitis was reported in an EV-D68-infected child and led to cardiopulmonary failure (90). A fatal meningoencephalitis was reported in a previously healthy child with EV-D68-associated AFM and severe pneumonia (7). Non-fatal aseptic meningitis has been reported in both children and adults (2, 6, 14, 91-93). Interestingly, the presence of EV-D68 RNA seems to be more often detected in patients with aseptic meningitis than in AFM patients (91).

Diagnostic of enterovirus D68 in CNS diseases

Diagnostics for EV-D68-associated CNS complications are challenging since the virus or the viral RNA is rarely detected in CSF with only 3% chance of detection compared to 40% RNA detection in respiratory or stool samples (94). However, the detection of viral RNA in respiratory samples is also challenging since samples need to be collected relatively early after disease onset (4). The detection rate of viral RNA in CSF among different EVs varies, where EV-D68 viral RNA in CSF is detected only 1% of the cases (83). Plausible explanations for the rare detection of EV-D68 RNA in the CSF could be lacking of virus shedding from CNS parenchyma into the intrathecal compartment. Alternatively, virus might not yet be present, or already cleared from the CSF at the moment of sampling. Therefore, alternative diagnostic tools are needed, and the presence of EV-specific antibodies would be such an alternative as it provides indirect evidence for EV infection in the CNS.

When validating the detection of virus specific antibody in the CSF, it is important to take into account that blood-CSF barrier function may be impaired during the infection, resulting in leakage of systemic antibodies into the CSF. Therefore, a Reiber diagram which can discriminate between virus specific antibodies that are blood-derived or those that are synthesized locally in the CNS should be implemented (95). To avoid misdiagnosis, paired serum and CSF should be therefore collected from a patient with neurological complications besides a respiratory sample.

Pathogenesis

The unprecedented emergence of CNS complications associated with EV-D68 has raised several questions about how the virus enters and causes diseases in the CNS. Mechanisms of virus entry and the subsequent virus spread and associated immune response in the CNS in vivo is poorly studies. Lesions in the anterior horn of the spinal cord are associated with AFM, suggesting the involvement of motor neuron in the pathogenesis of EV-D68-associated AFM (11, 87). Lesions in the cranial motor nuclei of the pons, medulla and midbrain are associated with cranial nerve dysfunction (89, 96). Whether these lesions are a direct result of virus-infected cells needs to be confirmed, but detection of EV-D68 RNA in the CSF of AFM patients suggests that virus invades the CNS (2, 7, 14, 91, 96). To understand more about the pathogenesis of EV-D68 infections in the CNS, we will discuss the possible routes for neuroinvasion and subsequent virus replication within the CNS and associated inflammatory responses.

Neuroinvasion

In general, viruses can gain access into the CNS via peripheral nerves or the hematogenous route. Virus entry into the CNS via peripheral nerves requires axonal transport. Mice inoculated intramuscularly with paralytogenic EV-D68 isolates developed paralysis within 3 to 4 dpi associated with motor neuron loss (31). The same study also showed that axonal retrograde transport of EV-D68 could occur in motor neurons derived from human induced pluripotent stem cells (hiPSCs). Anterograde

transport of EV-D68 could not be detected in the same system (31). Intraperitoneal inoculation of newborn mice or IFN-α/β/γ receptor-deficient mice with recent USA isolates of EV-D68 resulted in infection of muscle cells of the limb, followed by detection of virus in the spinal cord (59, 81, 97, 98). This suggests that EV-D68 virus can enter motor neurons via the neuromuscular junction, which is the direct connection between the muscle cells and the motor neurons. However, replication in muscle cells detected in mice after intranasal infection with clinical (isolated in 2014 in USA) or mouse adapted EV-D68 isolates did not always lead to neuroinvasion and/or the development of paralysis (51, 81).

Cranial nerve dysfunction has been observed in a number of patients without limb paralysis (11). Since affected cranial nerves, like the facial, abducens, glossopharyngeal and vagus nerves innervate muscles of the face, respiratory tract, oral cavity and tongue with nerve endings of motor neurons or directly innervate the respiratory tract and oral cavity with sensory neurons, EV-D68 might use these to enter the CNS without systemic spread. If EV-D68 can enter the CNS via cranial nerves and the exact mechanism requires further investigation.

To date, there is no direct evidence that EV-D68 invades the CNS through the blood-brain-barrier (BBB) or blood-CSF barrier. Since EV-D68 can be detected in the blood circulation, the virus could possibly invade the CNS and spread across the BBB or blood-CSF barrier. Other viruses, such as poliovirus, have been suggested to cause leakage of the BBB through direct infection of brain microvascular endothelial cells in vitro and in vivo (68, 99). Another possible route for EV-D68 neuroinvasion is through the infection of lymphocytes or other immune cells and utilize these cells as a Trojan horse to enter the CNS. Nonetheless, the mechanism of CNS invasion of EV-D68 in vivo requires more in-depth studies as various routes of entry may result in the different presentation of CNS diseases. Possible replication sites and dissemination route in the CNS are summarized and illustrated in Fig 2C.

Taken together, EV-D68 infection can leads to a wide spectrum of CNS diseases, ranging from AFM to cranial nerve dysfunction and meningoencephalitis. Even though the exact mechanism of CNS invasion is not known, it is possible that different invasion strategies used by the virus can explain the different disease presentations.

Replication in the CNS

Post-mortem examination has given some insights into the tropism of EV-D68 in the CNS and the associated lesions. In a patient with fatal meningomyeloencephalitis, pathological investigations revealed an extensive lymphocytic meningomyelitis and encephalitis associated with neuronophagia in motor nuclei in meninges, cerebellum, midbrain, pons, medulla and cervical cord. In the spinal cord infiltrating CD3+ T cells were observed around motor nuclei and infiltrating CD20+ B cells in perivascular areas (7). Detection of EV-D68 proteins or viral RNA was not included making it challenging

to link histological findings directly with local virus replication, even though EV-D68 RNA was detected in the CSF. In other EV-D68 patients, brainstem lesions were also observed by MRI although these were not further investigated (11, 87, 89).

In vivo, viral RNA and virus antigen have been detected in the spinal cord of intraperitoneally and intracranially inoculated mice (59, 97, 98). Intracranial inoculation of mice with USA clinical isolates from 2014 and prototype strain of EV-D68 resulted in minimal to absent virus replication in the cerebrum and cerebellum but efficient replication in motor neurons in the anterior horn of the spinal cord. This suggest that EV-D68 viruses can spread through the CNS towards the motor neurons in the spinal cord (98).

Current understanding on the cell tropism of EV-D68 in the CNS relies in part on in vitro studies, which do not always correspond to in vivo observations. In vitro, human (SH-SY5Y and SK-N-SH) and mouse neuroblastoma cell lines (24, 25, 100), together with motor neurons, cortical neurons and astrocytes derived from hiPSCs are permissive for EV-D68 infection (31, 100). Motor neurons derived from hiPSCs were able to facilitate multiple rounds of viral replication over 72 hours in the absence of cytopathic effect, in contrast to the death of motor neurons in intramuscularly inoculated mice (24). Moreover, in other in vivo studies, virus replication within the brain of intracranially inoculated mice was limited to the spinal cord and motor neurons (98), while in vitro data based on hiPSCs showed permissiveness of human cortical neurons and astrocytes (100). Another available model that was developed to study the replication of EV-D68 in the CNS is the ex vivo model. EV-D68 isolates from 2014 from USA replicated efficiently in ex vivo organotypic brain slices of neonatal mice, but the phenotype of EV-D68-infected cells in this model was not determined (100).

The functional receptor or receptors of EV-D68 in the CNS are not known. Both sialic acids and ICAM-5 could facilitate virus entry into the neuronal cells (30, 31). However, ICAM-5 is not expressed on motor neurons (31) (Table 1). Another possible receptor that may play a role in the neurotropism of EV-D68 is heparan sulfate, since it is abundantly expressed on cells of the CNS (27). These observations suggest that EV-D68 could possibly infect and replicate in neurons and astrocytes. Whether this also occurs in vivo and whether the cell tropism contributes to differences in the clinical presentation requires further investigations.

Taken together, data from humans, in vivo mice models and in vitro studies suggest that EV-D68 has a preference for motor neurons while the susceptibility of other cells of the CNS varies among studies. Whether infection of motor neurons is necessary to cause paralysis remains unclear. In vivo studies in mice have shown that infection of muscle tissues without lesions in the spinal cord or motor neuron depletion resulted in paralysis (81). It is plausible that paralysis and muscle atrophy, which are commonly observed within weeks to months after weakness onset, are a result of viral-induced

myositis, destruction of motor neurons, or a combination of both. To get more insight into the pathogenesis of EV-D68-associated paralysis and to monitor potential development of myositis to limb weakness, future *in vivo* studies should include analysis of muscle enzymes in the blood, together with the detection of viral RNA and antigen in muscle tissues and CSF during the course of infection.

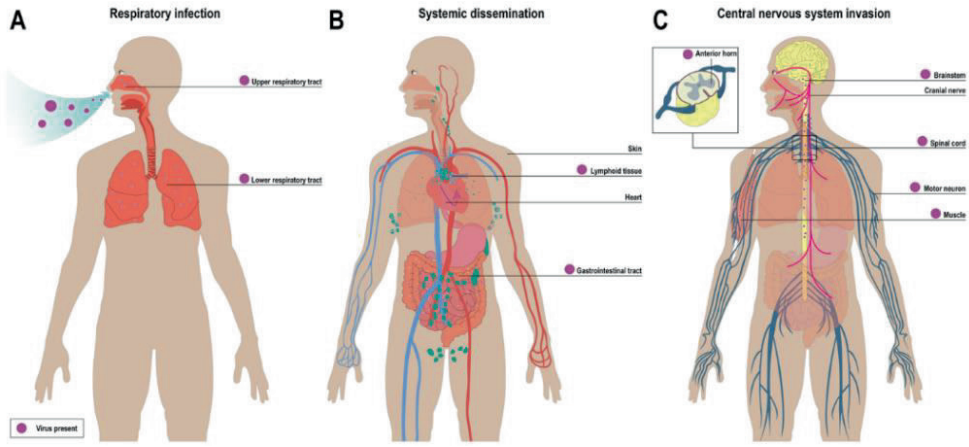

Figure 2. Hypothetical model of pathogenesis of EV-D68 infection based on findings from EV-D68 infected patients and experimental in vivo and in vitro studies. (A) EV-D68 infection in the respiratory tract: Inhaled virus particles firstly replicate in the upper respiratory tract and might spread to the lower respiratory tract. (B) EV-D68 infection outside the respiratory tract: Systemic dissemination of virus into the bloodstream and/or draining lymph nodes, resulting in viremia and infection of extra-respiratory tissues including the gastrointestinal tract, skin and heart. (C) EV-D68 infection in the CNS: EV-D68 may invade the CNS through infection of the muscles and subsequent spread via the neuromuscular junction to motor neurons in the anterior horn of the spinal cord using retrograde axonal transport. Other possible invasion mechanisms into the CNS are via the blood-brain barrier, blood-CSF barrier or cranial nerves. Purple dot represents EV-D68. Purple arrow represents the flow of EV-D68 systemic dissemination in the circulation

Viral factors important for the pathogenesis of EV-D68

Even though different clades of EV-D68 have circulated globally over time, the role of viral factors in the pathogenesis of EV-D68-associated respiratory and neurological diseases remains unknown. During the re-emergence of EV-D68 in 2014, multiple clades co-circulated but subclade B1 was predominant and associated with the development of severe respiratory diseases and AFM (14). After 2014, epidemiological and clinical data have reported AFM in patients that were infected with different clades, including subclades B1, B3 and D1 (or A2) (16, 101, 102). Whether genetic changes in were responsible for the increased disease severity and occurrence of neurological diseases since 2014 remains unclear (14, 103). Sequence analyses of subclade B1 isolates from the outbreaks in 2014 revealed 12 specific amino acid substitutions in both structural and non-structural viral proteins compared those of clades A, C, subclade B3 and Fermon strains. These substitutions were found in the 5'UTR as well

as different viral proteins, including VP2, VP3, 2A, 2B, 2C and 3D. Some of these amino acids are also observed in other neurotropic enteroviruses, e.g. poliovirus, EV-A71 and EV-D70 (103). Whether these amino acid substitutions are associated with an increased pathogenicity in vivo has not been shown.

Phenotypic characterization of different EV-D68 isolates from different clades has been performed to identify possible viral factors important for the pathogenicity of EV-D68. Structure and sequencing analyses of several clade B isolates from the outbreaks in 2014 have shown high genetic variation in VP1 protein (104). Despite this high genetic variation, in vitro and in vivo studies did not reveal difference in the replication efficiency between strains belonging to the clades derived before and after 2014 (25, 100). Nonetheless, one study showed that EV-D68 isolates from 2014 were able to replicate in neuroblastoma SH-SY5Y cells but not isolates from before 2014 (24). Recently it was shown that amino acid substitutions were easily acquired in clinical EV-D68 isolated while passaging the virus in cell culture, and that these substitutions led to the recognition of heparan sulfate as an additional receptor for EV-D68. The recognition of heparan sulfate was associated with large phenotypic changes in vitro, which emphasizes the necessity to sequence virus stocks used in studies to maintain the phenotypic characteristics of clinical isolates (25).

Several EV-D68 nonstructural proteins 3C and 2A have been shown to play a role in the suppression of innate immune responses in vitro (53-55). The 3C protein has been shown to play a role in the suppression of type I IFNs through cleavage of IFN regulatory factor 7 (IRF7) (53) or through binding to melanoma differentiation-associated gene 5 (MDA5), consequently inhibiting its interaction with downstream adaptor protein MAVS (54). The 2A protein also plays a role in the viral immune evasion by cleaving tumor necrosis factor receptor-associated factor 3 (TRAF3) (55). Whether different EV-D68 strains utilize different strategies to evade the innate immune responses and whether these strategies differ in different cell types remains to be determined.

Overall, how the evolution of EV-D68 clades in past years is associated with the cell tropism and pathogenesis of EV-D68 are undetermined. Also, the possible role of individual viral factors in the re-emergence of EV-D68 remains unclear. Therefore, further studies should provide more insight into phenotypic differences among the different clades circulating, and how these influences the pathogenesis.

Thesis outline

In recent years, EV-D68 outbreaks have been associated with severe respiratory illness and extra-respiratory complications, of which neurological complications occurred most frequently. However, how EV-D68 infection results in the development of severe disease and the underlying mechanism are largely unknown. This thesis aims to expand our knowledge on the systemic pathogenesis of EV-D68-associated disease focusing on the systemic dissemination and neurotropism of EV-D68 as well as to improve diagnostics for of EV-D68 associated CNS diseases. In **Chapter 1**, I discussed the different stages in the pathogenesis of EV-D68 infection – infection of the respiratory tract, systemic dissemination and infection of the CNS – based on observations in humans as well as experimental in vitro and in vivo studies.

As the systemic dissemination of EV-D68 via the hematogenous route is essential for the systemic spread, I explored in **Chapter 2** the potential role of immune cells in the systemic disseminations in EV-D68 infection.

During the 2014 outbreak, multiple clades were circulating of which subclade B1 was the most prevalent, and therefore associated with the development of neurological complications. In **Chapter 3,** I investigated whether the ability of EV-D68 viruses to replicate in cells of the CNS is a clade specific feature, and which viral factors are important for virus replication in vitro.

Acute flaccid myelitis is the most common CNS complications associated with EV-D68 infections, while encephalitis and meningoencephalitis are infrequently reported. In **Chapter 4**, I investigated the cell tropism and replication efficiency of different EV-D68 isolates from before-and after-2014 in spinal motor neurons and cortical neurons derived from human pluripotent stem cells as well as the associated effect of virus infection on motor neurons.

Diagnostics of EV-D68-associated CNS diseases are challenging because virus antigen or viral RNA are rarely detected in CSF. In **Chapter 5**, I evaluated use of a quantitative EV IgG ELISA in combination with Reiber diagram analysis and AI-calculation as a diagnostic tool for EV-associated CNS disease, including EV-D68.

Finally, the findings presented in this thesis are evaluated in the summarizing discussion **Chapter 6**.

References

1. Waghmare A, Pergam SA, Jerome KR, Englund JA, Boeckh M, Kuypers J. Clinical disease due to enterovirus D68 in adult hematologic malignancy patients and hematopoietic cell transplant recipients. Blood. 2015;125(11):1724-9.
2. Giombini E, Rueca M, Barberi W, Iori AP, Castilletti C, Scognamiglio P, et al. Enterovirus D68-Associated Acute Flaccid Myelitis in Immunocompromised Woman, Italy. Emerg Infect Dis. 2017;23(10):1690-3.
3. Poelman R, Schuffenecker I, Van Leer-Buter C, Josset L, Niesters HG, Lina B, et al. European surveillance for enterovirus D68 during the emerging North-American outbreak in 2014. J Clin Virol. 2015;71:1-9.
4. Messacar K, Abzug MJ, Dominguez SR. The Emergence of Enterovirus-D68. Microbiol Spectr. 2016;4(3).
5. Ayscue P, Van Haren K, Sheriff H, Waubant E, Waldron P, Yagi S, et al. Acute flaccid paralysis with anterior myelitis - California, June 2012-June 2014. MMWR Morb Mortal Wkly Rep. 2014;63(40):903-6.
6. Esposito S, Chidini G, Cinnante C, Napolitano L, Giannini A, Terranova L, et al. Acute flaccid myelitis associated with enterovirus-D68 infection in an otherwise healthy child. Virol J. 2017;14(1):4.
7. Kreuter JD, Barnes A, McCarthy JE, Schwartzman JD, Oberste MS, Rhodes CH, et al. A fatal central nervous system enterovirus 68 infection. Arch Pathol Lab Med. 2011;135(6):793-6.
8. Benschop KS, Albert J, Anton A, Andres C, Aranzamendi M, Armannsdottir B, et al. Re-emergence of enterovirus D68 in Europe after easing the COVID-19 lockdown, September 2021. Euro Surveill. 2021;26(45).
9. Paul JR. Poliomyelitis attack rates in American troops, 1940-1948. Am J Hyg. 1949;50(1):57-62.
10. Garon JR, Cochi SL, Orenstein WA. The Challenge of Global Poliomyelitis Eradication. Infect Dis Clin North Am. 2015;29(4):651-65.
11. Messacar K, Schreiner TL, Maloney JA, Wallace A, Ludke J, Oberste MS, et al. A cluster of acute flaccid paralysis and cranial nerve dysfunction temporally associated with an outbreak of enterovirus D68 in children in Colorado, USA. Lancet. 2015;385(9978):1662-71.
12. Top FH. Incidence of cranial nerve paralysis in poliomyelitis in relation to presence or absence of tonsils. II. In a largely rural area. Pediatrics. 1958;21(1):106-11.
13. Baggen J, Thibaut HJ, Strating J, van Kuppeveld FJM. The life cycle of non-polio enteroviruses and how to target it. Nat Rev Microbiol. 2018;16(6):368-81.
14. Greninger AL, Naccache SN, Messacar K, Clayton A, Yu G, Somasekar S, et al. A novel outbreak enterovirus D68 strain associated with acute flaccid myelitis cases in the USA (2012-14): a retrospective cohort study. Lancet Infect Dis. 2015;15(6):671-82.
15. Knoester M, Scholvinck EH, Poelman R, Smit S, Vermont CL, Niesters HG, et al. Upsurge of Enterovirus D68, the Netherlands, 2016. Emerg Infect Dis. 2017;23(1):140-3.
16. Bal A, Sabatier M, Wirth T, Coste-Burel M, Lazrek M, Stefic K, et al. Emergence of enterovirus D68 clade D1, France, August to November 2018. Euro Surveill. 2019;24(3).

17. Hadfield J, Megill C, Bell SM, Huddleston J, Potter B, Callender C, et al. Nextstrain: real-time tracking of pathogen evolution. Bioinformatics. 2018;34(23):4121-3.
18. Sagulenko P, Puller V, Neher RA. TreeTime: Maximum-likelihood phylodynamic analysis. Virus Evol. 2018;4(1):vex042.
19. Baggen J, Thibaut HJ, Staring J, Jae LT, Liu Y, Guo H, et al. Enterovirus D68 receptor requirements unveiled by haploid genetics. Proc Natl Acad Sci U S A. 2016;113(5):1399-404.
20. Liu Y, Sheng J, Baggen J, Meng G, Xiao C, Thibaut HJ, et al. Sialic acid-dependent cell entry of human enterovirus D68. Nat Commun. 2015;6:8865.
21. de Graaf M, Fouchier RA. Role of receptor binding specificity in influenza A virus transmission and pathogenesis. Embo J. 2014;33(8):823-41.
22. Nicholls JM, Bourne AJ, Chen H, Guan Y, Peiris JS. Sialic acid receptor detection in the human respiratory tract: evidence for widespread distribution of potential binding sites for human and avian influenza viruses. Respir Res. 2007;8(1):73.
23. Sauer AK, Liang CH, Stech J, Peeters B, Quéré P, Schwegmann-Wessels C, et al. Characterization of the sialic acid binding activity of influenza A viruses using soluble variants of the H7 and H9 hemagglutinins. PLoS One. 2014;9(2):e89529.
24. Brown DM, Hixon AM, Oldfield LM, Zhang Y, Novotny M, Wang W, et al. Contemporary Circulating Enterovirus D68 Strains Have Acquired the Capacity for Viral Entry and Replication in Human Neuronal Cells. mBio. 2018;9(5).
25. Sooksawasdi Na Ayudhya S, Meijer A, Bauer L, Oude Munnink B, Embregts C, Leijten L, et al. Enhanced Enterovirus D68 Replication in Neuroblastoma Cells Is Associated with a Cell Culture-Adaptive Amino Acid Substitution in VP1. mSphere. 2020;5(6).
26. Baggen J, Liu Y, Lyoo H, van Vliet ALW, Wahedi M, de Bruin JW, et al. Bypassing pan-enterovirus host factor PLA2G16. Nat Commun. 2019;10(1):3171.
27. Tseligka ED, Sobo K, Stoppini L, Cagno V, Abdul F, Piuz I, et al. A VP1 mutation acquired during an enterovirus 71 disseminated infection confers heparan sulfate binding ability and modulates ex vivo tropism. PLoS Pathog. 2018;14(8):e1007190.
28. Jenniskens GJ, Oosterhof A, Brandwijk R, Veerkamp JH, van Kuppevelt TH. Heparan sulfate heterogeneity in skeletal muscle basal lamina: demonstration by phage display-derived antibodies. J Neurosci. 2000;20(11):4099-111.
29. Farhy Tselnicker I, Boisvert MM, Allen NJ. The role of neuronal versus astrocyte-derived heparan sulfate proteoglycans in brain development and injury. Biochem Soc Trans. 2014;42(5):1263-9.
30. Wei W, Guo H, Chang J, Yu Y, Liu G, Zhang N, et al. ICAM-5/Telencephalin Is a Functional Entry Receptor for Enterovirus D68. Cell Host Microbe. 2016;20(5):631-41.
31. Hixon AM, Clarke P, Tyler KL. Contemporary Circulating Enterovirus D68 Strains Infect and Undergo Retrograde Axonal Transport in Spinal Motor Neurons Independent of Sialic Acid. J Virol. 2019;93(16).
32. Gahmberg CG, Tian L, Ning L, Nyman-Huttunen H. ICAM-5--a novel two-facetted adhesion molecule in the mammalian brain. Immunol Lett. 2008;117(2):131-5.
33. Kim M, Yu JE, Lee JH, Chang BJ, Song CS, Lee B, et al. Comparative analyses of influenza virus receptor distribution in the human and mouse brains. J Chem Neuroanat. 2013;52:49-57.

34. Sakabe S, Iwatsuki-Horimoto K, Takano R, Nidom CA, Le MTQ, Nagamura-Inoue T, et al. Cytokine production by primary human macrophages infected with highly pathogenic H5N1 or pandemic H1N1 2009 influenza viruses. J Gen Virol. 2011;92(Pt 6):1428-34.
35. Videira PA, Amado IF, Crespo HJ, Algueró MC, Dall'Olio F, Cabral MG, et al. Surface alpha 2-3- and alpha 2-6-sialylation of human monocytes and derived dendritic cells and its influence on endocytosis. Glycoconj J. 2008;25(3):259-68.
36. Eash S, Tavares R, Stopa EG, Robbins SH, Brossay L, Atwood WJ. Differential distribution of the JC virus receptor-type sialic acid in normal human tissues. Am J Pathol. 2004;164(2):419-28.
37. Yang H. Structure, Expression, and Function of ICAM-5. Comp Funct Genomics. 2012;2012:368938.
38. Fadnes B, Husebekk A, Svineng G, Rekdal O, Yanagishita M, Kolset SO, et al. The proteoglycan repertoire of lymphoid cells. Glycoconj J. 2012;29(7):513-23.
39. Wegrowski Y, Milard AL, Kotlarz G, Toulmonde E, Maquart FX, Bernard J. Cell surface proteoglycan expression during maturation of human monocytes-derived dendritic cells and macrophages. Clin Exp Immunol. 2006;144(3):485-93.
40. Itagaki T, Aoki Y, Matoba Y, Tanaka S, Ikeda T, Mizuta K, et al. Clinical characteristics of children infected with enterovirus D68 in an outpatient clinic and the association with bronchial asthma. Infect Dis (Lond). 2018;50(4):303-12.
41. Schuster JE, Selvarangan R, Hassan F, Briggs KB, Hays L, Miller JO, et al. Clinical Course of Enterovirus D68 in Hospitalized Children. Pediatr Infect Dis J. 2017;36(3):290-5.
42. Schuster JE, Miller JO, Selvarangan R, Weddle G, Thompson MT, Hassan F, et al. Severe enterovirus 68 respiratory illness in children requiring intensive care management. J Clin Virol. 2015;70:77-82.
43. Korematsu S, Nagashima K, Sato Y, Nagao M, Hasegawa S, Nakamura H, et al. "Spike" in acute asthma exacerbations during enterovirus D68 epidemic in Japan: A nation-wide survey. Allergol Int. 2018;67(1):55-60.
44. Foster CB, Coelho R, Brown PM, Wadhwa A, Dossul A, Gonzalez BE, et al. A comparison of hospitalized children with enterovirus D68 to those with rhinovirus. Pediatr Pulmonol. 2017;52(6):827-32.
45. Kusabe Y, Takeshima A, Seino A, Nishida M, Takahashi M, Yamada S, et al. [An Adult Case of Enterovirus D68 Encephalomyelitis Presenting as Bilateral Facial Nerve Palsy and Dysphagia]. Brain Nerve. 2017;69(8):957-61.
46. Ward NS, Hughes BL, Mermel LA. Enterovirus D68 Infection in an Adult. Am J Crit Care. 2016;25(2):178-80.
47. Matsumoto M, Awano H, Ogi M, Tomioka K, Unzaki A, Nishiyama M, et al. A pediatric patient with interstitial pneumonia due to enterovirus D68. J Infect Chemother. 2016;22(10):712-5.
48. Essaidi-Laziosi M, Brito F, Benaoudia S, Royston L, Cagno V, Fernandes-Rocha M, et al. Propagation of respiratory viruses in human airway epithelia reveals persistent virus-specific signatures. J Allergy Clin Immunol. 2018;141(6):2074-84.
49. Patel MC, Wang W, Pletneva LM, Rajagopala SV, Tan Y, Hartert TV, et al. Enterovirus D-68 Infection, Prophylaxis, and Vaccination in a Novel Permissive Animal Model, the Cotton Rat (Sigmodon hispidus). PLoS One. 2016;11(11):e0166336.

50. Zheng HW, Sun M, Guo L, Wang JJ, Song J, Li JQ, et al. Nasal Infection of Enterovirus D68 Leading to Lower Respiratory Tract Pathogenesis in Ferrets (Mustela putorius furo). Viruses. 2017;9(5).
51. Evans WJ, Hurst BL, Peterson CJ, Van Wettere AJ, Day CW, Smee DF, et al. Development of a respiratory disease model for enterovirus D68 in 4-week-old mice for evaluation of antiviral therapies. Antiviral Res. 2019;162:61-70.
52. Rajput C, Han M, Bentley JK, Lei J, Ishikawa T, Wu Q, et al. Enterovirus D68 infection induces IL-17-dependent neutrophilic airway inflammation and hyperresponsiveness. JCI Insight. 2018;3(16).
53. Xiang Z, Liu L, Lei X, Zhou Z, He B, Wang J. 3C Protease of Enterovirus D68 Inhibits Cellular Defense Mediated by Interferon Regulatory Factor 7. J Virol. 2016;90(3):1613-21.
54. Rui Y, Su J, Wang H, Chang J, Wang S, Zheng W, et al. Disruption of MDA5-Mediated Innate Immune Responses by the 3C Proteins of Coxsackievirus A16, Coxsackievirus A6, and Enterovirus D68. J Virol. 2017;91(13).
55. Kang J, Pang Z, Zhou Z, Li X, Liu S, Cheng J, et al. Enterovirus D68 Protease 2A(pro) Targets TRAF3 To Subvert Host Innate Immune Responses. J Virol. 2021;95(3).
56. Chong PF, Kira R, Mori H, Okumura A, Torisu H, Yasumoto S, et al. Clinical Features of Acute Flaccid Myelitis Temporally Associated With an Enterovirus D68 Outbreak: Results of a Nationwide Survey of Acute Flaccid Paralysis in Japan, August-December 2015. Clin Infect Dis. 2018;66(5):653-64.
57. Imamura T, Suzuki A, Lupisan S, Kamigaki T, Okamoto M, Roy CN, et al. Detection of enterovirus 68 in serum from pediatric patients with pneumonia and their clinical outcomes. Influenza Other Respir Viruses. 2014;8(1):21-4.
58. Hurst BL, Evans WJ, Smee DF, Van Wettere AJ, Tarbet EB. Evaluation of antiviral therapies in respiratory and neurological disease models of Enterovirus D68 infection in mice. Virology. 2019;526:146-54.
59. Zhang C, Zhang X, Dai W, Liu Q, Xiong P, Wang S, et al. A Mouse Model of Enterovirus D68 Infection for Assessment of the Efficacy of Inactivated Vaccine. Viruses. 2018;10(2).
60. Zheng H, Wang J, Li B, Guo L, Li H, Song J, et al. A Novel Neutralizing Antibody Specific to the DE Loop of VP1 Can Inhibit EV-D68 Infection in Mice. J Immunol. 2018;201(9):2557-69.
61. Shen L, Chen CY, Huang D, Wang R, Zhang M, Qian L, et al. Pathogenic Events in a Nonhuman Primate Model of Oral Poliovirus Infection Leading to Paralytic Poliomyelitis. J Virol. 2017;91(14).
62. Smura T, Ylipaasto P, Klemola P, Kaijalainen S, Kyllonen L, Sordi V, et al. Cellular tropism of human enterovirus D species serotypes EV-94, EV-70, and EV-68 in vitro: implications for pathogenesis. J Med Virol. 2010;82(11):1940-9.
63. Corona AK, Saulsbery HM, Corona Velazquez AF, Jackson WT. Enteroviruses Remodel Autophagic Trafficking through Regulation of Host SNARE Proteins to Promote Virus Replication and Cell Exit. Cell Rep. 2018;22(12):3304-14.
64. Liang CC, Sun MJ, Lei HY, Chen SH, Yu CK, Liu CC, et al. Human endothelial cell activation and apoptosis induced by enterovirus 71 infection. J Med Virol. 2004;74(4):597-603.

65. Bozym RA, Morosky SA, Kim KS, Cherry S, Coyne CB. Release of intracellular calcium stores facilitates coxsackievirus entry into polarized endothelial cells. PLoS Pathog. 2010;6(10):e1001135.
66. Conaldi PG, Serra C, Mossa A, Falcone V, Basolo F, Camussi G, et al. Persistent infection of human vascular endothelial cells by group B coxsackieviruses. J Infect Dis. 1997;175(3):693-6.
67. Couderc T, Barzu T, Horaud F, Crainic R. Poliovirus permissivity and specific receptor expression on human endothelial cells. Virology. 1990;174(1):95-102.
68. Coyne CB, Kim KS, Bergelson JM. Poliovirus entry into human brain microvascular cells requires receptor-induced activation of SHP-2. Embo J. 2007;26(17):4016-28.
69. Saijets S, Ylipaasto P, Vaarala O, Hovi T, Roivainen M. Enterovirus infection and activation of human umbilical vein endothelial cells. J Med Virol. 2003;70(3):430-9.
70. Wang W, Sun J, Wang N, Sun Z, Ma Q, Li J, et al. Enterovirus A71 capsid protein VP1 increases blood-brain barrier permeability and virus receptor vimentin on the brain endothelial cells. J Neurovirol. 2020;26(1):84-94.
71. Zanone MM, Favaro E, Conaldi PG, Greening J, Bottelli A, Perin PC, et al. Persistent infection of human microvascular endothelial cells by coxsackie B viruses induces increased expression of adhesion molecules. J Immunol. 2003;171(1):438-46.
72. Pham NTK, Thongprachum A, Baba T, Okitsu S, Trinh QD, Komine-Aizawa S, et al. A 3-Month-Old Child with Acute Gastroenteritis with Enterovirus D68 Detected from Stool Specimen. Clin Lab. 2017;63(7):1269-72.
73. Van Haren K, Ayscue P, Waubant E, Clayton A, Sheriff H, Yagi S, et al. Acute Flaccid Myelitis of Unknown Etiology in California, 2012-2015. Jama. 2015;314(24):2663-71.
74. Fall A, Ndiaye N, Jallow MM, Barry MA, Touré CSB, Kebe O, et al. Enterovirus D68 Subclade B3 Circulation in Senegal, 2016: Detection from Influenza-like Illness and Acute Flaccid Paralysis Surveillance. Sci Rep. 2019;9(1):13881.
75. Williams CJ, Thomas RH, Pickersgill TP, Lyons M, Lowe G, Stiff RE, et al. Cluster of atypical adult Guillain-Barre syndrome temporally associated with neurological illness due to EV-D68 in children, South Wales, United Kingdom, October 2015 to January 2016. Euro Surveill. 2016;21(4).
76. Guo H, Li Y, Liu G, Jiang Y, Shen S, Bi R, et al. A second open reading frame in human enterovirus determines viral replication in intestinal epithelial cells. Nat Commun. 2019;10(1):4066.
77. Antona D, Kossorotoff M, Schuffenecker I, Mirand A, Leruez-Ville M, Bassi C, et al. Severe paediatric conditions linked with EV-A71 and EV-D68, France, May to October 2016. Euro Surveill. 2016;21(46).
78. Chang TH, Yang TI, Hsu WY, Huang LM, Chang LY, Lu CY. Case report: painful exanthems caused by enterovirus D68 in an adolescent. Medicine (Baltimore). 2019;98(33):e16493.
79. Midgley SE, Benschop K, Dyrdak R, Mirand A, Bailly JL, Bierbaum S, et al. Co-circulation of multiple enterovirus D68 subclades, including a novel B3 cluster, across Europe in a season of expected low prevalence, 2019/20. Euro Surveill. 2020;25(2).
80. Barnadas C, Midgley SE, Skov MN, Jensen L, Poulsen MW, Fischer TK. An enhanced Enterovirus surveillance system allows identification and characterization of rare and emerging respiratory enteroviruses in Denmark, 2015-16. J Clin Virol. 2017;93:40-4.

81. Morrey JD, Wang H, Hurst BL, Zukor K, Siddharthan V, Van Wettere AJ, et al. Causation of Acute Flaccid Paralysis by Myelitis and Myositis in Enterovirus-D68 Infected Mice Deficient in Interferon alphabeta/gamma Receptor Deficient Mice. Viruses. 2018;10(1).
82. Cabrerizo M, Garcia-Iniguez JP, Munell F, Amado A, Madurga-Revilla P, Rodrigo C, et al. First Cases of Severe Flaccid Paralysis Associated With Enterovirus D68 Infection in Spain, 2015-2016. Pediatr Infect Dis J. 2017;36(12):1214-6.
83. Sejvar JJ, Lopez AS, Cortese MM, Leshem E, Pastula DM, Miller L, et al. Acute Flaccid Myelitis in the United States, August-December 2014: Results of Nationwide Surveillance. Clin Infect Dis. 2016;63(6):737-45.
84. Pfeiffer HC, Bragstad K, Skram MK, Dahl H, Knudsen PK, Chawla MS, et al. Two cases of acute severe flaccid myelitis associated with enterovirus D68 infection in children, Norway, autumn 2014. Euro Surveill. 2015;20(10):21062.
85. Hu YL, Huang LM, Lu CY, Fang TY, Cheng AL, Chang LY. Manifestations of enterovirus D68 and high seroconversion among children attending a kindergarten. J Microbiol Immunol Infect. 2019;52(6):858-64.
86. ElBadry M, Lednicky J, Cella E, Telisma T, Chavannes S, Loeb J, et al. Isolation of an Enterovirus D68 from Blood from a Child with Pneumonia in Rural Haiti: Close Phylogenetic Linkage with New York Strain. Pediatr Infect Dis J. 2016;35(9):1048-50.
87. Messacar K, Schreiner TL, Van Haren K, Yang M, Glaser CA, Tyler KL, et al. Acute flaccid myelitis: A clinical review of US cases 2012-2015. Ann Neurol. 2016;80(3):326-38.
88. Nelson GR, Bonkowsky JL, Doll E, Green M, Hedlund GL, Moore KR, et al. Recognition and Management of Acute Flaccid Myelitis in Children. Pediatr Neurol. 2016;55:17-21.
89. Maloney JA, Mirsky DM, Messacar K, Dominguez SR, Schreiner T, Stence NV. MRI findings in children with acute flaccid paralysis and cranial nerve dysfunction occurring during the 2014 enterovirus D68 outbreak. AJNR Am J Neuroradiol. 2015;36(2):245-50.
90. Yogo N, Imamura T, Muto Y, Hirai K. Cardiopulmonary failure as a result of brainstem encephalitis caused by enterovirus D68. BMJ Case Rep. 2019;12(11).
91. Esposito S, Lunghi G, Zampiero A, Tagliabue C, Orlandi A, Torresani E, et al. Enterovirus-D68 in the Cerebrospinal Fluid of Two Children with Aseptic Meningitis. Pediatr Infect Dis J. 2016;35(5):589-91.
92. Lang M, Mirand A, Savy N, Henquell C, Maridet S, Perignon R, et al. Acute flaccid paralysis following enterovirus D68 associated pneumonia, France, 2014. Euro Surveill. 2014;19(44).
93. Wali RK, Lee AH, Kam JC, Jonsson J, Thatcher A, Poretz D, et al. Acute Neurological Illness in a Kidney Transplant Recipient Following Infection With Enterovirus-D68: An Emerging Infection? Am J Transplant. 2015;15(12):3224-8.
94. Lopez A, Lee A, Guo A, Konopka-Anstadt JL, Nisler A, Rogers SL, et al. Vital Signs: Surveillance for Acute Flaccid Myelitis - United States, 2018. MMWR Morb Mortal Wkly Rep. 2019;68(27):608-14.
95. Reiber H, Peter JB. Cerebrospinal fluid analysis: disease-related data patterns and evaluation programs. J Neurol Sci. 2001;184(2):101-22.
96. Ruggieri V, Paz MI, Peretti MG, Rugilo C, Bologna R, Freire C, et al. Enterovirus D68 infection in a cluster of children with acute flaccid myelitis, Buenos Aires, Argentina, 2016. Eur J Paediatr Neurol. 2017;21(6):884-90.

97. Sun S, Bian L, Gao F, Du R, Hu Y, Fu Y, et al. A neonatal mouse model of Enterovirus D68 infection induces both interstitial pneumonia and acute flaccid myelitis. Antiviral Res. 2019;161:108-15.
98. Hixon AM, Yu G, Leser JS, Yagi S, Clarke P, Chiu CY, et al. A mouse model of paralytic myelitis caused by enterovirus D68. PLoS Pathog. 2017;13(2):e1006199.
99. Ohka S, Nihei C, Yamazaki M, Nomoto A. Poliovirus trafficking toward central nervous system via human poliovirus receptor-dependent and -independent pathway. Front Microbiol. 2012;3:147.
100. Rosenfeld AB, Warren AL, Racaniello VR. Neurotropism of Enterovirus D68 Isolates Is Independent of Sialic Acid and Is Not a Recently Acquired Phenotype. MBio. 2019;10(5).
101. Dyrdak R, Grabbe M, Hammas B, Ekwall J, Hansson KE, Luthander J, et al. Outbreak of enterovirus D68 of the new B3 lineage in Stockholm, Sweden, August to September 2016. Euro Surveill. 2016;21(46).
102. Piralla A, Principi N, Ruggiero L, Girello A, Giardina F, De Sando E, et al. Enterovirus-D68 (EV-D68) in pediatric patients with respiratory infection: The circulation of a new B3 clade in Italy. J Clin Virol. 2018;99-100:91-6.
103. Zhang Y, Cao J, Zhang S, Lee AJ, Sun G, Larsen CN, et al. Genetic changes found in a distinct clade of Enterovirus D68 associated with paralysis during the 2014 outbreak. Virus Evol. 2016;2(1):vew015.
104. Du J, Zheng B, Zheng W, Li P, Kang J, Hou J, et al. Analysis of Enterovirus 68 Strains from the 2014 North American Outbreak Reveals a New Clade, Indicating Viral Evolution. PLoS One. 2015;10(12):e0144208.

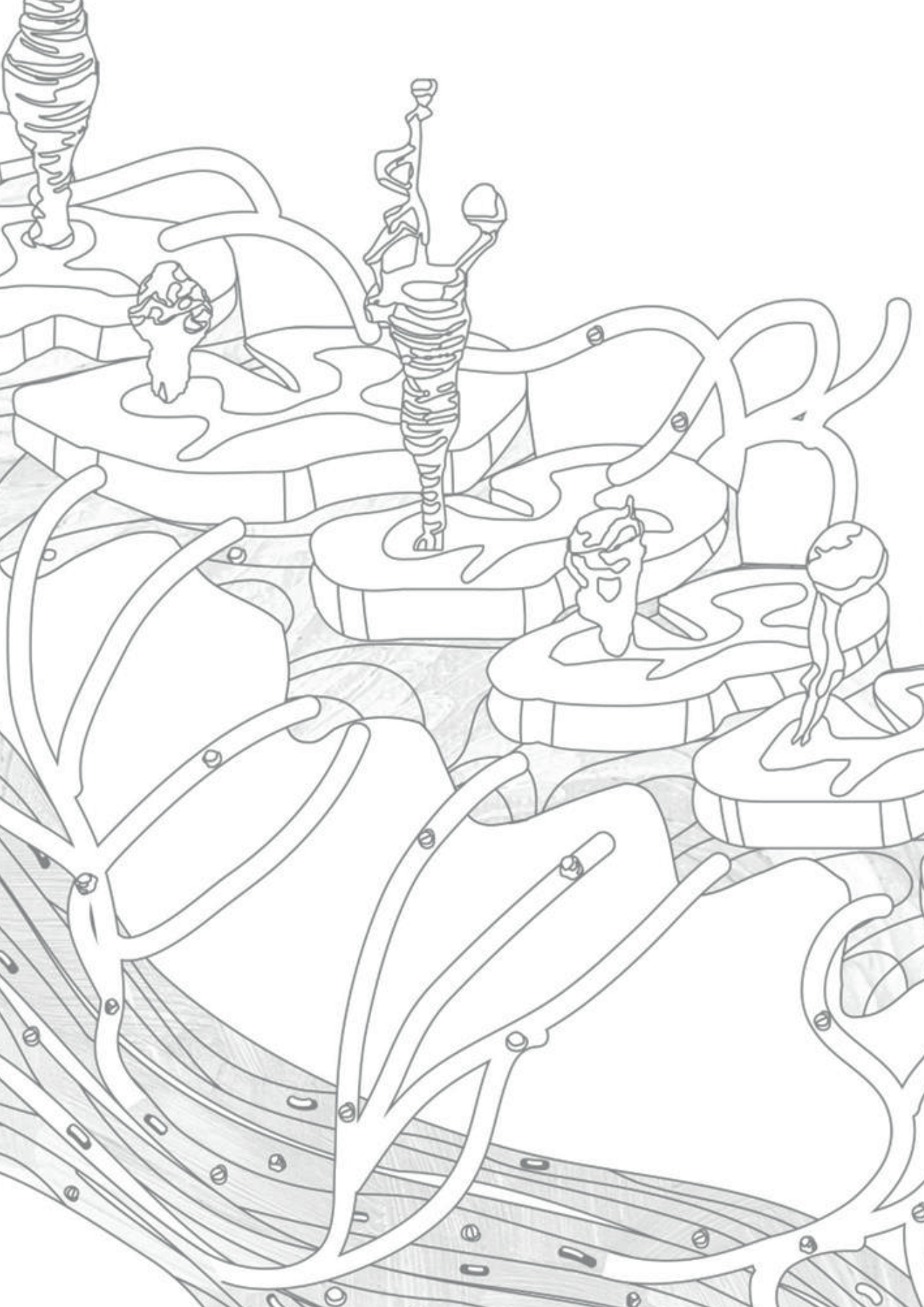

Chapter

2

The potential role of human immune cells in the systemic dissemination of enterovirus D68

Brigitta M. Laksono*, Syriam Sooksawasdi Na Ayudhya*,
Muriel Aguilar-Bretones, Carmen W. E. Embregts,
Gijsbert P van Nierop, Debby van Riel

* These authors contributed equally to this work

Submitted

Abstract

Enterovirus-D68 (EV-D68) are predominantly associated with mild respiratory infections, but can also cause severe respiratory disease and extra-respiratory complications, including acute flaccid myelitis (AFM). Systemic dissemination of EV-D68 is crucial for the development of extra-respiratory diseases, but it is currently unclear how EV-D68 spreads systemically (viremia). We hypothesize that immune cells contribute to the systemic dissemination of EV-D68, as this is a mechanism commonly used by other enteroviruses. Therefore, we investigated the susceptibility and permissiveness of human primary immune cells for different EV-D68 isolates. In human peripheral blood mononuclear cells (PBMC) inoculated with EV-D68, only B cells were susceptible but virus replication was limited. However, in B cell-rich cultures, such as Epstein-Barr virus-transformed B-lymphoblastoid cell line (BLCL) and primary lentivirus-transduced B cells, which better represent lymphoid B cells, were productively infected. In BLCL, neuraminidase treatment to remove α2,6- and α2,3-linked sialic acids resulted in a significant decrease of EV-D68 infected cells, suggesting that sialic acids are the functional receptor on B cells. Subsequently, we showed that dendritic cells (DCs), particularly immature DCs, are susceptible and permissive for EV-D68 infection and that they can spread EV-D68 to autologous BLCL. Altogether, our findings suggest that immune cells, especially B cells and DCs, could play an important role in the systemic dissemination of EV-D68 during an infection, which is an essential step towards the development of extra-respiratory complications.

Importance

Enterovirus D68 (EV-D68) is an emerging respiratory virus that has caused outbreaks worldwide since 2014. EV-D68 infects primarily respiratory epithelial cells resulting in mild respiratory diseases. However, EV-D68 infection is also associated with extra-respiratory complications, including polio-like paralysis. It is unclear how EV-D68 spreads systemically and infects other organs. We investigated if immune cells could play a role in the extra-respiratory spread of EV-D68. We showed that EV-D68 can infect and replicate in specific immune cells, *i.e.* B cells and dendritic cells (DCs), and that virus could be transferred from DCs to B cells. Our data reveal a potential role of immune cells in the systemic spread of EV-D68. Intervention strategies that prevent EV-D68 infection of immune cells will therefore potentially prevent systemic spread of virus and thereby severe extra-respiratory complications.

Introduction

Enterovirus D68 (EV-D68) is a small non-enveloped, positive single-stranded RNA virus that belongs to the family *Picornaviridae*, genus Enterovirus. Although EV-D68 infections causes predominantly mild upper respiratory tract symptoms, severe respiratory diseases were reported worldwide in 2014. In addition, in some individuals, EV-D68 was associated with neurological complications, of which acute flaccid myelitis (AFM) was reported most frequently (1-4). Since then, EV-D68 has caused biennial outbreaks of severe respiratory disease and AFM up to 2018 (3, 5). EV-D68 circulation was limited during the pandemic, partly due to COVID-19 measures, but EV-D68-associated severe respiratory illnesses have been rising in several countries since 2021 and 2022 due to easing of COVID-19 measures (6, 7). Throughout the years, multiple clades of EV-D68 circulated, but so far there is little evidence for differences in the virulence of these viruses (1, 8, 9).

The ability of EV-D68 to disseminate from the respiratory tract, which is the primary replication site of the virus, to other organs, such as the central nervous system (CNS), is essential for the development of extra-respiratory complications. Studies in mice, ferrets and patient samples have shown that the virus or viral RNA can be detected in the circulation (viremia and RNAemia, respectively) and extra-respiratory tissues (1, 10-17). In intranasally inoculated mice, virus was detected in the blood within 24 hours post-inoculation (hpi), and in extra-respiratory tissues, such as the spleen and skeletal muscles (10, 11). In intranasally inoculated ferrets, virus was detected in axillary lymph nodes at multiple days post-inoculation (earliest detection at day 5 post-inoculation) (12). In humans, virus and viral RNA have been detected in serum of EV-D68 patients, but it is currently unknown how frequent viremia occurs during an EV-D68 infection (13-17). However, despite the importance of viremia in the pathogenesis of EV-D68 infection, the mechanism that leads to it is poorly understood. In addition, it is unclear whether the virus detected in the circulation is a direct spill-over from the respiratory tract or whether virus first spreads to and replicates in other tissues, *e.g.* lymphoid tissues, before disseminating into the circulation.

Other EVs can infect various immune cells with different replication efficiency. Coxsackievirus type B3 (CVB3) infects murine splenic B cells resulting in production of new virus particles (18). Poliovirus productively infects dendritic cells (DCs) and macrophages *in vitro* (human PBMC) and *in vivo* (non-human primates) (19, 20). Echoviruses and EV-A71 have also been reported to infect human immature DCs (imDCs) and mature DCs (mDCs) (21, 22). Some EVs, for example, poliovirus and EV-A71 are known to replicate in lymphoid tissues, resulting in a sustained production of infectious viruses and subsequent spill-over into the circulation (23-27). For EV-D68, the role of immune cells and lymphoid tissues in the development of a viremia remains unclear. Previous studies have shown that EV-D68 productively infects several human immune cell lines, such as granulocytic (KG-1), monocytic (U-937), T (Jurkat and MOLT) and B (Raji) cell lines (28), suggesting that immune cells or lymphoid tissues may play a

role in the development of EV-D68 viremia. Here, we investigated the susceptibility and permissiveness of human primary immune cells, B cells enriched models and monocytic-derived DCs to infection of EV-D68 from different subclades to unravel the potential role of immune cells in the development of viremia and to investigate if there are clade-specific differences in the susceptibility and permissiveness of these cells. Subsequently, we investigated whether DCs can transmit virus to other immune cells, such as B cells.

Materials and methods

Ethics statement

PBMC were obtained from healthy adult donors after obtaining written informed consent. The studies were approved by the medical ethical committee of Erasmus MC, the Netherlands (MEC-2015-095). For experiment involving human buffy coats, written informed consent for research use was obtained by the Sanquin blood bank.

Cells

Human PBMC were isolated from blood (n = 10 healthy donors) by Ficoll density gradient centrifugation. BLCL were established from 7 donors by transformation with Epstein-Barr virus as previously described (43). PBMC and BLCL were cultured in RPMI-1640 medium (Capricorn) supplemented with 10% fetal bovine serum (FBS) and 100 IU/ml of penicillin, 100 µg/ml of streptomycin and 2 mM L-glutamine (PSG). After virus inoculation, supernatants and cell lysates were collected and frozen and thawed three times prior to sample processing.

Germinal center-like B cell clones were generated from 3 donors. Synthetic cDNA encoding a self-cleaving polyprotein Bcl-6.t2A.Blc-xL to express the germinal center B cell-associated transcription factors Bcl-6 and Bcl-xL was synthesized (B6L; Integrated DNA Technologies) and cloned in pENTR/D-TOPO (Thermo Fisher), generating pENTR.B6L (35, 44). The B6L cDNA was subsequently transferred to pLenti6.3/V5-DEST using Gateway LR Clonase II (Thermo Fisher), generating pLV-B6L. Subsequently, lentiviral vector stocks (LV-B6L) were generated, all according to manufacturer's instructions (Thermo Fisher). Primary $CD19^+$ B cells were isolated from human PBMC using the EasySep human CD19 positive selection kit II (StemCell Technologies) and transduced using LV.B6L as described elsewhere (35). LV-B6L transduced B cells were cultured in AIM-V AlbuMAX medium (Gibco) supplemented with 10% FBS, PSG, 50 µM beta-mercaptoethanol (Sigma), 25 ng/ml recombinant human IL-21 (Peprotech) and growth-arrested 40 gray gamma-irradiated L-CD40L feeder cells. Every 3 to 4 days, new culture medium was added with 25 ng/ml recombinant human IL-21 and new growth-arrested 40 gray gamma-irradiated L-CD40L feeder cells. Clonal B cell cultures from each donor were generated using limiting dilution. Absence of antibody reactivity towards EV-D68 was confirmed to exclude antibody-mediated effects on EV-D68

infection (data not shown). After virus inoculation, supernatants and cell lysates were collected and frozen and thawed three times prior to sample processing.

Human rhabdomyosarcoma (RD) cells were cultured in DMEM (Lonza) supplemented with 10% FBS and PSG.

Viruses

EV-D68 strains included in this study were isolated from clinical specimens at the National Institute of Public Health and the Environment (RIVM), Bilthoven, the Netherlands. The viruses were isolated on RD cells (ATCC) at 33°C at RIVM from respiratory samples from patients with EV-D68-associated respiratory disease. Virus stocks for the studies were grown in RD cells at 33°C in 5% CO_2. The viruses included in this study with virus reference number, year of isolation an accession number are as follows: subclade A (or A1; 4311200821; 2012, accession number MN954536), subclade A2 (previously known as D; 4311400720; 2014, accession number MN954537) and subclade B2 (4311201039; 2012, accession number MN954539). All virus stocks were sequenced for their whole genome, and there was no evidence for cell culture adaptive mutations. For heat-inactivated virus controls, the same viruses from subclades A, B2 or A2 were heat-inactivated at 70 °C for 30 min prior to inoculation.

Virus titration

Virus titers were assessed by end-point titrations in RD cells and were expressed in median tissue culture infectious dose ($TCID_{50}$/ml). In brief, 10-fold serial dilutions of a virus stock were prepared in triplicate and inoculated onto a monolayer of RD cells. The inoculated plates were incubated at 33°C in 5% CO_2. Cytopathic effect (CPE) was determined at day 5, and virus titers were determined using the Spearman-Kärber method (45).

Differentiation of monocyte-derived DCs

Human monocytes were isolated from buffy coats (n= 5 donors) by Ficoll density gradient centrifugation and selected for $CD14^+$ cells using magnetic beads. Monocytes were cultured in RPMI-1640 medium supplemented with 1X Glutamax, 10% FBS, 100 IU/ml of penicillin and 100 µg/ml of streptomycin. Subsequently, monocytes were differentiated into imDCs in the presence of human interleukin 4 (IL-4; 20ng/ml; PEPROTECH; 200-04) and human granulocyte-macrophage colony-stimulating factor (GM-CSF; 20ng/ml; MILTENYI BIOTEC; 130-093-866). At day 5, monocyte-derived imDCs were further differentiated into mature DCs by adding lipopolysaccharide (LPS; 1ug/ml; Thermo Fisher Scientific; L8274-10MG) into the medium. mDCs were defined by the increased expression of HLA-DR, CD86, PD-L1 and CD83 compared to imDCs (S3) and the determination of the cellular marker expression by flow cytometry is described below.

EV-D68 infection of PBMC, BLCL and lentivirus-transduced B cells

Freshly isolated PBMCs, BLCLs or lentivirus-transduced B cells (1×10^6 cells) were inoculated with EV-D68 or heat-inactivated EV-D68 at multiplicity of infection (MOI) of 0.1 for 1 h at 37°C in 5% CO_2. The inoculum was removed and cells were seeded in new medium into a U-bottomed 96-well plate. Cells and supernatants were collected at 0, 6, 8, 12, 24, 48 and 72 h post-inoculation (hpi). The collected specimens were frozen and thawed three times to allow release of intracellular virus before further used for virus titration. Cells were also collected at 6, 24, 48 and 72 hpi for detection of intracellular capsid protein VP1 (10 µg/ml; GeneTex; GTX132313) by flow cytometry as described below. Normal rabbit serum was included as VP1 isotype control in PBMC.

Removal of cell surface sialic acids on BLCL

BLCLs were incubated with 50 mU/ml *Arthrobacter ureafaciens* neuraminidase (Roche) in serum-free medium for 2 h at 37°C in 5% CO_2. Removal of α(2,3)-linked and α(2,6)-linked sialic acids on the cell surface was verified by staining with biotinylated *Maackia amurensis* lectin (MAL) I (5 µg/ml; Vector Laboratories; B-1265-1) or fluorescein-labeled *Sambucus nigra* lectin (SNA) (5 µg/ml; EY Laboratories; BA-6802-1), respectively. Biotin was detected using a streptavidin-conjugated AlexaFluor488 (5 µg/ml; Thermo Fisher Scientific; S11223). Virus and mock inoculations in non-enzymatic-treated cells were included as positive and negative infection controls, respectively. Infection of BLCL in different conditions were performed as describe above and intracellular capsid protein VP1 were detected by flow cytometry as described below.

EV-D68 inoculation of DCs and co-culture of DCs and BLCLs

ImDCs and mDCs in a flat-bottomed 96-well plate (1×10^5 cells/well) were inoculated with EV-D68/A at MOI of 1. After 1 h, the inoculum was removed and the monocytes-derived imDCs were supplemented with complete RPMI-1640 containing human IL-4 and GM-CSF, while mDCs were supplemented with complete RPMI-1640 containing human IL-4, GM-CSF and LPS. Cells and supernatants were collected at 0, 2, 4, 6, 8, 10, 24 and 48 hpi for virus titration or at 6 hpi for detection of intracellular expression of capsid protein VP1 by flow cytometry as described below.

For co-culture assay, infected imDCs (1×10^5 cells/well) as describe above were incubated with (2×10^5 BLCL/well; BLCL+DC) or without autologous BLCL (DC only). To investigate whether imDCs transfer virus particles directly to autologous BLCL or indirectly by release of infectious virus, the supernatant from imDCs that were infected with EV-D68/A for 6 hours, were transferred to autologous BLCL (BLCL+t6 DC sup). As a control, to show that infected BLCL is not due to the leftover of virus inoculum, supernatant from the last washing step in infected imDCs were transferred to the autologous BLCL (BLCL+t0 DC sup). The schematic representation of the co-culture assay is presented in Fig 5A. The intracellular expression of capsid protein VP1 was

detected at 6 and 24 hpi by flow cytometry as described below. Cells and supernatant were collected to detect infectious virus particles at different time points.

Flow cytometry

For determination of immune cell phenotypes, human PBMC were incubated with monoclonal antibodies against CD19 (PE-Cy7; Beckman Coulter; IM3628), CD3 (PerCP; BD Biosciences; 345766), CD4 (V450; BD Biosciences; 560811), CD8 (AmCyan; BD Biosciences; 339188), CD14 (BV711; BD Biosciences; 740773) and CD16 (AlexaFluor647; BD Biosciences; 302020). For determination of DC phenotypes, DCs were incubated with monoclonal antibodies against HLA-DR (Pacific Blue; BioLegend; 307624), CD83(PE-Cy7; BioLegend; 305326), CD86 (AF647; BioLegend; 305416) and PD-L1 (BV785; BioLegend; 320736). For determination of cell phenotypes in DC-BLCL co-cultures, the cells were incubated with monoclonal antibodies against HLA-DR (Pacific Blue; BioLegend; 307624), CD86 (AF647; BioLegend; 305416), CD19 (PE-Cy7; Beckman Coulter; IM3628). Cells were fixed and permeabilized with BD Cytofix/Cytoperm Fixation and Permeabilization kit according to the manufacturer's instructions (BD Biosciences). The presence of intracellular capsid protein VP1 was determined by staining with polyclonal rabbit anti-EV-D68 VP1 (10 µg/ml; Genetex; GTX132313) and goat anti-rabbit IgG (FITC; BD Biosciences; 554020). Flow cytometry was performed using BD FACS Lyric (BD Biosciences, USA). Data were acquired with BD Suite software and analyzed with FlowJo software. Gating strategies to define different cell phenotypes and to define $VP1^+$ cells are presented in S4 – 7.

Statistical analyses

Statistical analyses were performed using GraphPad Prism 9.0 software (La Jolla, CA, USA). Specific tests are described in the figure legends. P values of ≤ 0.05 were considered significant. All data were expressed as standard error of mean (SEM).

Data availability

The viruses included in this study are available under accession numbers MN954536, MN954537 and MN954539.

Results

Susceptibility and permissiveness of human immune cells to EV-D68 infections

To investigate whether human immune cell subsets are susceptible to EV-D68 infection, human peripheral blood mononuclear cells (PBMC) were inoculated with EV-D68 strains from subclades A, B2 and A2 (previously known as D). At 24 hpi, we detected EV-D68/A- (mean 3% ± standard error of mean (SEM) 0.9) and EV-D68/B2- (3% ± 0.7) but not for EV-D68/A2-infected cells, based on intracellular expression of EV-D68 capsid protein VP1. In two donors, 1% of monocytes were susceptible to infection with EV-D68/B2. We did not observe any $VP1^+$ cells in $CD4^+$ nor $CD8^+$ T cell population. (Fig 1A). Isotype controls were included, and to confirm that the VP1 signal that was detected was due to infection and not phagocytosis of the virus inoculum, heat-inactivated EV-D68/B2 was included as a control. We did not observe $VP1^+$ cells in cells inoculated with heat-inactivated virus (S1).

Next, we investigated whether EV-D68 inoculation of PBMC resulted in the production of progeny viruses. Supernatant and cell lysate were collected and the presence of infectious virus particles at 0, 6, 8, 10, 24, 48 and 72 hpi was determined by virus titration. Despite the presence of infected cells after inoculation with EV-D68/A or EV-D68/B2, we did not observe an increase in infectious virus titer at any time point (Fig 1B). As human PBMC consists only of 4 – 14% of B cells (29), of which ~3% were infected by EV-D68, we cannot exclude the possibility that the replication in $VP1^+$ B cells was below the detection limit of the assay.

In order to determine whether B cells are susceptible and permissive for EV-D68, we utilized two B cell-rich models. We first inoculated Epstein-Barr virus-transformed B-lymphoblastoid cell line (BLCL) with EV-D68 strains from subclades A, B2 and A2. The inoculation resulted in 13% ± 4 EV-D68/A, 18% ± 5 EV-D68/B2 and 21% ± 4 EV-D68/A2 $VP1^+$ cells, without significant differences among the subclades. Furthermore, we observed variation among donors in the percentage of infected cells (Fig 2A). Production of progeny viruses (~2 – 3 logarithmic increase of $TCID_{50}$/ml within 24 hours) was detected after inoculation with all three viruses, in which EV-D68/B2 and EV-D68/A2 replicated faster than EV-D68/A, albeit without any statistical differences (Fig 2B). Heat-inactivated viruses were included as controls. We did not observe $VP1^+$ cells in cells inoculated with heat-inactivated virus (S2).

To confirm the susceptibility and permissiveness of B cells, B cell clones were inoculated with EV-D68 strains from subclades A, B2 and A2. These cells originated from PBMC B cells and were lentivirus-transduced to express the germinal center-associated B cell lymphoma-6 (Bcl-6) and Bcl-xL in order to endow a stable proliferative state, thus representing germinal center B cells. This resulted in 11% ± 2 EV-D68/A, 27% ± 8 EV-D68/B2 and 14% ± 6 EV-D68/A2 $VP1^+$ cells (Fig 2C). The inoculation also resulted in

production of new infectious viruses (~2 – 3 logarithmic increase within 10 to 24 hours), without any statistical differences among the different EV-D68 subclades (Fig 2D).

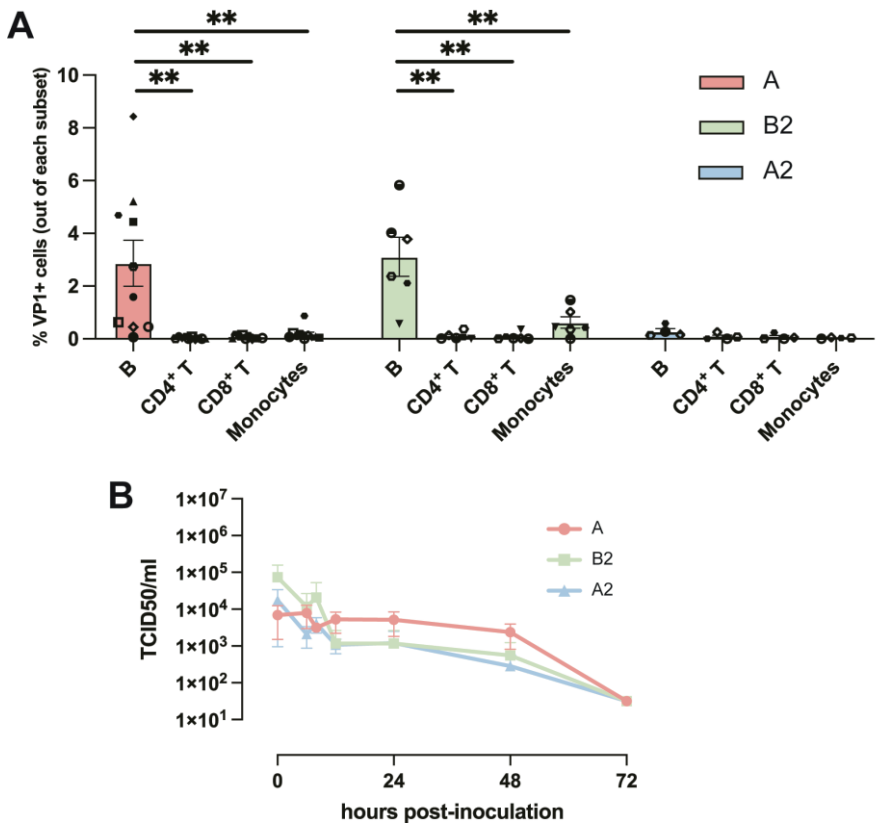

Fig 1. Susceptibility and permissiveness of human PBMC to EV-D68 infection. (A) Percentage of EV-D68 VP1⁺ immune cell subsets 24 h after inoculation with EV-D68 strains from subclades A (n = 10 donors), B2 (n = 6 donors) and A2 (n = 4 donors). Each symbol represents one donor. Statistical analysis was performed using unpaired t-test. Error bars denoted SEM. (B) Production of infectious virus in EV-D68-inoculated PBMC. PBMC: peripheral blood mononuclear cells; SEM: standard error of mean **: P<0.01.

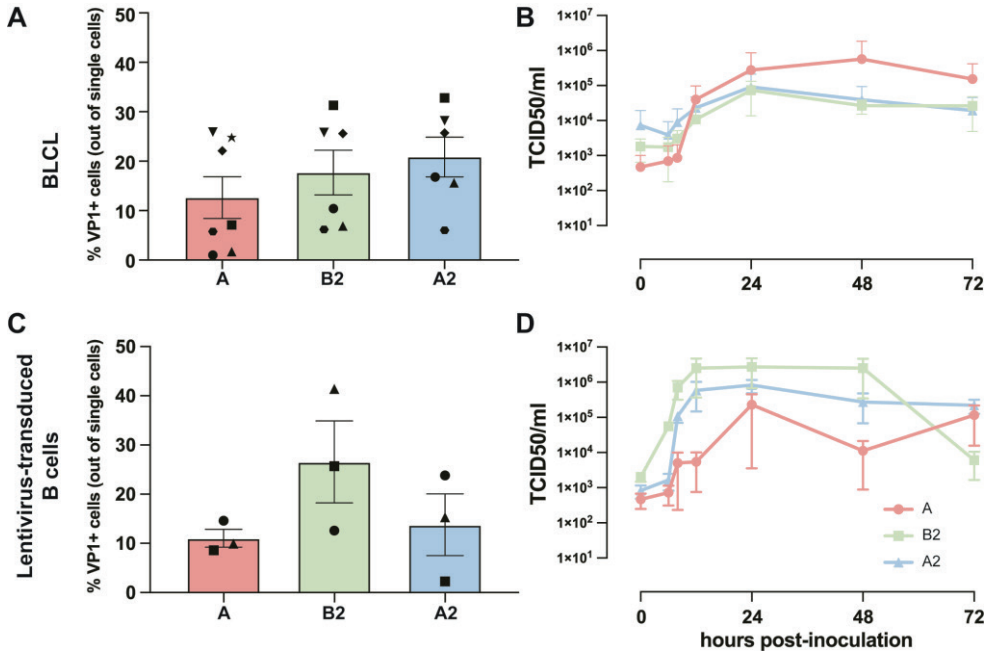

Fig 2. Susceptibility and permissiveness of B cell-rich models to EV-D68 infection. BLCL and lentivirus-transduced B cells were inoculated with EV-D68 strains from subclades A (n = 7), B2 (n = 6) and A2 (n = 6) as models for EV-D68 infection in B cell-rich environment. (A – B) Percentage of EV-D68 VP1⁺ cells at 24 hpi and production of infectious viruses in EV-D68-inoculated BLCL over time, respectively. (C – D) Percentage of VP1⁺ cells at 24 hpi and production of infectious viruses in EV-D68-inoculated lentivirus-transduced B-cells. Each symbol in (A) and (C) represents one donor. No statistically significant differences were observed in the percentages of VP1⁺ cells among the different virus subclades. Statistical analysis was performed using a one-way ANOVA with multiple comparison test. Error bars denote SEM. BLCL: B-lymphoblastoid cell line; hpi: hours post-inoculation; SEM: standard error of mean.

Infection of BLCL is largely mediated by the presence of α2,3- and α2,6-linked SAs

Several immune cells, including B cells, express α2,6-linked and α2,3-linked sialic acids (SAs), which can function as receptors for EV-D68 to initiate binding and virus entry (30-32). To investigate whether α2,3- and α2,6-linked SAs mediate EV-D68 infection of BLCL, cell surface SAs were removed by *Arthrobacter ureafaciens* neuraminidase (ANA) prior to inoculation with EV-D68 strains. Upon ANA treatment, the average percentages of α2,3-linked SA⁺ BLCL decreased from 77% ± 9 to 38% ± 3 and of α2,6-linked SA⁺ cells from 89% ± 1 to 5% ± 1 (Fig 3A). ANA treatment of BLCL prior to inoculation resulted in a significant decrease of VP1⁺ cells at 24 hpi, with only 2% ± 1 EV-D68/A, 5% ± 2 EV-D68/B2 and 5% ± 1 EV-D68/A2 VP1⁺ cells (Fig 3B).

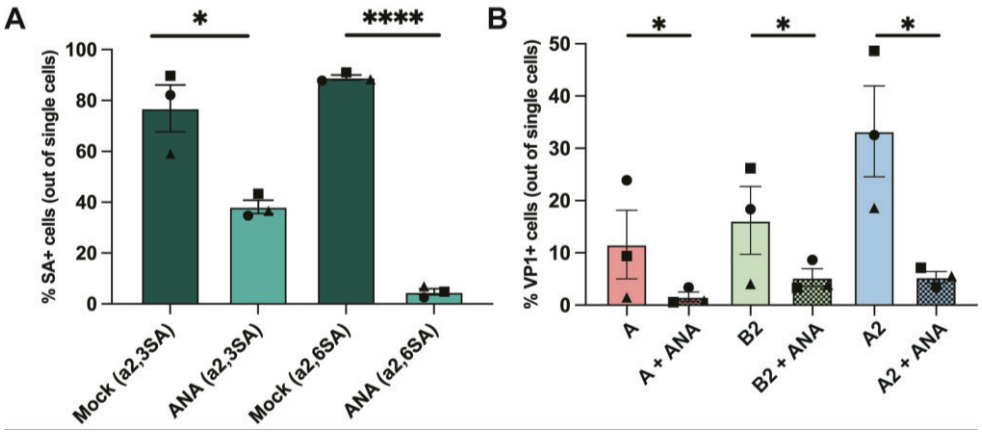

Fig 3. Percentages of α2,3-and α2,6-linked SAs⁺ and EV-D68 VP1⁺ BLCL upon neuraminidase treatment. (A) Percentage of BLCL expressed α2,3- (n=3) and α2,6- (n=3) linked SAs with and without ANA treatment. (B) Percentage of VP1⁺ BLCL (n=3) with and without ANA treatment inoculated with EV-D68 from subclades A, B2 and A2, measured 24 hpi. Statistical analysis was performed with unpaired t-test. Error bars denote SEM. BLCL: B-lymphoblastoid cell line. ANA: *Arthrobacter ureafaciens* neuraminidase; SAs: sialic acids; hpi: hours post-inoculation; SEM: standard error of mean. *: P<0.05; ****: P≤0.0001.

Dendritic cells (DCs) are susceptible and permissive to EV-D68 infection

Dendritic cells are a subset of immune cells that are attracted to sites of inflammation, but not abundantly present in PBMC (33). To investigate whether DCs are susceptible and permissive to EV-D68 infection, monocytes were differentiated in immature and mature DCs (imDCs and mDCs, respectively), and inoculated with EV-D68 strain from subclade A as a representative strain. Increased expression of maturation markers (HLA-DR, CD86, PD-L1 and CD83) was used to confirm differentiation of imDCs to mDCs (S3). The average percentage of VP1⁺ cells in imDCs (10% ± 1) was significantly higher than in mDCs (4% ± 1) at 6 hpi (Fig 4A). From 2 to 10 hpi, viral titers in the supernatants increased ~1 logarithmic $TCID_{50}$/ml in imDCs and ~0.5 logarithmic $TCID_{50}$/ml in mDCs inoculated with EV-D68/A, after which the virus titers decreased. Despite this decrease, at 48 hpi, virus titer in the supernatants of imDCs were significantly higher than in mDCs (Fig 4B).

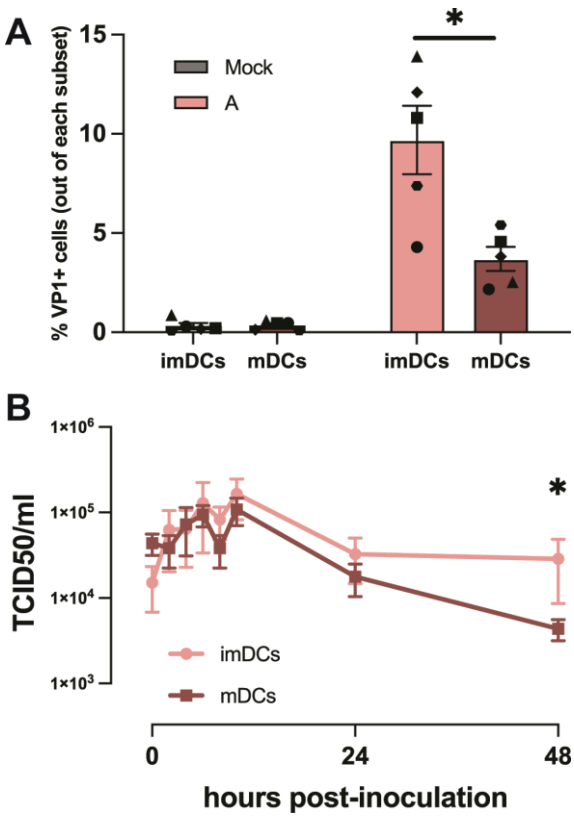

Fig 4. Susceptibility and permissiveness of imDCs and mDCs to EV-D68 infection. (A) Percentage of EV-D68 VP1⁺ imDCs (n = 5) and mDCs (n = 5) measured at 6 hpi. (B) Production of infectious viruses in EV-D68/A-inoculated imDCs (n = 3) and mDCs (n = 3). Samples for virus titration were collected at 0, 2, 4, 6, 8, 10, 24 and 48 hpi. All statistical analyses in this figure were performed with unpaired t-test. Error bars denote SEM. imDCs: immature dendritic cells; mDCs: mature dendritic cells; hpi: hours post-inoculation; SEM: standard error of mean. *: P<0.05.

imDCs can transfer EV-D68 to autologous BLCL

Dendritic cells are important for local antiviral responses and phagocytosis of viral antigens triggers DC migration to lymphoid tissues (33). Therefore, we investigated whether imDCs can transmit EV-D68 infection to B cells. EV-D68/A-inoculated imDCs were co-cultured with autologous BLCL (BLCL+DC), after which the percentages of $VP1^+$ BLCLs were determined. The following controls were included: (1) EV-D68/A-inoculated imDCs (DC only); (2) BLCL cultured with supernatant from EV-D68/A-inoculated imDCs collected at 0 hpi, directly after the virus inoculation for 1 hour and the subsequent washing steps (BLCL + t0 DC sup) and (3) BLCL cultured with supernatant collected around the peak of virus shedding (6 hpi) from EV-D68/A-inoculated imDCs (BLCL + t6 DC sup). The schematic representation of this experiment is presented in Fig 5A. As observed previously, inoculation of imDCs in the absence of their autologous BLCL resulted in an average of 11% ± 2 $VP1^+$ cells at 6 hpi and the percentage remained stable at 24 hpi. In imDCs co-cultured with BLCL, we observed an average percentage of 10% ± 4 $VP1^+$ imDCs at 6 hpi, although this percentage decreased at 24 hpi (4% ± 2) (Fig 5B). When BLCLs were inoculated with supernatants from EV-D68-inoculated imDCs collected at 0 or 6 hpi, only very few B cells were infected, with average percentages of 0.5% $VP1^+$ BLCLs in BLCL+t0 DC sup and 1% $VP1^+$ BLCLs in BLCL+t6 DC sup at 24 hpi. When BLCLs were co-cultured with EV-D68-inoculated imDCs, the percentage of infected BLCL increased from 2%±1 at 6 hpi to 6% ± 1 at 24 hpi (Fig 5C).

The inoculation of imDCs in the absence of BLCL resulted in production of new infectious virus particles (~1 logarithmic increase of $TCID_{50}$/ml) within 24 h. Detection of infectious virus particles in the supernatants of the BLCL+DC co-culture showed a stably higher virus titer (~1 – 1.5 logarithmic increase of $TCID_{50}$/ml) within the same period of time. Very few, if any, new infectious virus particles were produced by BLCL inoculated with t0 or t6 DC supernatants (Fig 5D). Statistical analysis was performed but there was no significant difference in virus titer at 0, 24 and 48 hpi. Together, the results suggested that imDCs might be capable to transmit virus to other susceptible immune cells, such as B cells, which subsequently become productively infected.

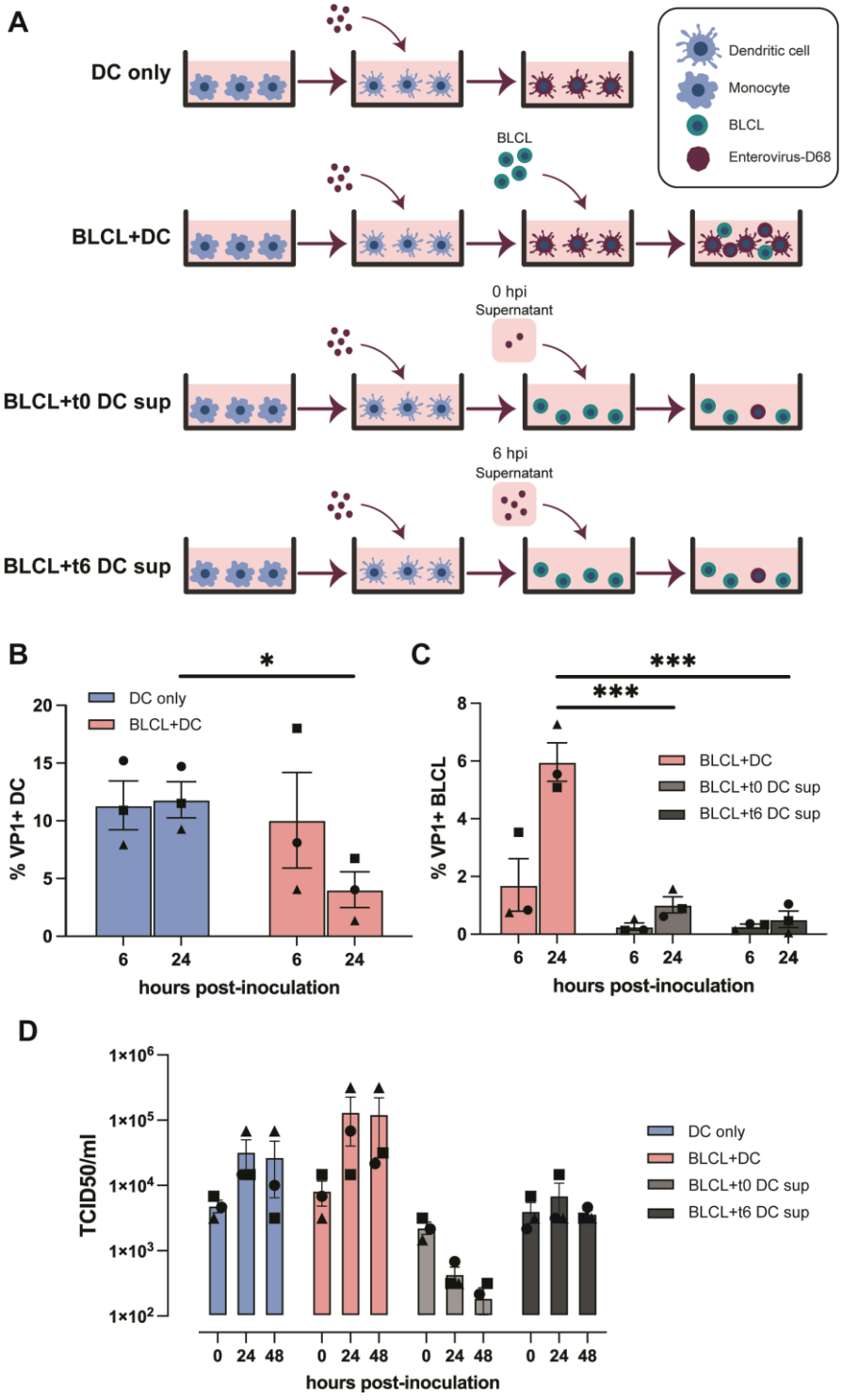
A
DC only
BLCL+DC
BLCL
0 hpi
Supernatant
BLCL+t0 DC sup
6 hpi
Supernatant
BLCL+t6 DC sup
Dendritic cell
Monocyte
BLCL
Enterovirus-D68
B
*
DC only
BLCL+DC
% VP1+ DC
20
15
10
5
0
6
24
6
24
hours post-inoculation
C
***
***
% VP1+ BLCL
8
6
4
2
0
BLCL+DC
BLCL+t0 DC sup
BLCL+t6 DC sup
6
24
6
24
6
24
hours post-inoculation
D
TCID50/ml
1×10^6
1×10^5
1×10^4
1×10^3
1×10^2
0
24
48
0
24
48
0
24
48
0
24
48
hours post-inoculation
DC only
BLCL+DC
BLCL+t0 DC sup
BLCL+t6 DC sup

Fig 5. Co-culture of EV-D68-inoculated imDCs with their autologous BLCL. (A) Schematic representation of the experimental setup and controls. (B) Percentages of EV-D68 VP1^{+} imDCs and (C) BLCL in different culture conditions at 6 and 24 hpi. (D) Production of infectious viruses in different culture conditions. Statistical analysis in (B) was performed with unpaired t-test. Statistical analysis in (C) and (D) were performed with a one-way ANOVA with multiple comparison test and compared to BLCL+t0 DC sup and BLCL+t6 sup, respectively. Error bars denote SEM. BLCL: B-lymphoblastoid cell line; imDCs: immature dendritic cells; hpi: hours post-inoculation; SEM: standard error of mean; BLCL+t0 DC sup: autologous BLCL co-cultured with supernatant collected from EV-D68/A-inoculated imDCs at 0 hpi. BLCL+t6 DC sup: autologous BLCL co-cultured with supernatant collected from EV-D68/A-inoculated imDCs at 6 hpi. *: P<0.05; ***: P≤0.001.

Discussion

The systemic dissemination of EV-D68 is an essential step for extra-respiratory spread of the virus and the development of associated complications, such as AFM. In this study, we reveal the potential role of immune cells in the systemic dissemination of EV-D68. We show that human B cells and DCs are susceptible and permissive to EV-D68 infection and that DCs may play a role in the transmission of virus to B cells.

Immune cells are susceptible to infection of other members of *Picornaviridae*. Coxsackievirus type B infects murine splenic B cells resulting in production of new virus particles (18), and poliovirus productively infects DCs and macrophages in vitro (human PBMC) and in vivo (non-human primates) (19, 20). Echoviruses and EV-A71 have also been reported to infect human imDCs and mDCs (21, 22). Here, we showed that human B cells and DCs are susceptible and permissive to EV-D68 infection, which fits with findings in a cohort study that detected enterovirus RNA in peripheral blood B cells and DCs (34). In B cells, this tropism is facilitated by the presence of α2,6- and/or α2,3-linked SAs. Productive infection was only detected in more activated B cell populations, *i.e.* BLCLs and lentivirus-transduced B cells, of which the latter resembles activated germinal center B cells (35). In addition, we observed that imDCs were more susceptible and permissive to EV-D68 infection than mDCs. It is possible that the different susceptibility to EV-D68 infection between imDCs and mDCs is due to the higher expression of α2,6-linked SA on imDCs than mDCs (36). It is also likely that the activation or maturation state of immune cells plays an important role in the susceptibility for EV-D68 infection. This has been shown for other enteroviruses, where activated and/or immortalized B cells were more susceptible to CVB3 infection than primary immune cells, and imDCs were more susceptible to poliovirus infection than mDCs (19, 37). As for the permissiveness to EV-D68 infection, or enteroviruses in general, metabolic activity of different immune cell subtypes may play a role and therefore requires further investigation.

We observed differences in the susceptibility and permissiveness to EV-D68 infection among viruses or donors included in this study. Differences in the susceptibility to different EV-D68 subclades were observed in B cells within the PBMCs, but this was not observed in BLCLs and lentivirus-transduced B cells. Donor variation was observed in

PBMCs and all B cell models, and in two PBMC donors, we observed a low percentage of EV-D68/B2-infected monocytes. The underlying mechanism for these differences among donors and possibly among different virus subclades, as well as their association with the risk of the development of extra-respiratory diseases, are still unclear.

Virus replication within immune cells and/or lymphoid tissues is likely important for the development of a viremia. Due to the susceptibility and permissiveness of immune cells to EV-D68 infection, an immune cell-rich environment, such as a lymphoid tissue, can serve as a secondary replication site for EV-D68, from where the virus can spread into the circulation. Since poliovirus viremia is essential for virus spread to the CNS and the subsequent development of poliomyelitis (38), it can be speculated that EV-D68 viremia is essential for virus entry into the CNS and the subsequent development of AFM (4, 13). In addition, a viremia could lead to virus spread to other organ system contributing to non-neurological complications associated with EV-D68 infection, including acute gastroenteritis, myocarditis and skin rash (39-41). Prevention of spread to, or productive infection of lymphoid tissues may prevent systemic dissemination, as observed in poliovirus infection, in which vaccination prevents viral spread to other organs (42).

Based on our findings, we propose a model that explains the systemic dissemination of EV-D68 (Fig 6). EV-D68 infects respiratory epithelial cells, which results in the production of infectious virus particles and the recruitment of immune cells, such as imDCs. From the respiratory tract, cell-free virus can spill over into the circulatory and lymphatic systems and spread into lymphoid tissues. Alternatively, imDCs can become infected, and migrate to the lymphoid tissues, where they release newly produced viruses or spread virus to resident DCs or B cells. Lymphoid tissues can be the secondary replication site for EV-D68, from where the virus is released in the bloodstream. Prevention of virus spread to and amplification in lymphoid tissues can therefore prevent the development of a subsequent viremia and severe extra-respiratory complications caused by EV-D68.

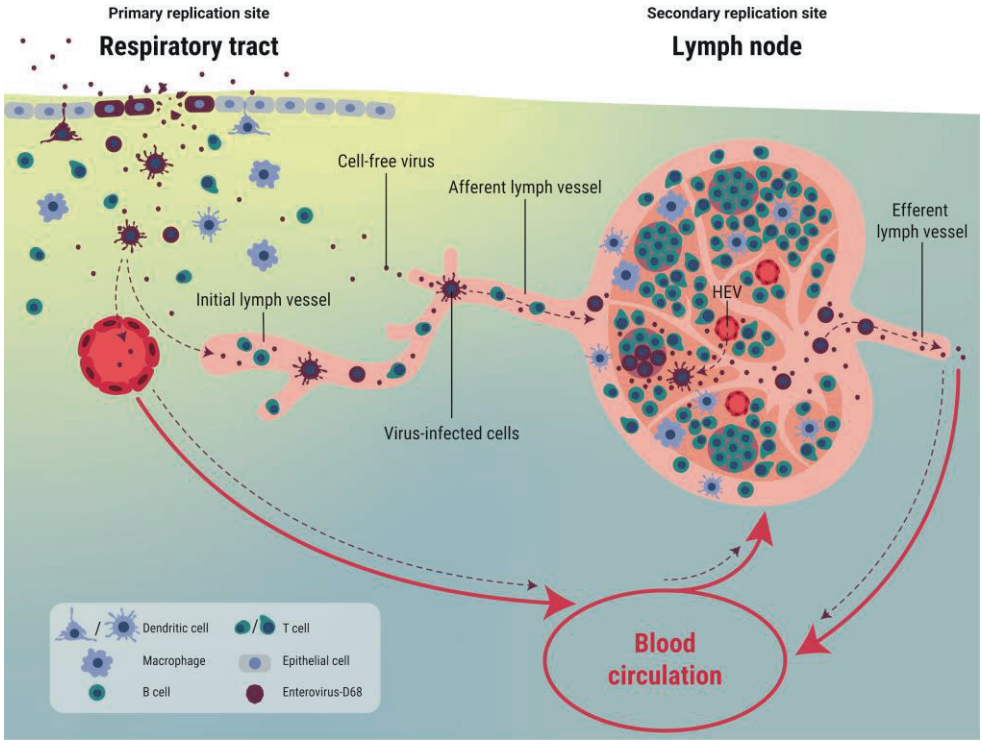

Fig 6. Proposed model for systemic dissemination of EV-D68. EV-D68 enters the respiratory tract and initially infects respiratory epithelial cells. The infection will result in the recruitment of immune cells, including imDCs. Subsequently, cell-free EV-D68 can spread to lymphoid tissues by spilling over into the circulatory or lymphatic system. Alternatively, it can infect imDCs, which can transfer the virus to lymphoid tissues. These lymphoid tissues can function as a secondary replication site, where EV-D68 infects mDCs and B cells. From this site, cell-free virus or virus-infected immune cells can enter the blood circulation and spread virus to other tissues. HEV: high endothelial venule. Red arrow: blood circulation; purple dotted arrow: potential routes of EV-D68 spread.

Funding

This work was funded by a fellowship to DvR from the Netherlands Organization for Scientific Research (VIDI contract 91718308). SSNA received the Royal Thai Government Scholarship supported by the Ministry of Science and Technology of Thailand to perform her doctoral study. GPvN received financial supports from the European Union's Horizon 2020 research and innovation program under grant agreements no. 874735 (VEO) and no. 101003589 (RECoVER), and the Dutch Research Council (NWO) project no. 109986 (One Health Pact). The funders had no role in study design, data collection and analysis, decision to publish or preparation of the manuscript.

Acknowledgment

The authors would like to thank Nuder Nizam, Thomas Langerak, Lisa Bauer, Feline Benavides, Lonneke Leijten, Daryl Geers, Laurine Rijsbergen and Rik de Swart for technical assistance, Adam Meijer for providing the virus isolates, and Rory de Vries for helpful discussion.

Supplementary Information

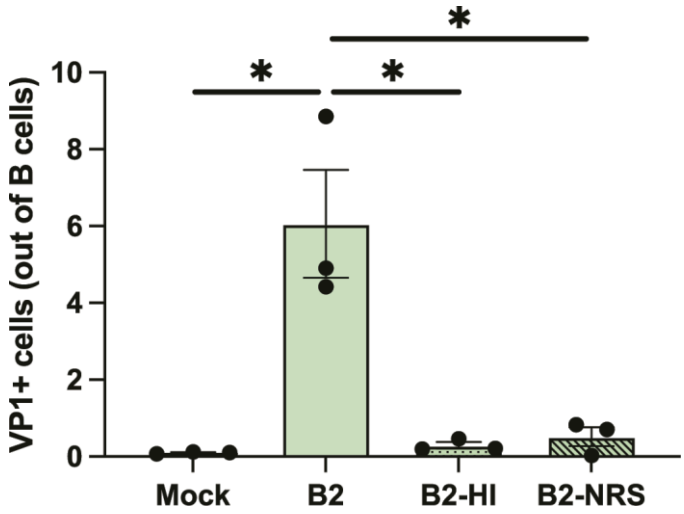

S1. Heat-inactivated virus and isotype controls for the inoculation of PBMC with EV-D68/B2. Inoculation of PBMCs with EV-D68/B2, but not with heat-inactivated EV-D68/B2 (B2-HI), results in detection of $VP1^+$ signal in B cells. EV-D68/B2-inoculated PBMC were incubated with normal rabbit serum (B2-NRS) as a staining isotype control. Statistical analysis was performed with unpaired t-test. *: P<0.05

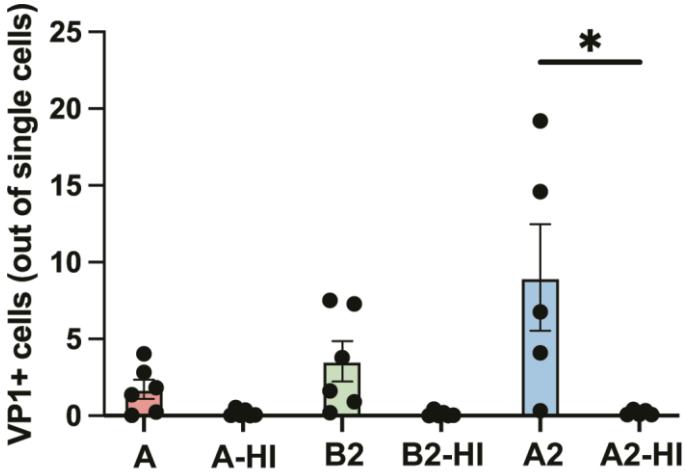

S2. Heat-inactivated virus controls for the inoculation of BLCL with EV-D68. BLCL were inoculated with EV-D68/A (n = 4), EV-D68/B2 (n = 4), EV-D68/A2 (n = 5) and their heat-inactivated counterparts (A-HI, B2-HI and A2-HI). $VP1^+$ cells were only detected in cells inoculated with virus, and not when BLCLs were inoculated with heat-inactivated virus. Statistical analysis was performed with unpaired t-test. *: P<0.05

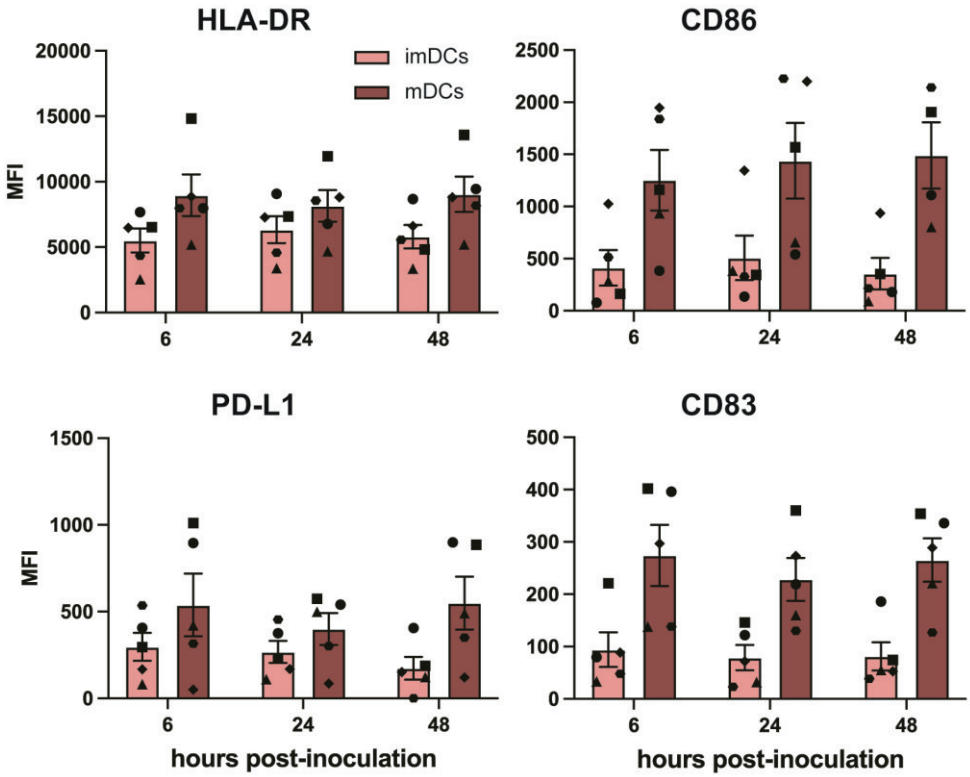

S3. The expression of dendritic cell maturation markers in immature and mature dendritic cells (imDCs and mDCs). mDCs were defined by the upregulation of surface HLA-DR, CD86, PD-L1 and CD83 after treatment of monocyte-derived imDCs with lipopolysacharride. Each symbol represents one donor. Error bars denote standard error of mean. MFI: median fluorescence intensity.

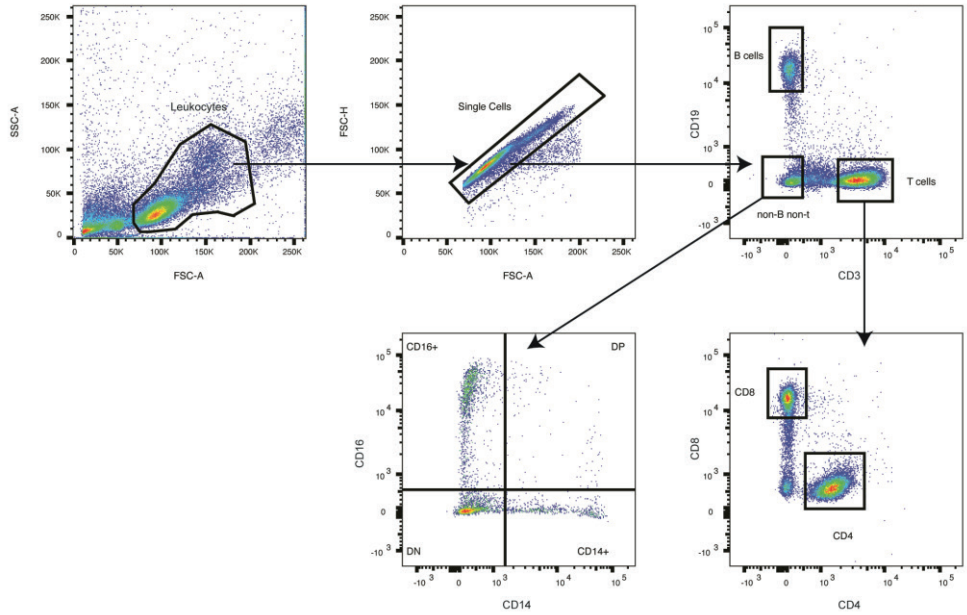

S4. Representative gating strategy for peripheral blood mononuclear cell subpopulations. B cells were defined as $CD3^{-}CD19^{+}$ cells; $CD4^{+}$T cells as $CD3^{+}CD19^{-}CD4^{+}CD8^{-}$ cells; $CD8^{+}$T cells as $CD3^{+}CD19^{-}CD4^{-}CD8^{+}$ cells; and monocytes as $CD3^{-}CD19^{-}CD14^{-/+}CD16^{-/+}$ cells.

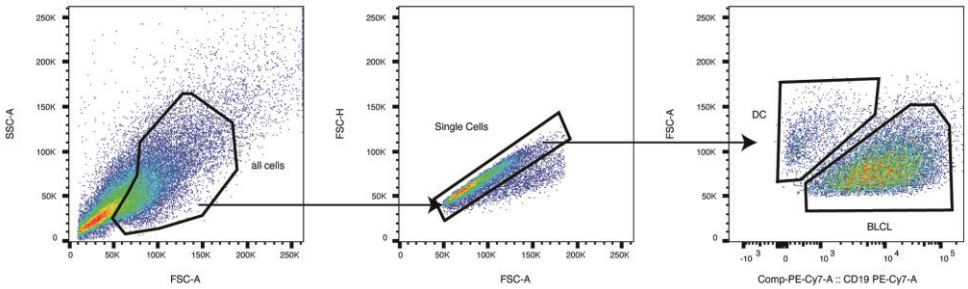

S5. Representative gating strategy for EV-D68-inoculated immature dendritic cells (imDCs) co-cultured with autologous B-lymphoblastoid cell line (BLCL). imDCs were defined as $CD19^{-}$ cells; BLCL were defined as $CD19^{+}$ cells.

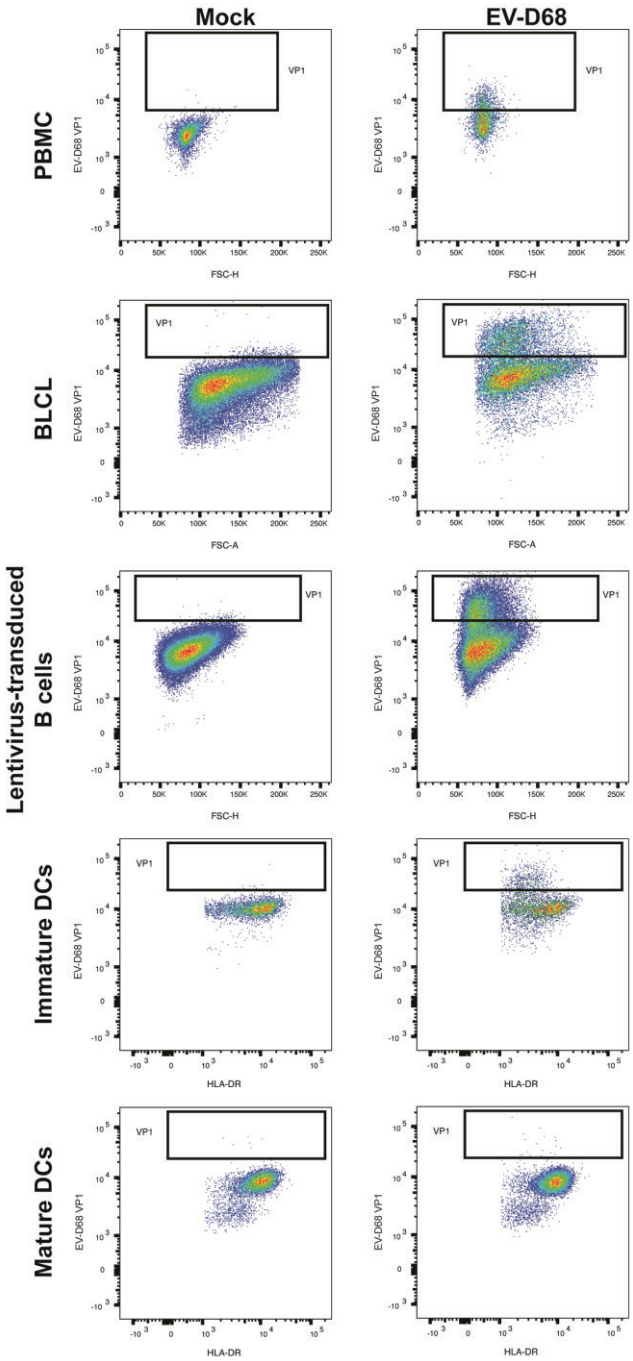

S6. Representative gating strategies for EV-D68 VP1⁺ cells. PBMC: peripheral blood mononuclear cells; BLCL: B-lymphoblastoid cell line; DCs: dendritic cells.

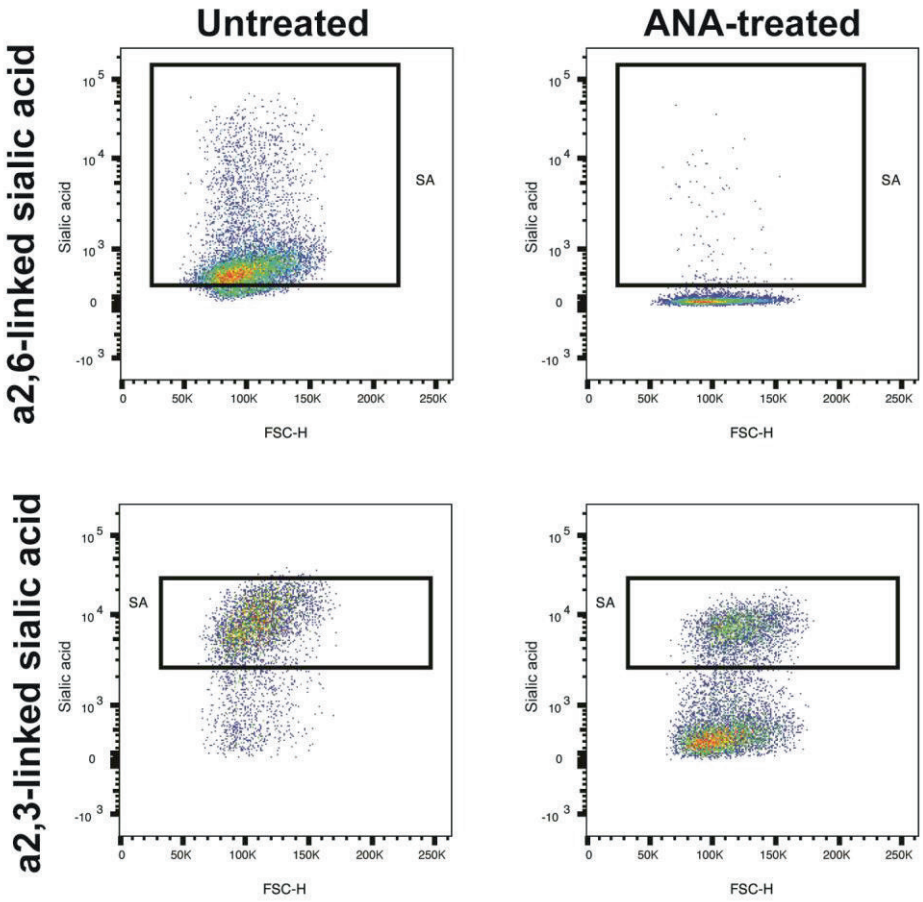

S7. Representative gating strategy to determine percentages of α2,3- and α2,6-linked sialic acid$^+$ (SAs$^+$) BLCL. Percentages of SA$^+$ cells were determined at 0 h post-inoculation. ANA: *Arthrobacter ureafaciens* neuraminidase; BLCL: B-lymphoblastoid cell line.

References

1. Greninger AL, Naccache SN, Messacar K, Clayton A, Yu G, Somasekar S, et al. A novel outbreak enterovirus D68 strain associated with acute flaccid myelitis cases in the USA (2012-14): a retrospective cohort study. Lancet Infect Dis. 2015;15(6):671-82.
2. Messacar K, Abzug MJ, Dominguez SR. The Emergence of Enterovirus-D68. Microbiol Spectr. 2016;4(3).
3. Messacar K PK, Reno S, Dominguez SR. Continued biennial circulation of enterovirus D68 in Colorado. J Clin Virol. 2019;113:24-6.
4. Messacar K, Schreiner TL, Van Haren K, Yang M, Glaser CA, Tyler KL, et al. Acute flaccid myelitis: A clinical review of US cases 2012-2015. Ann Neurol. 2016;80(3):326-38.
5. Kramer R, Sabatier M, Wirth T, Pichon M, Lina B, Schuffenecker I, et al. Molecular diversity and biennial circulation of enterovirus D68: a systematic screening study in Lyon, France, 2010 to 2016. Euro Surveill. 2018;23(37).
6. Ma KC, Winn A, Moline HL, Scobie HM, Midgley CM, Kirking HL et al. Increase in Acute Respiratory Illnesses Among Children and Adolescents Associated with Rhinoviruses and Enteroviruses, Including Enterovirus D68 — United States, July–September 2022. MMWR Morb Mortal Wkly Rep. 2022; 7;71(40):1265-1270.
7. Benschop KS, Albert J, Anton A, Andres C, Aranzamendi M, Armannsdottir B, et al. Re-emergence of enterovirus D68 in Europe after easing the COVID-19 lockdown, September 2021. Euro Surveill. 2021;26(45).
8. Wang G, Zhuge J, Huang W, Nolan SM, Gilrane VL, Yin C, et al. Enterovirus D68 Subclade B3 Strain Circulating and Causing an Outbreak in the United States in 2016. Sci Rep. 2017;7(1):1242.
9. Yip CCY LJ, Sridhar S, Lung DC, Luk S, Chan KH et al. First Report of a Fatal Case Associated with EV-D68 Infection in Hong Kong and Emergence of an Interclade Recombinant in China Revealed by Genome Analysis. Int J Mol Sci. 2017;16(18).
10. Evans WJ, Hurst BL, Peterson CJ, Van Wettere AJ, Day CW, Smee DF, et al. Development of a respiratory disease model for enterovirus D68 in 4-week-old mice for evaluation of antiviral therapies. Antiviral Res. 2019;162:61-70.
11. Zhang C, Zhang X, Dai W, Liu Q, Xiong P, Wang S, et al. A Mouse Model of Enterovirus D68 Infection for Assessment of the Efficacy of Inactivated Vaccine. Viruses. 2018;10(2).
12. Zheng HW, Sun M, Guo L, Wang JJ, Song J, Li JQ, et al. Nasal Infection of Enterovirus D68 Leading to Lower Respiratory Tract Pathogenesis in Ferrets (Mustela putorius furo). Viruses. 2017;9(5).
13. Esposito S, Chidini G, Cinnante C, Napolitano L, Giannini A, Terranova L, et al. Acute flaccid myelitis associated with enterovirus-D68 infection in an otherwise healthy child. Virol J. 2017;14(1):4.
14. Justin D. Kreuter M, Arti Barnes M, James E. McCarthy M, Joseph D. Schwartzman M, M. Steven Oberste P, C. Harker Rhodes P, MD; , et al. A fatal CNS EV68 infection. Arch Pathol Lab Med2011.
15. Kusabe Y, Takeshima A, Seino A, Nishida M, Takahashi M, Yamada S, et al. [An Adult Case of Enterovirus D68 Encephalomyelitis Presenting as Bilateral Facial Nerve Palsy and Dysphagia]. Brain Nerve. 2017;69(8):957-61.

16. Chong PF, Kira R, Mori H, Okumura A, Torisu H, Yasumoto S, et al. Clinical Features of Acute Flaccid Myelitis Temporally Associated With an Enterovirus D68 Outbreak: Results of a Nationwide Survey of Acute Flaccid Paralysis in Japan, August-December 2015. Clin Infect Dis. 2018;66(5):653-64.
17. Imamura T, Suzuki A, Lupisan S, Kamigaki T, Okamoto M, Roy CN, et al. Detection of enterovirus 68 in serum from pediatric patients with pneumonia and their clinical outcomes. Influenza Other Respir Viruses. 2014;8(1):21-4.
18. Mena I, Perry CM, Harkins S, Rodriguez F, Gebhard J, Whitton JL. The role of B lymphocytes in coxsackievirus B3 infection. Am J Pathol. 1999;155(4):1205-15.
19. Wahid R, Cannon MJ, Chow M. Dendritic Cells and Macrophages Are Productively Infected by Poliovirus. Journal of Virology. 2005;79(1):401-9.
20. Shen L, Chen CY, Huang D, Wang R, Zhang M, Qian L, et al. Pathogenic Events in a Nonhuman Primate Model of Oral Poliovirus Infection Leading to Paralytic Poliomyelitis. J Virol. 2017;91(14).
21. Kramer M, Schulte BM, Toonen LW, de Bruijni MA, Galama JM, Adema GJ, et al. Echovirus infection causes rapid loss-of-function and cell death in human dendritic cells. Cell Microbiol. 2007;9(6):1507-18.
22. Lin YW, Wang SW, Tung YY, Chen SH. Enterovirus 71 infection of human dendritic cells. Exp Biol Med (Maywood). 2009;234(10):1166-73.
23. Racaniello VR. One hundred years of poliovirus pathogenesis. Virology. 2006;344(1):9-16.
24. Solomon T, Lewthwaite P, Perera D, Cardosa MJ, McMinn P, Ooi MH. Virology, epidemiology, pathogenesis, and control of enterovirus 71. Lancet Infect Dis. 2010;10(11):778-90.
25. Zhao T, Zhang Z, Zhang Y, Feng M, Fan S, Wang L, et al. Dynamic Interaction of Enterovirus 71 and Dendritic Cells in Infected Neonatal Rhesus Macaques. Front Cell Infect Microbiol. 2017;7:171.
26. Xing J, Wang K, Wang G, Li N, Zhang Y. Recent advances in enterovirus A71 pathogenesis: a focus on fatal human enterovirus A71 infection. Arch Virol. 2022.
27. He Y, Ong KC, Gao Z, Zhao X, Anderson VM, McNutt MA, et al. Tonsillar crypt epithelium is an important extra-central nervous system site for viral replication in EV71 encephalomyelitis. Am J Pathol. 2014;184(3):714-20.
28. Smura T, Ylipaasto P, Klemola P, Kaijalainen S, Kyllonen L, Sordi V, et al. Cellular tropism of human enterovirus D species serotypes EV-94, EV-70, and EV-68 in vitro: implications for pathogenesis. J Med Virol. 2010;82(11):1940-9.
29. Laksono BM, Grosserichter-Wagener C, de Vries RD, Langeveld SAG, Brem MD, van Dongen JJM, et al. In Vitro Measles Virus Infection of Human Lymphocyte Subsets Demonstrates High Susceptibility and Permissiveness of both Naive and Memory B Cells. J Virol. 2018;92(8).
30. Sakabe S, Iwatsuki-Horimoto K, Takano R, Nidom CA, Le MTQ, Nagamura-Inoue T, et al. Cytokine production by primary human macrophages infected with highly pathogenic H5N1 or pandemic H1N1 2009 influenza viruses. J Gen Virol. 2011;92(Pt 6):1428-34.

31. Videira PA, Amado IF, Crespo HJ, Algueró MC, Dall'Olio F, Cabral MG, et al. Surface alpha 2-3- and alpha 2-6-sialylation of human monocytes and derived dendritic cells and its influence on endocytosis. Glycoconj J. 2008;25(3):259-68.
32. Eash S, Tavares R, Stopa EG, Robbins SH, Brossay L, Atwood WJ. Differential distribution of the JC virus receptor-type sialic acid in normal human tissues. Am J Pathol. 2004;164(2):419-28.
33. Cao W, Liu YJ. Innate immune functions of plasmacytoid dendritic cells. Curr Opin Immunol. 2007;19(1):24-30.
34. Sioofy-Khojine AB, Richardson SJ, Locke JM, Oikarinen S, Nurminen N, Laine AP, et al. Detection of enterovirus RNA in peripheral blood mononuclear cells correlates with the presence of the predisposing allele of the type 1 diabetes risk gene IFIH1 and with disease stage. Diabetologia. 2022.
35. Kwakkenbos MJ, Diehl SA, Yasuda E, Bakker AQ, van Geelen CM, Lukens MV, et al. Generation of stable monoclonal antibody-producing B cell receptor-positive human memory B cells by genetic programming. Nat Med. 2010;16(1):123-8.
36. Jenner J, Kerst G, Handgretinger R, Muller I. Increased alpha2,6-sialylation of surface proteins on tolerogenic, immature dendritic cells and regulatory T cells. Exp Hematol. 2006;34(9):1212-8.
37. Vuorinen T, Vainionpää R, Kettinen H, Hyypiä T. Coxsackievirus B3 infection in human leukocytes and lymphoid cell lines. Blood. 1994;84(3):823-9.
38. Horstmann DM. Poliomyelitis virus in blood of orally infected monkeys and chimpanzees. Proc Soc Exp Biol Med. 1952;79(3):417-9.
39. Pham NTK, Thongprachum A, Baba T, Okitsu S, Trinh QD, Komine-Aizawa S, et al. A 3-Month-Old Child with Acute Gastroenteritis with Enterovirus D68 Detected from Stool Specimen. Clin Lab. 2017;63(7):1269-72.
40. Antona D, Kossorotoff M, Schuffenecker I, Mirand A, Leruez-Ville M, Bassi C, et al. Severe paediatric conditions linked with EV-A71 and EV-D68, France, May to October 2016. Eurosurveillance. 2016;21(46):11-4.
41. Chang TH, Yang TI, Hsu WY, Huang LM, Chang LY, Lu CY. Case report: painful exanthems caused by enterovirus D68 in an adolescent. Medicine (Baltimore). 2019;98(33):e16493.
42. Zhu Q, Berzofsky JA. Oral vaccines: directed safe passage to the front line of defense. Gut Microbes. 2013;4(3):246-52.
43. van Binnendijk RS, Poelen MC, de Vries P, Voorma HO, Osterhaus AD, Uytdehaag FG. Measles virus-specific human T cell clones. Characterization of specificity and function of CD4+ helper/cytotoxic and CD8+ cytotoxic T cell clones. J Immunol. 1989;142(8):2847-54.
44. Wang Y, Wang F, Wang R, Zhao P, Xia Q. 2A self-cleaving peptide-based multi-gene expression system in the silkworm Bombyx mori. Sci Rep. 2015;5:16273.
45. Atkinson GF. The Spearman-Karber Method of Estimating 50% Endpoints. Cornell University. Dept. of Biometrics.: Biometrics Unit Technical Reports;; 1961. Contract No.: BU-141-M.

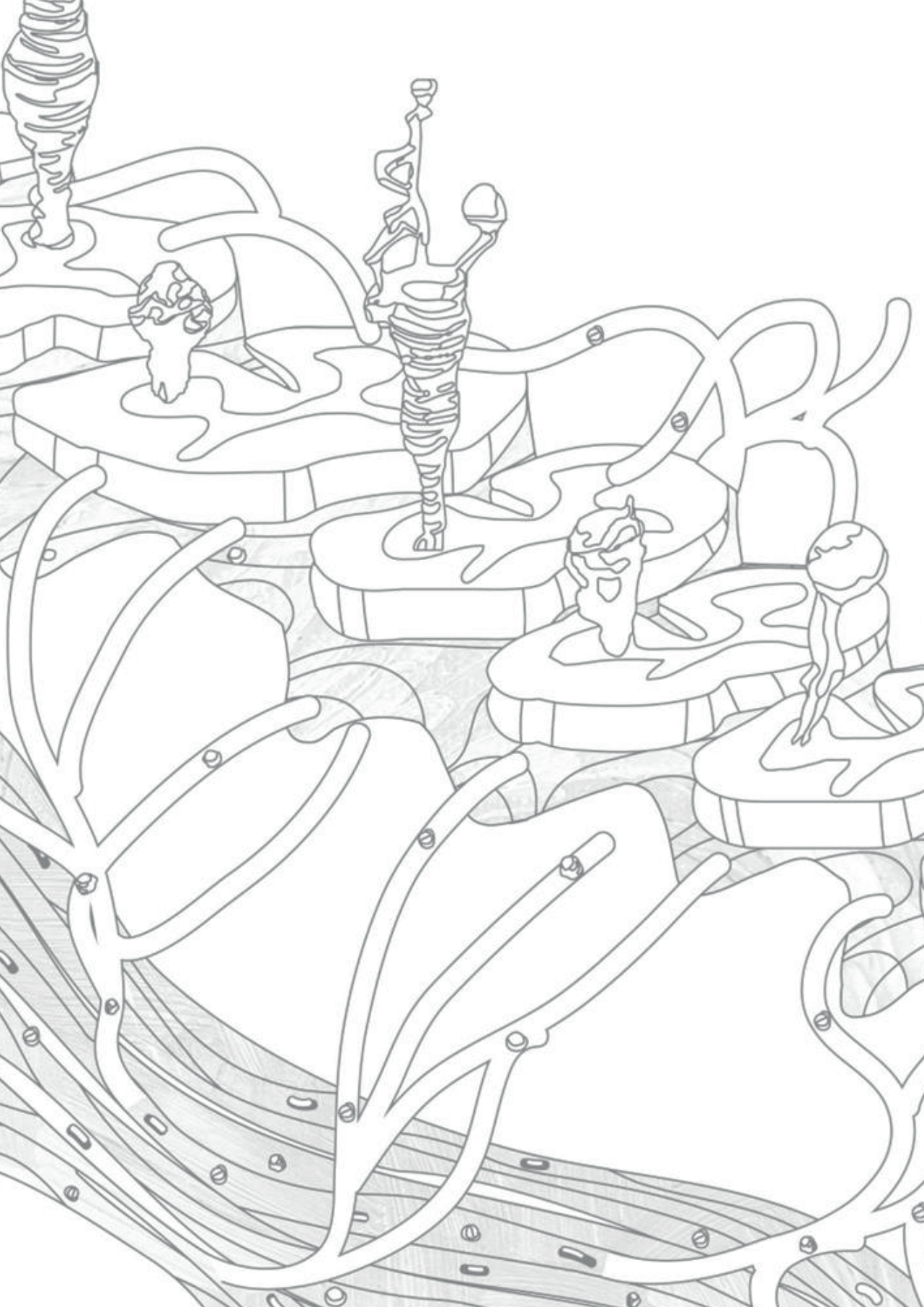

Chapter

3

Enhanced enterovirus D68 replication in neuroblastoma cells is associated with a cell culture adaptive amino acid substitution in VP1

Syriam Sooksawasdi Na Ayudhya, Adam Meijer, Lisa Bauer, Bas Oude Munnink, Carmen W.E. Embregts, Lonneke Leijten, Jurre Y. Siegers, Brigitta M. Laksono, Frank van Kuppeveld, Thijs Kuiken, Corine H. GeurtsvanKessel, Debby van Riel

msphere.2020 Nov 4;5(6):e00941-20

Abstract

Since the emergence in the United States in 2014, Enterovirus D68 (EV-D68) has been associated with severe respiratory diseases and acute flaccid myelitis. Even though EV-D68 has been shown to replicate in different neuronal cells in vitro, it is currently poorly understood which viral factors contribute to the ability to replicate efficiently in cells of the central nervous system and whether this feature is a clade specific feature. Here, we determined the replication kinetics of clinical EV-D68 isolates from (sub)clade A, B1, B2, B3 and D1 in human neuroblastoma cells (SK-N-SH). Subsequently, we compared sequences to identify viral factors associated with increased viral replication. All clinical isolates replicated in SK-N-SH cells, although there was a large difference in efficiency. Efficient replication of clinical isolates was associated with an amino acid substitution at position 271 of VP1 (E271K), which was acquired during virus propagation in vitro. Viruses with recognized heparan sulfate in addition to sialic acids, which was associated with increased attachment, infection and replication. Removal of heparan sulfate resulted in a decrease in attachment, internalization and replication of viruses with E271K. Taken together, our study suggests that the replication kinetics of EV-D68 isolates in SK-N-SH cells is not a clade specific feature. However, recognition of heparan sulfate as an additional receptor had a large effect on phenotypic characteristic in vitro. These observations emphasize the need to compare sequences from virus stocks with clinical isolates in order to retrieve phenotypic characteristics from original virus isolates.

Importance

Enterovirus D68 (EV-D68) causes mild to severe respiratory disease associated with acute flaccid myelitis since 2014. Currently, the understanding of the ability of EV-D68 to replicate in the central nervous system (CNS), and whether it is associated with a specific clade of EV-D68 viruses or specific viral factors is lacking. Comparing difference EV-D68 clades did not reveal clade specific phenotypic characteristics. However, we did show that viruses which acquired a cell culture adapted amino acid substitution in VP1 (E271K), recognized heparan sulfate as an additional receptor. Recognition of heparan sulfate resulted in an increase in attachment, infection and replication in neuroblastoma cells compared with viruses without this specific amino acid substitution. The ability of EV-D68 viruses to acquire cell-culture adaptive substitution which have a large effect in experimental settings emphasizes the need to sequence virus stocks.

Introduction

Enterovirus D68 (EV-D68) is known to cause mild to severe respiratory infections, but since 2014 it has been increasingly associated with neurological complications (1-3). After its discovery in 1962, cases were only sporadically reported (4). EV-D68 caused a large outbreak of severe respiratory disease across the U.S. of which about 10.4 % of symptomatic cases developed acute flaccid myelitis (AFM) from August 2014 to January 2015 (5). During this outbreak, more than 2,000 cases of EV-D68 infections were reported in 20 countries (6-9) of which about 7% of symptomatic cases developed acute flaccid myelitis (AFM) (10). Other neurological complications like cranial nerve dysfunction and encephalitis were occasionally reported (11-13). Since then, biennial epidemics of EV-D68 globally occur with the largest epidemic in 2018 (14-17).

EV-D68 belongs to the Enterovirus genus in the *Picornaviridae* family. It is a non-enveloped, positive-sense, single-stranded RNA virus. Within the capsid, the structural protein VP1 plays an important role in the attachment to host cells, and its gene is the most variable part of the genome and used for genotyping (18). Circulating EV-D68 isolates use cell surface glycoproteins including sialylated glycoproteins or glycolipid as a receptor. These sialylated receptors bind to the canyon in VP1 which leads to conformational change, subsequent dysregulation of stability and thereby initiates uncoating (19). However, recent studies have identified non-sialylated receptors, such as ICAM-5 and heparan sulfate glycosaminoglycans (GAGs), for specific EV-D68 isolates (20, 21).

To date, EV-D68 is divided in four clades, from A to D, although the initial division in three clades A, B and C with subclades A1 and A2 is also being used. Some researchers use A for A1 and D for A2 (22, 23). EV-D68 clade B is subdivided in subclades B1, B2 and B3 (24), and clade D has recently been subdivided in subclade D1 and D2 (25). Multiple clades circulated during the 2014 outbreak, but subclade B1 was the most prevalent and was also associated with neurological complications. Based on this observation, it was initially thought that the ability to invade and replicate in the central nervous system (CNS) was a recently acquired feature and clade specific (2, 3, 8, 10, 26). However, since 2016, subclade B3 and to a lesser extent subclade D1 became predominant and both were associated with neurological complications (27-30). In addition, recent studies have shown that multiple isolates from different clades are able to infect both neuronal cells and neuroblastoma cell lines (31), and that non-subclade B1 and B3 isolates were able to cause paralysis in mice after intracranial inoculation. Interestingly, isolates from the same clade differed in their ability to cause paralysis in mice (32). Altogether, this suggests that the ability to invade and replicate in the CNS is not a clade-specific feature. Even though several studies have determined the in vitro phenotypic characteristics of EV-D68 isolates in cells of the CNS, viral factors associated with efficient attachment, infection and replication have not been identified yet. In addition, genetic analysis of EV-D68 isolates associated with phenotypic characteristics in vitro have not been determined in previous studies.

In this study, we investigated the ability of EV-D68 isolates from different clades to attach and infect human neuroblastoma cells (SK-N-SH) and determined their replication kinetics. Subsequently, we compared viral sequences in order to identify viral factors associated with increased viral replication.

Materials and methods

Cells

Rhabdomyosarcoma (RD cells) (ATCC) were maintained in Dulbecco's Modified Eagle Medium (DMEM; Lonza, Basel, Switzerland) supplemented with 10% (v/v) fetal calf serum (FCS; Sigma-Aldrich, St. Louis,MO, USA), 100 IU/ml penicillin (Lonza), 100 IU/ml streptomycin (Lonza), 2 mM L-glutamine (Lonza), at 37°C with 5% CO_2. Neuroblastoma cells SK-N-SH (Sigma-Aldrich) were maintained in Eagle's Minimum Essential Medium (EMEM) and Earle's Balanced Salt Solution (EBSS) (Lonza), 10% (v/v) FCS, 100 IU/ml penicillin (Lonza), 100 µg/ml streptomycin (Lonza), 2 mM L-glutamine (Lonza), 1% nonessential amino acids (Lonza), 1 mM sodium pyruvate (Thermo Fisher Scientific, Waltham, MA, USA), and 1.5 mg/ml sodium bicarbonate (Lonza), at 37°C with 5% CO_2. All SK-N-SH cells used in the study were from the same batch and maintained up to 15 passages.

Viruses

Enterovirus D68 included in this study were isolated from clinical specimens at the National Institute of Public Health and the Environment (RIVM), Bilthoven, The Netherlands. The viruses were initially isolated on RD cells at 33°C at RIVM from patients with respiratory disease caused by EV-D68 infection. Virus stocks for the *in vitro* studies were grown at Viroscience laboratory, EMC, Rotterdam, The Netherlands in RD cells (ATCC) at 33°C in 5% CO_2. The viruses included in this study, with virus reference number, year of collection and isolation, passage number and accession number; clade A (or A1) (4311200821; 2012, passage RD3, accession number MN954536) (46), D subclade D1 (or A2) (4311400720; 2014, passage RD4, accession number MN954537) (46), B1 (4311300117; 2013, passage RD4, accession number MN954538 (46), B2/039 (4311201039; 2012, passage RD3, accession number MN954539) (46), B2/947 (4310900947; 2009, passage RD4, accession number MN954540 (19, 47)and B3 (4311601013; 2016, passage RD4, accession number MN954541). EV-D68 prototype Fermon were provided by Prof. Frank van Kupperveld, Utrecht University, Utrecht, The Netherlands.

Virus titrations

Virus titers (median tissue culture infectious dose, TCID50) of the virus stocks were determined by endpoint titrations in RD cells. Briefly, ten-fold serial dilutions were made and inoculated onto a monolayer of RD cells. The inoculated plates were

incubated at 33°C in 5% CO_2. CPE was determined at day 5, and virus titers were determined using the Spearman-Kärber method (48).

Replication kinetics, virus infection and internalization

Virus infection of EV-D68 isolates were determined using a multiplicity of infection (MOI) of 0.01 or 1. Monolayer of SK-N-SH and RD cells in a 6-well plate or a 96-well plate were inoculated with the different EV-D68 viruses for 1 hour at 37°C in 5% CO_2, or cell culture medium as a control. After 1 hour of virus adsorption, the inoculum was removed, and cells were washed once with PBS before the cells were lysed with lysis buffer (Roche, the Netherlands) for qPCR analysis or replenished with culture medium and incubated at 37°C in 5% CO_2. The supernatant was collected at indicated hour post inoculation (hpi), and stored at -80°C for subsequent virus titration.

Percentage of infections

SK-N-SH and RD cells (~80% confluent) in a 96-well plate were infected with EV-D68 at a MOI of 2. Mock-infected cells were included as a negative control. EV-D68 infected SK-N-SH and RD cells were incubated at 37°C and 33°C in 5% CO_2, respectively. After 8 hpi, cells were fixed with 4% paraformaldehyde (PFA) for 20 minutes at room temperature, washed with PBS and permeabilized with 70% ethanol. Cells were first incubated with 5% bovine serum albumin (BSA; Aurion, Wageningen, the Netherlands) in PBS for 30 minutes before incubating with rabbit anti-EV-D68 VP1 (20 µg/ml; GeneTex, Alton Pkwy Irvine, USA) for 1 h. Cells were washed twice with PBS and incubated with goat anti-rabbit IgG conjugated with Alexa Fluor 594 (10 µg/ml; Life Technologies, Inc., the Netherlands) in PBS with 0.1% BSA (Aurion) for 1 h. Cells were washed 3 times with PBS and mounted with ProLong Diamond Antifade with DAPI (Life Technologies) to visualize nuclei. Each experiment included negative and omission control. EV-D68 VP1 positive cells were identified using a Zeiss LSM 700 laser scanning microscope. All images were processed using Zen 2010 software. Per sample, 3 high-power fields were photographed and the number of infected cells was calculated by counting virus-infected/uninfected cells in 3 randomly chosen panels. All experiments were performed in triplicate.

Next-Generation Sequencing

After pre-treatment of the virus stock with OmniCleaveTM (Lucigen, Halle-Zoersel, Belgium), RNA was extracted using Nucleospin RNA II kit (Bioke, Leiden, the Netherlands) according to the manufacturer's instructions. First-strand complementary DNA (cDNA) was synthesized from using random hexamers and Superscript IV (ThermoFisher Scientific). Double-stranded DNA was generated using Klenow (NEB). For library preparation, the KAPA HyperPlus library preparation kit (Roche, Basel, Switzerland) was used according to the manufacturer's instructions with minor modifications. Adapters were diluted 1:10 and a second wash step was performed after

adapter ligation. The samples were sequenced on an Illumina MiSeq to generate 2x300bp sequence reads.

Data analysis for Illumina sequencing

Raw sequences reads were quality controlled using fastp (49). The quality controlled reads were normalized using bbnorm (50) and subsequently de novo assembled using SPAdes (51). Minimap2 (52) was used to align the quality controlled reads against the obtained contigs and the obtained bam files was loaded into Geneious (53) for minor variant determination with a 20% cut-off.

Sequencing alignment

Each segment of viral genome was aligned using the CLUSTAL W algorithm in MEGA5 (54). Next, sequences of all individual isolated were aligned using the Bioedit version 7.0. 5' UTR or non-coding region was resected from sequences.

Virus attachment

Cell suspensions of SK-N-SH or RD cells were incubated with EV-D68 strains for 1 h at 4°C using a MOI of 1. As a negative control, viruses were heat inactivated at 62°C for 10 minutes before incubation with the cells. Subsequently, cells were washed with PBS, fixed with 4% PFA for 15 minutes, and blocked for 30 minutes with PBS containing 5% normal goat serum (DAKO, Denmark). Cells were incubated with rabbit anti-EV-D68 VP1 (20 µg/ml; GeneTex) in 2mM EDTA (Sigma-Aldrich) and 0.1% BSA (Aurion) FACS buffer for 1 h at 4°C. After washing 3 times, cells were incubated with a secondary goat-anti rabbit IgG conjugated Alexa Fluor 594 (10 µg/ml; Life Technologies) in FACS buffer. After incubation, cells were washed 3 times in FACS buffer and analyzed using a BD FACS Lyrics flowcytometer (BD Bioscience, USA). The percentage of cells to which virus attached was determined using FlowJo 10 software (Ashland, OR, USA). Experiments were performed at least 3 times, and each experiment was performed in duplicates.

Removal of cell-surface sialic acid and heparan sulfate

Cell suspensions of SK-N-SH or RD cells were incubated with 100 mU/ml *Arthobactor ureafaciens* neuraminidase (Roche) or 10 mIU/ml heparinase iii (Sigma-Aldrich) in serum-free medium for 1 h at 37°C. To prevent the cell surface sulfation, cells were cultured for 5 days with sodium chlorate ($NaClO_3$) 80 mM (Sigma-Aldrich, 1.06420 EMD Millipore). Removal of α (2,3)-linked sialic acid and α (2,6)-linked sialic acid on cell surface was confirmed by staining with fluorescein-labeled Sambucus nigra lectin (SNA) (5 µg/ml; Vector laboratories, CA, USA) and biotinylated Maackia amurensis lectin (MAL) I (5 µg/ml; Vector laboratories). The sialylated cells were detected by streptavidin conjugated Alexa Flour 488 (5 µg/ml; Thermo Fisher Scientific). Removal of heparan sulfate on cell surface was confirmed using a mouse anti-heparan sulfate monoclonal Antibody (10 µg/ml; Amsbio, Frankfurt, Germany). No virus inoculation control and virus inoculation in non-enzymatic treatment control were included as a

negative control and positive control respectively in all assays. Mean fluorescence intensity (MFI) was measured with BD FACS Lyrics (BD Bioscience). Subsequently, virus attachment was determined as described above. Data were analyzed using FlowJo 10 software (Ashland). The experiments were performed at least 3 times, and each experiment was performed in duplicates.

RT-qPCR

Total nucleic acid was extracted from cell lysis using Magna Pure MagNA Pure LC Total Nucleic Acid Isolation Kit (Roche) according to manufacturer's instruction. The total nucleic acid was eluted in 50 µl. For viral RNA quantification, real-time Taqman RT-PCR assay was performed using Applied Biosystems 7500 Real-Time PCR System (Thermo Fisher Scientific). The experiments were carried out by adding forward and reverse EV-D68 primer (75 pmol/µl) and the probes (10 pmol/µl). The following sequences including EV-D68 specific primer and probe: forward primer, 5'-TGTTCCCACGGTTGAAAACAA-3', reverse primer 5'-TGTCTAGCGTCTCATGGTTTTCAC -3', the probe1 5'-TCCGCTATAGTACTTCG -3' and the probe2 5'-ACCGCTATAGTACTTCG-3'. The following reaction conditions were applied for all PCR reaction experiment: 5 min at 50 °C and 20 s at 95 °C, followed by 45 cycles at 95°C for 3 s, and 60 °C for 31 s.

Statistical analyses

Statistical analyses were performed using GraphPad Prism 6.0h software (La Jolla, CA, USA). Specific tests were described in the figure legends. P values of ≤ 0.05 were considered significant. All data were expressed as mean ± standard deviations (SDs). Experiments were performed at least in biological triplicates and technical duplicates.

Results

Clinical enterovirus D68 isolates from different clades replicate in human neuroblastoma cells with different efficiency

Growth curves using a multiplicity of infection (MOI) of 0.01 were generated for clinical isolates of clade A (or A1; subsequently we use A), subclade B1, subclade B2 (B2/039 and B2/947), subclade B3, subclade D1 (or A2; subsequently we use D1), and the prototype Fermon strain in SK-N-SH and RD cells. Growth curves showed that all viruses replicate in SK-N-SH cells, but virus titers of subclade B2/947, B3, and Fermon were significantly higher than those of clade A, subclade D1, B1 and B2/039 from 24 hours post inoculation (hpi) onwards (Fig 1A). Remarkable, large differences between the two subclade B2 isolates were observed in growth kinetics on SK-N-SH cells. The same pattern was observed in RD cells, but the differences among isolates were smaller. Isolates that replicated most efficiently on SK-N-SH cells also did in RD cells. (Fig 1B). Overall, these data show that EV-D68 isolates from all clades are able to replicate in SK-N-SH and RD cells, but do so with different efficiency.

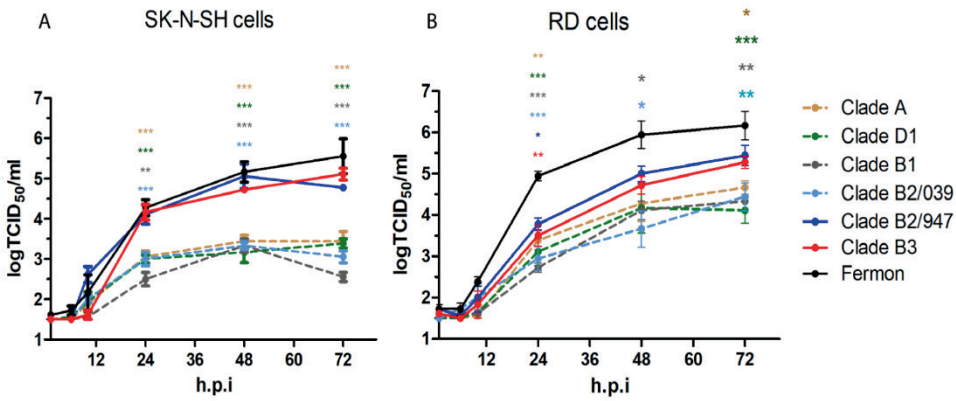

Figure 1. Growth curves of EV-D68 isolations in SK-N-SH and D cells. Growth curve of clinical isolates of (sub)clade A, B1, B2, B3, D1 and prototype EV-D68 strain Fermon in SK-N-SH cells (A) and RD cells (B) at MOI 0.01. Statistical analysis was performed using the One-way ANOVA compared to Fermon. Data are shown as mean ± SD of three independent experiments: *, P≤0.05; **, P≤0.01; ***, P≤0.001.

Replication efficiency is associated with higher infection percentages

To study whether the replication efficiency was associated with the infection efficiency of the different EV-D68 isolates, the percentage of infection was determined by immunofluorescence using an anti-VP1 antibody after incubation of viruses on SK-N-SH and RD cells with a MOI of 2 for 8 hours. Viruses of clade B2/947 and Fermon, and to a lesser extent B3, which replicated most efficiently in SK-N-SH and RD cells, infected higher percentages of cells compared to other isolates (Fig 2A, 2B). These results suggest that the efficient replication measured by the growth kinetics was associated with efficient infection of cells.

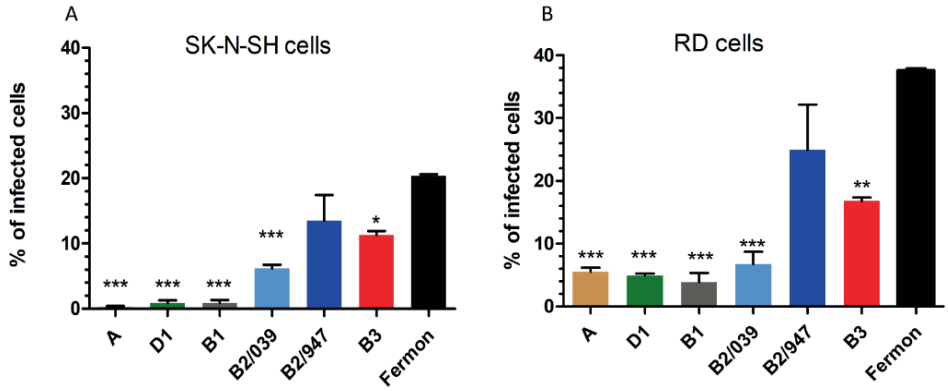

Figure 2. Infection efficiency of different EV-D68 isolates in SK-N-SH and RD cells. Percentage of infected SK-N-SH cells (A) and RD cells (B) after infection with clinical isolates from A, B1, B2, B3, D1 and prototype EV-D68 strain Fermon 8 hours post infection (MOI of 2). The infected cells were stained for VP1 antigen using immunofluorescence staining. Three high-power fields were captured per samples. Statistical analysis was performed using the One-way ANOVA in comparison with Fermon. Data are shown as mean ± SD of three independent experiments: *, P≤0.05; **, P≤0.01; ***, P≤0.001.

Amino acid differences between viruses of subclade B2

Since we observed a large difference in the replication kinetics between the two isolates of subclade B2, we initially performed full genome sequencing analysis of the stocks from B2/039 and B2/947 isolates. There were 13 amino acid differences between these two viruses: V66A, R67K, K116R, V166I, R234G, V136M, D140N, E271K, R25K, I37V, K56R, I187V and S56R (Table 1). These amino acid differences were present in both structural proteins (VP4, VP2, VP3 and VP1) and non-structural proteins (2A, 3C and 3D).

Table 1. Amino acid differences between clade B2/947 and clade B2/039 isolates

Isolate	VP4	VP2		VP3		VP1			2A		3C		3D
	66	67	116	166	234	136	140	271	25	37	56	187	56
B2/947	A	K	R	I	G	M	N	K	K	V	R	V	R
B2/039	V	R	K	V	R	V	D	E	R	I	K	I	S

A lysine is present at position 271 of capsid protein VP1 in isolates that replicate efficiently in SK-N-SH and RD cells.

After the identification of amino acid differences between the two clinical isolates of subclade B2, the 13 amino acid positions that differed were verified in the other clinical isolates to identify amino acid substitutions possibly associated with increased infection and replication efficiency. An amino acid lysine (K) at position 271 in the VP1 capsid protein was only observed in clade B2/947 and B3 viruses, the two clinical isolates that replicated most efficiently in SK-N-SH and RD cells. All other clinical isolates had a glutamic acid (E) or valine (V) at position 271 in VP1 and the lab-adapted Fermon carried an aspartic acid (D) (Table 2). At all other positions that differed between the clade B2 isolates, no common differences were observed between the viruses with different replication efficiencies (Table 2). This indicates that the amino acid substitution E271K might be a determinant for increased infection and replication in SK-N-SH cells *in vitro*.

Table 2. Amino acids present in clinical isolates of (sub)clade A, B1, B2, B3, and D1 at the positions that differed between low and high replicating isolates

Isolate	VP4	VP2		VP3		VP1			2A		3C		3D
	66	67	116	166	234	136	140	271	25	37	56	187	56
B2/947*	A	K	R	I	G	M	N	K	K	V	R	V	R
B3*	A	R	K	I	G	V	D	K	R	I	R	V	S
B2/039	V	R	K	V	R	V	D	E	R	I	K	I	S
A	A	K	K	V	R	T	D	E	R	V	K	V	S
D1	A	K	K	V	A	M	D	E	R	I	K	V	S
B1	A	K	K	I	G	V	D	V	R	V	R	V	S
Fermon*	A	R	K	I	G	M	D	D	R	V	R	V	S

*isolates that replicate efficiently in SK-N-SH cells.

The lysine at position 271 in VP1 is acquired during *in vitro* passaging

The clinical isolates used in this study were passaged in RD cells to produce virus stocks. To investigate whether a lysine at position 271 in VP1 was present in the original isolate of the patient, sequences from clinical specimens, previous passages and virus stocks used in this study were generated and aligned. In the clinical specimens, a glutamic acid (E) was found at position 271 in VP1 of both subclade B2/947 (21) and subclade B3. Furthermore, sequencing analysis of all virus passages showed the acquisition of a lysine (K) in passage 3 of subclade B2/947 and passage 2 of subclade B3 on RD cells (Table 3). There were no minor variants present at position 271 of sequences derived from clinical specimens and stock B2/947 and B3 viruses using a 20% cut-off (Table 3). This indicates that viruses with high replication and infection efficiency acquired the E271K amino acid substitution during passaging in RD cells.

Table 3. Amino acid at position 271 of VP1 in isolate B2/947 and B3 from original clinical specimens and historical passages

Isolate	Clinical specimen / Virus isolate passage	Amino acid at position 271	Frequent variant; method	GenBank accession
B2/947*	Clinical specimen	E	100%; Illumina	.
	Passage 1	Position not sequenced	100%; Sanger	.
	Passage 2	E	100%; Sanger	KT231897
	Passage 3	K	100%; Sanger	KT231898
	Passage 3	K	100%; Illumina	MN954540
B3	Clinical specimen	E	100%; Sanger	.
	Passage 1	E	100%; Sanger	.
	Passage 2	K	100%; Illumina	.
	Passage 3	K	100%; Illumina	.
	Passage 4	K	100%; Illumina	MN954541

Viruses with E271K substitution in VP1 attached more efficiently to SK-N-SH and RD cells

Since the amino acid at position 271 of EV-D68 resides within the canyon, close to the sialic acid binding site (19), we investigated whether EV-D68 isolates with the specific E271K amino acid substitution attached to higher percentages of SK-N-SH and RD cells. We observed that the subclade B2/947 and subclade B3 isolates which acquired the E271K substitution attached to higher percentages of SK-N-SH and RD cells than all other isolates. Fermon attached to lower percentages of SK-N-SH and RD cells despite efficient replication and infection (Fig 3A, 3B). Overall, these observations suggest that the E271K substitution is associated with increased virus attachment in vitro.

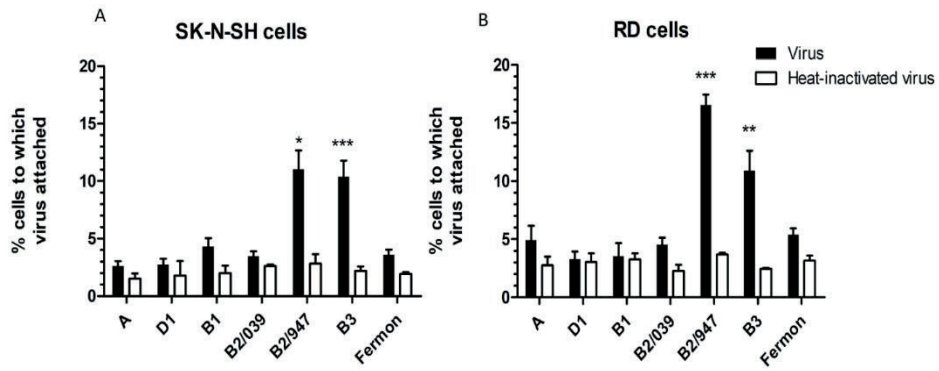

Figure 3. Virus attachment of EV-D68 viruses to SK-N-SH and RD cells. Experiments were performed by Flow cytometry. Attachment of clinical isolates from (sub)clade A, B1, B2, B3, D1 and prototype EV-D68 strain Fermon to SK-N-SH cells (A) and RD cells (B). Heat-in-activated viruses were included as negative control. Statistical analysis was performed using the One-way ANOVA in comparison with Fermon. Data are shown as mean ± SD of three independent experiments: *, P≤0.05; **, P≤0.01; ***, P≤0.001.

Viruses with E271K substitution in VP1 recognized sialic acid and heparan sulfate

A previous study has shown that among several EV-D68 strains, subclade B2/947 can recognize heparan sulfate as an additional receptor to sialic acid (21). To investigate whether our viruses with a E271K substitution were able to recognize both sialic acid and heparan sulfate, we determined the ability of these viruses to attach to cells that were pretreated with Arthobacter ureafaciens neuraminidase and heparinase iii to remove sialic acids or heparan sulfate respectively. Subclade B2/947 and B3 isolates carrying the E271K substitution, and subclade B2/039 isolate (271E) as control were included in these analyses. Removal of sialic acids and heparan sulfate was confirmed by measuring mean fluorescent intensity (MFI) with MAL for α (2,3)-linked sialic acid and SNA α (2,6)-linked sialic acid, and with an antibody that recognizes heparan sulfate (Fig 4A, 4D). Percentage of cells to which the virus attached was significantly decreased for all viruses in both SK-N-SH and RD cells after neuraminidase treatment (Fig 4B, 4C).

In contrast, heparinase iii treatment resulted in decreased attachment of only viruses with E271K substitution (Fig 4E,4F). Overall, these results showed that the viruses with E271K substitution recognize both sialic acid and heparan sulfate on cellular surface.

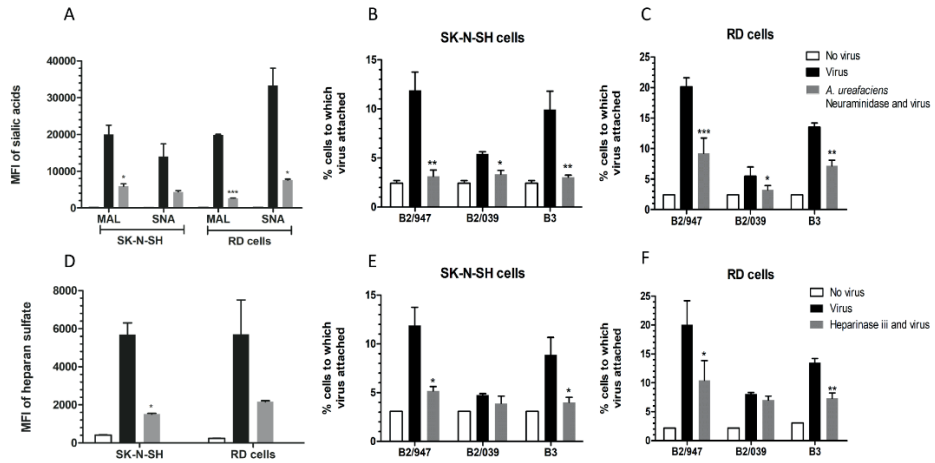

Figure 4. Virus attachment of clinical isolates B2/039, B2/947 and B3 after neuraminidase and heparinase iii treatment. Mean fluorescent intensity (MFI) levels of MAL (α (2,3)-linked sialic acid) and SNA (α (2,6)-linked sialic acid) with and without neuraminidase treatment (A). Percentage of attachment of isolates B2/039, B2/947 and B3 with and without neuraminidase treatment of SK-N-SH cells (B) and RD cells (C). MFI levels of heparan sulfate with and without heparinase iii treatment (D). Attachment of clinical isolates B2/039, B2/947 and B3 with and without heparinase iii treatment of SK-N-SH cells (E) and RD cells (F). Statistical analysis was performed by paired t-test. Data are shown as mean ± SD of three independent experiments: *, P≤0.05; **, P≤0.01; ***, P≤0.001.

Attachment, internalization and replication of viruses with E271K substitution in VP1 depend in part on heparan sulfate recognition

To investigate if heparan sulfate is required for attachment, internalization and replication of viruses with an E271K substitution, heparan sulfate was removed on SK-N-SH and RD cells by either heparinase iii or $NaClO_3$ which prevents cell surface sulfation (21). Treated and untreated cells were inoculated with a MOI 1 of B2/947, B3 and B2/039. After 1 hpi at 37°C the amount of attached and internalized viral RNA of B2/947 and B3 was lower in the heparinase iii or $NaClO_3$ treated cells compared to untreated cells by qPCR. Viral RNA for B2/039 was not reduced in the heparinase or NaClO3 treated cells, with the exception of a minimal but significant reduction of viral RNA in SK-N-SH cells treated with $NaClO_3$ but not in RD cells (Fig 5A, 5B). Virus replication of both B2/947 and B3 were significantly decreased in SK-N-SH and RD cells treated with heparinase iii or $NaClO_3$, while replication of B2/039 was similar in treated and untreated cells (Fig 5C, 5D and Fig S1). Together, these results indicate that the recognition of heparan sulfate is important for facilitating virus attachment, internalization and replication.

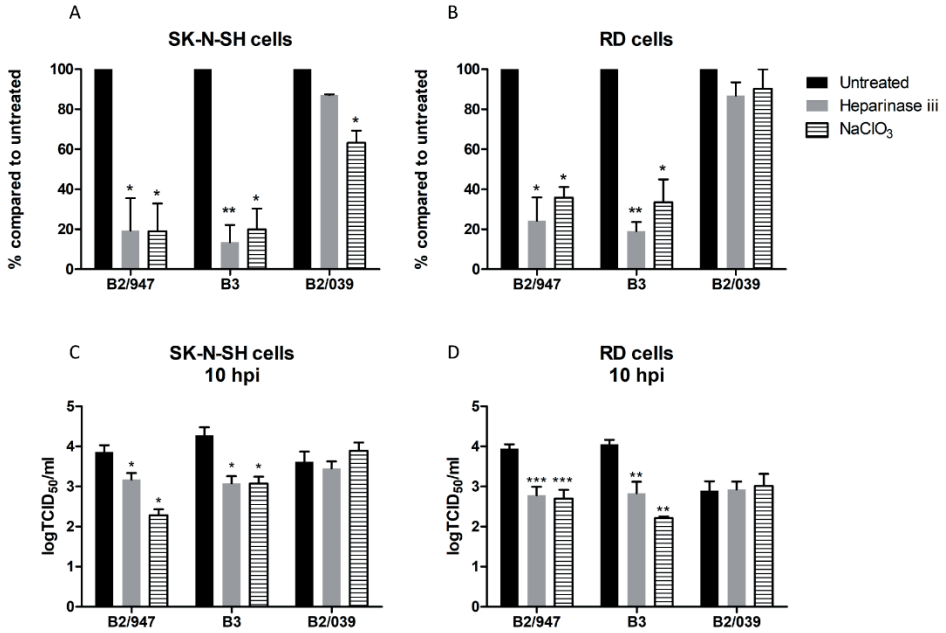

Figure 5. Attachment, internalization and replication of clinical isolates B2/947, B3 and B2/039 in SK-N-SH and RD cells after heparinase iii and $NaClO_3$, treatment. SK-N-SH and RD cells were treated for one hour with heparinase iii or cells were cultured for 5 days with $NaClO_3$. After the treatment, cells were infected with clinical isolates at MOI 1. To remove the unbound viruses, cells were washed three times with PBS before cell lysis (A) Attach and intracellular viral RNA levels were determined by qPCR 1 hour post infection. Percentage of viral RNA levels were compared to untreated in SK-N-SH and RD cells. (B) Infectious virus particles of the supernatants were determined by TCID50, 10 hours post infection. Statistical analysis was performed using the One-way ANOVA. Data are shown as mean ± SD of three independent experiments: *, P≤0.05; **, P≤0.01; ***, P≤0.001.

Discussion

Here we report that EV-D68 isolates from (sub)clade A, B1, B2, B3 and D1 replicated in human neuroblastoma SK-N-SH cells; however, large differences were observed in replication efficiency. Subsequent genotypic analysis revealed that viruses replicating most efficiently had a specific amino acid substitution in VP1 (E271K). This substitution was acquired during cell culture propagation and was associated with the recognition of heparan sulfate. Furthermore, attachment, internalization and replication depended in part on heparan sulfate recognition for viruses with the E271K substitution in VP1. These findings suggest that efficient replication of EV-D68 isolates in vitro in human neuroblastoma cells is not a clade specific feature, but at least in part associated with the usage of heparan sulfate as an additional receptor.

The amino acid substitution at position 271 of VP1 (E271K) acquired during in vitro passaging in 2 out of the 6 viruses included in our study was associated with the

recognition of heparan sulfate as an additional receptor (21), which had a large impact on the phenotypic characteristics of EV-D68 viruses. Heparan sulfate is abundantly present on RD cells (33), and associated with increased virus attachment, infection efficiency and virus replication in cells in vitro. The ability of EV-D68 in replicating in a mouse neuroblastoma cell line and human induced pluripotent stem cell motor neuron cells were independent of sialic acid recognition, although the usage of heparan sulfate was not investigated (31, 34). In our study unfortunately viruses from earlier passages without E271K in VP1 were not available and an infectious clone of the clinical isolate B2/947 with the original VP1 amino acid E271 could not be recovered (21), which made a direct comparison of viruses with and without E271K in VP1 not possible. The lysine at position 271 of VP1 is positively charged, which contributes to the formation of a basic patch that interacts with negatively charged heparan sulfate proteoglycan (21). This mechanism has been described previously for other picornaviruses which acquired the recognition of heparan sulfate during passaging of viruses in vitro (35-37).

It was initially thought that the neurotropic potential of EV-D68 was a feature recently acquired, and associated to subclade B1. However, epidemiological and clinical data have shown that different subclades, namely B3 and D1, beside subclade B1 have also been associated with AFM cases after 2014 (28-30). In addition, most *in vitro* studies, including ours, and in vivo studies do not reveal phenotypic difference between clades or recent and older EV-D68 isolates (31, 32, 38). In vivo, EV-D68 isolates from multiple clades (e.g. clade A and subclade B1) were able to cause paralysis after intracranial inoculation (32). In vitro we and other showed that EV-D68 isolates from multiple clades were able to replicate in neuroblastoma cells (38). Furthermore, we did not detect phenotypic differences between viruses isolated before and after 2014 independent of the clade, which correlates with the study of Rosenfeld et al. (31), but not with a study performed by Brown et al. (38). Unfortunately, virus stocks were not compared with clinical isolates in these studies. All together these data suggest that the ability to replicate in cells of the CNS is not a clade specific feature.

The role of heparan sulfate as an additional receptor in the pathogenesis in vivo remains unclear. Although the presence of the E271K substitution in human EV-D68 isolates has not been studied, we found that only a very few EV-D68 VP1 sequences available in GenBank have a lysine at position 271 of VP1; by 15 December 2019, 17 out of 1737 (<1%), and they fall in a wide range of old and current clades. However, of most sequences the source, clinical material or virus isolate and passage history, is not known. Interestingly, acquisition of heparan sulfate recognition in an immunocompromised patient with Enterovirus 71 (EV-71) was associated with systemic spread, including the CNS. In this patient a mutation in the VP1 responsible for heparan sulfate recognition was only detected in extra-respiratory samples (39). Since heparan sulfate is not expressed on the apical site of respiratory epithelial cells, but abundantly in cells outside the respiratory tract, such as cells of the CNS and muscle cells (39, 40), in vivo acquisition of E271K might—just like EV71—occur outside the respiratory tract and

would therefore hardly be found in respiratory samples. Sequence analysis from respiratory and extra-respiratory samples from the same patient should reveal if heparan sulfate recognition is important for the pathogenesis of EV-D68 in vivo.

It remains unclear why there is an increase of AFM cases associated with EV-D68 since 2014, since epidemiological and serological studies suggest that EV-D68 has been circulating throughout the population for decades (41, 42). Currently, the pathogenesis of neurological disease associated with EV-D68 infection is not fully understood. Both a direct effect of virus entry and replication in the nervous system or an indirect effect of systemic cytokines could contribute. However, the detection of EV-D68 or virus specific antibodies in the cerebrospinal fluid suggest that virus enters and replicates in the CNS in at least part of the patients (43, 44). As there are more cases with severe respiratory disease caused by EV-D68 since 2014 (9, 45), it might be that recent EV-D68 viruses replicate to higher titers in the respiratory tract, thereby increasing the risk of systemic spread including to the CNS. However, the exact mechanism of systemic spread of EV-D68 in vivo requires more in-depth pathogenesis studies

Taken together, we demonstrate that the replication of EV-D68 isolates in the neuroblastoma cell line SK-N-SH is not a clade specific phenotype of EV-D68. However, large phenotypic differences that we did observe in vitro could be linked to the substitution E271K in VP1 leading to the recognition of heparan sulfate as an additional receptor, which resulted in increased attachment, internalization and replication. Therefore, we recommend to sequence virus stocks in order to get the virus that resemble those of the clinical isolates in order to study phenotypic characteristics of EV-D68 isolates in vitro and in vivo.

Acknowledgements

This work was funded by a fellowship to DvR from the Netherlands Organization for Scientific Research (VIDI contract 91718308) and the Erasmus MC Foundation. Syriam Sooksawasdi Na Ayudhya received the Royal Thai Government Scholarship supported by the Ministry of Science and Technology of Thailand to perform her doctoral study. The authors would like to thank Claudia Schapendonk, Jim Baggen, Gabriel Goderski, Ton Marzec, Pieter Overduin and Thierry Janssens for technical advices and assistances.

Supplementary Figure

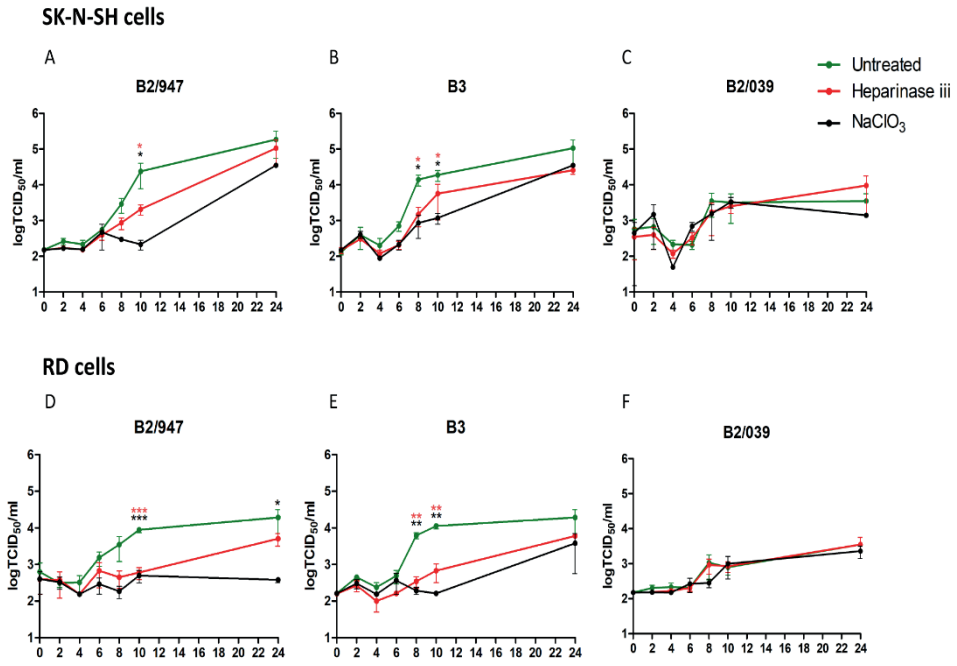

Fig S.1. Growth curves of subclade B2/947, B3, B2/039 isolates in SK-N-SH and RD cells after heparinase iii and NaClO3 treatment. Growth curve of clinical isolates of subclade B2/947, B3 and B2/039 in SK-N-SH cells (A) and RD cells (B) at MOI 1. Statistical analysis was performed using the One-way ANOVA compared to untreated. Data are shown as mean ± SD of three independent experiments: *, P ≤ 0.05; **, P ≤ 0.01; ***, P ≤ 0.001.

References

1. Imamura T, Oshitani H. 2015. Global reemergence of enterovirus D68 as an important pathogen for acute respiratory infections. Rev Med Virol 25:102-14.
2. Messacar K, Schreiner TL, Maloney JA, Wallace A, Ludke J, Oberste MS, Nix WA, Robinson CC, Glodé MP, Abzug MJ, Dominguez SR. 2015. A cluster of acute flaccid paralysis and cranial nerve dysfunction temporally associated with an outbreak of enterovirus D68 in children in Colorado, USA. The Lancet 385:1662-1671.
3. Alexander L Greninger, Samia N Naccache, Kevin Messacar, Anna Clayton, Guixia Yu, Sneha Somasekar, Scot Federman, Doug Stryke, Christopher Anderson, Shigeo Yagi, Sharon Messenger, Debra Wadford, Dongxiang Xia, James P Watt, Keith Van Haren, Samuel R Dominguez, Carol Glaser, Prof Grace Aldrovandi, Dr Charles Y Chiu. 2015. A novel outbreak enterovirus D68 strain associated with acute flaccid myelitis cases in the USA (2012–14): a retrospective cohort study. The Lencet Infectious Diseases 15:p671–682.
4. CarinaHolm EM, Thea Kolsen Fischer. 2016. Global emergence of enterovirus D68: a systematic review. The Lancet Infectious Disease 16:64-75.
5. Dyda A, Stelzer-Braid S, Adam D, Chughtai AA, MacIntyre CR. 2018. The association between acute flaccid myelitis (AFM) and Enterovirus D68 (EV-D68) - what is the evidence for causation? Euro Surveill 23.
6. Knoester M, Scholvinck EH, Poelman R, Smit S, Vermont CL, Niesters HG, Van Leer-Buter CC. 2017. Upsurge of Enterovirus D68, the Netherlands, 2016. Emerg Infect Dis 23:140-143.
7. Furuse Y, Chaimongkol N, Okamoto M, Imamura T, Saito M, Tamaki R, Saito M, Tohoku RCRT, Lupisan SP, Oshitani H. 2015. Molecular epidemiology of enterovirus D68 from 2013 to 2014 in Philippines. J Clin Microbiol 53:1015-8.
8. Messacar K, Abzug MJ, Dominguez SR. 2016. 2014 outbreak of enterovirus D68 in North America. J Med Virol 88:739-45.
9. Midgley CM, Jackson MA, Selvarangan R, Turabelidze G, Obringer E, Johnson D, Giles BL, Patel A, Echols F, Oberste MS, Nix WA, Watson JT, Gerber SI. 2014. Severe respiratory illness associated with enterovirus D68 - Missouri and Illinois, 2014. MMWR Morb Mortal Wkly Rep 63:798-9.
10. Zhang Y, Cao J, Zhang S, Lee AJ, Sun G, Larsen CN, Zhao H, Gu Z, He S, Klem EB, Scheuermann RH. 2016. Genetic changes found in a distinct clade of Enterovirus D68 associated with paralysis during the 2014 outbreak. Virus Evol 2:vew015.
11. Yogo N, Imamura T, Muto Y, Hirai K. 2019. Cardiopulmonary failure as a result of brainstem encephalitis caused by enterovirus D68. BMJ Case Rep 12.
12. Esposito S, Chidini G, Cinnante C, Napolitano L, Giannini A, Terranova L, Niesters H, Principi N, Calderini E. 2017. Acute flaccid myelitis associated with enterovirus-D68 infection in an otherwise healthy child. Virol J 14:4.

13. Kreuter JD, Barnes A, McCarthy JE, Schwartzman JD, Oberste MS, Rhodes CH, Modlin JF, Wright PF. 2011. A fatal central nervous system enterovirus 68 infection. Arch Pathol Lab Med 135:793-6.
14. Messacar K PK, Reno S, Dominguez SR. 2019. Continued biennial circulation of enterovirus D68 in Colorado. J Clin Virol 113:24-26.
15. Carballo CM EM, Sordelli N, Vazquez G, Mistchenko AS, Cejas C, Rodriguez M,, Cisterna DM FM, Contrini MM, Lopez EL. 2019. Acute Flaccid Myelitis Associated with Enterovirus D68 in Children, Argentina, 2016. Emerg Infect Dis 25:573-576.
16. Pellegrinelli L GF, Lunghi G, Uceda Renteria SC, Greco L,, Fratini A GC, Piralla A, Binda S, Pariani E, Baldanti, F. 2019. Emergence of divergent enterovirus (EV) D68 sub-clade D1 strains, northern Italy, September to October 2018. Euro Surveill 24.
17. Ramsay M DJ, Foulkes S, Lopez J, Bukasa A, Iyanger N,, Zambon M BK, Bradshaw D, Ladhani S, MacGregor V, Pebody, Donati M, Stowe J,, Williams C DM, Reynolds A, Marques D, McMenamin J, Templeton K, Lim M. 2019. An increase in reports of acute flaccid paralysis (AFP) in the United Kingdom, 1 January 2018-21 January 2019: early findings. Euro Surveill 24.
18. AL Cathcart EB, and BL Semler. 2015. Picornaviruses: Pathogenesis and Molecular Biology, 2014-12-15 ed doi:10.1016/B978-0-12-801238-3.00272-5 Elsevier Inc., University of California, Irvine, CA, USA.
19. Baggen J, Thibaut HJ, Staring J, Jae LT, Liu Y, Guo H, Slager JJ, de Bruin JW, van Vliet AL, Blomen VA, Overduin P, Sheng J, de Haan CA, de Vries E, Meijer A, Rossmann MG, Brummelkamp TR, van Kuppeveld FJ. 2016. Enterovirus D68 receptor requirements unveiled by haploid genetics. Proc Natl Acad Sci U S A 113:1399-404.
20. Wei W, Guo H, Chang J, Yu Y, Liu G, Zhang N, Willard SH, Zheng S, Yu XF. 2016. ICAM-5/Telencephalin Is a Functional Entry Receptor for Enterovirus D68. Cell Host Microbe 20:631-641.
21. Baggen J, Liu Y, Lyoo H, van Vliet ALW, Wahedi M, de Bruin JW, Roberts RW, Overduin P, Meijer A, Rossmann MG, Thibaut HJ, van Kuppeveld FJM. 2019. Bypassing pan-enterovirus host factor PLA2G16. Nat Commun 10:3171.
22. Wei HY, Yeh TK, Hsieh JY, Lin IP, Yang JY. 2018. Updates on the molecular epidemiology of Enterovirus D68 after installation of screening test among acute flaccid paralysis patients in Taiwan. J Microbiol Immunol Infect 51:688-691.
23. Fall A, Jallow MM, Kebe O, Kiori DE, Sy S, Goudiaby D, Boye CSB, Niang MN, Dia N. 2019. Low Circulation of Subclade A1 Enterovirus D68 Strains in Senegal during 2014 North America Outbreak. Emerg Infect Dis 25:1404-1407.
24. Anonymous. 2012. Virus taxonomy doi:10.1016/B978-0-12-384684-6.X0001-8. ELSEIVER, USA.
25. Yip CCY, Lo JYC, Sridhar S, Lung DC, Luk S, Chan KH, Chan JFW, Cheng VCC, Woo PCY, Yuen KY, Lau SKP. 2017. First Report of a Fatal Case Associated with EV-D68 Infection

in Hong Kong and Emergence of an Interclade Recombinant in China Revealed by Genome Analysis. Int J Mol Sci 18.
26. Messacar K, Schreiner TL, Van Haren K, Yang M, Glaser CA, Tyler KL, Dominguez SR. 2016. Acute flaccid myelitis: A clinical review of US cases 2012-2015. Ann Neurol 80:326-38.
27. Wang G, Zhuge J, Huang W, Nolan SM, Gilrane VL, Yin C, Dimitrova N, Fallon JT. 2017. Enterovirus D68 Subclade B3 Strain Circulating and Causing an Outbreak in the United States in 2016. Sci Rep 7:1242.
28. Dyrdak R, Grabbe M, Hammas B, Ekwall J, Hansson KE, Luthander J, Naucler P, Reinius H, Rotzen-Ostlund M, Albert J. 2016. Outbreak of enterovirus D68 of the new B3 lineage in Stockholm, Sweden, August to September 2016. Euro Surveill 21.
29. Piralla A, Principi N, Ruggiero L, Girello A, Giardina F, De Sando E, Caimmi S, Bianchini S, Marseglia GL, Lunghi G, Baldanti F, Esposito S. 2018. Enterovirus-D68 (EV-D68) in pediatric patients with respiratory infection: The circulation of a new B3 clade in Italy. J Clin Virol 99-100:91-96.
30. Pellegrinelli L, Giardina F, Lunghi G, Uceda Renteria SC, Greco L, Fratini A, Galli C, Piralla A, Binda S, Pariani E, Baldanti F. 2019. Emergence of divergent enterovirus (EV) D68 sub-clade D1 strains, northern Italy, September to October 2018. Euro Surveill 24.
31. Rosenfeld AB, Warren AL, Racaniello VR. 2019. Neurotropism of Enterovirus D68 Isolates Is Independent of Sialic Acid and Is Not a Recently Acquired Phenotype. MBio 10.
32. Hixon AM, Yu G, Leser JS, Yagi S, Clarke P, Chiu CY, Tyler KL. 2017. A mouse model of paralytic myelitis caused by enterovirus D68. PLoS Pathog 13:e1006199.
33. Tan CW, Poh CL, Sam IC, Chan YF. 2013. Enterovirus 71 uses cell surface heparan sulfate glycosaminoglycan as an attachment receptor. J Virol 87:611-20.
34. Hixon AM, Clarke P, Tyler KL. 2019. Contemporary Circulating Enterovirus D68 Strains Infect and Undergo Retrograde Axonal Transport in Spinal Motor Neurons Independent of Sialic Acid. J Virol 93.
35. Bochkov YA, Watters K, Basnet S, Sijapati S, Hill M, Palmenberg AC, Gern JE. 2016. Mutations in VP1 and 3A proteins improve binding and replication of rhinovirus C15 in HeLa-E8 cells. Virology 499:350-360.
36. Goodfellow IG, Sioofy AB, Powell RM, Evans DJ. 2001. Echoviruses bind heparan sulfate at the cell surface. J Virol 75:4918-21.
37. Tan CW, Sam IC, Lee VS, Wong HV, Chan YF. 2017. VP1 residues around the five-fold axis of enterovirus A71 mediate heparan sulfate interaction. Virology 501:79-87.
38. Brown DM, Hixon AM, Oldfield LM, Zhang Y, Novotny M, Wang W, Das SR, Shabman RS, Tyler KL, Scheuermann RH. 2018. Contemporary Circulating Enterovirus D68 Strains Have Acquired the Capacity for Viral Entry and Replication in Human Neuronal Cells. MBio 9.

39. Tseligka ED, Sobo K, Stoppini L, Cagno V, Abdul F, Piuz I, Meylan P, Huang S, Constant S, Tapparel C. 2018. A VP1 mutation acquired during an enterovirus 71 disseminated infection confers heparan sulfate binding ability and modulates ex vivo tropism. PLoS Pathog 14:e1007190.
40. Jenniskens GJ, Oosterhof A, Brandwijk R, Veerkamp JH, van Kuppevelt TH. 2000. Heparan sulfate heterogeneity in skeletal muscle basal lamina: demonstration by phage display-derived antibodies. J Neurosci 20:4099-111.
41. Karelehto E, Koen G, Benschop K, van der Klis F, Pajkrt D, Wolthers K. 2019. Enterovirus D68 serosurvey: evidence for endemic circulation in the Netherlands, 2006 to 2016. Euro Surveill 24.
42. Harrison CJ, Weldon WC, Pahud BA, Jackson MA, Oberste MS, Selvarangan R. 2019. Neutralizing Antibody against Enterovirus D68 in Children and Adults before 2014 Outbreak, Kansas City, Missouri, USA(1). Emerg Infect Dis 25:585-588.
43. Schubert RD, Hawes IA, Ramachandran PS, Ramesh A, Crawford ED, Pak JE, Wu W, Cheung CK, O'Donovan BD, Tato CM, Lyden A, Tan M, Sit R, Sowa GA, Sample HA, Zorn KC, Banerji D, Khan LM, Bove R, Hauser SL, Gelfand AA, Johnson-Kerner BL, Nash K, Krishnamoorthy KS, Chitnis T, Ding JZ, McMillan HJ, Chiu CY, Briggs B, Glaser CA, Yen C, Chu V, Wadford DA, Dominguez SR, Ng TFF, Marine RL, Lopez AS, Nix WA, Soldatos A, Gorman MP, Benson L, Messacar K, Konopka-Anstadt JL, Oberste MS, DeRisi JL, Wilson MR. 2019. Pan-viral serology implicates enteroviruses in acute flaccid myelitis. Nat Med 25:1748-1752.
44. Mishra N, Ng TFF, Marine RL, Jain K, Ng J, Thakkar R, Caciula A, Price A, Garcia JA, Burns JC, Thakur KT, Hetzler KL, Routh JA, Konopka-Anstadt JL, Nix WA, Tokarz R, Briese T, Oberste MS, Lipkin WI. 2019. Antibodies to Enteroviruses in Cerebrospinal Fluid of Patients with Acute Flaccid Myelitis. mBio 10.
45. Okumura A, Numoto S, Iwayama H, Kurahashi H, Natsume J, Saitoh S, Yoshikawa T, Fukao T, Hirayama M, Takahashi Y, Aichi Pediatric Clinical Study G. 2019. Respiratory illness and acute flaccid myelitis in the Tokai district in 2018. Pediatr Int.
46. Meijer A, Benschop KS, Donker GA, van der Avoort HG. 2014. Continued seasonal circulation of enterovirus D68 in the Netherlands, 2011-2014. Euro Surveill 19.
47. Meijer A, van der Sanden S, Snijders BE, Jaramillo-Gutierrez G, Bont L, van der Ent CK, Overduin P, Jenny SL, Jusic E, van der Avoort HG, Smith GJ, Donker GA, Koopmans MP. 2012. Emergence and epidemic occurrence of enterovirus 68 respiratory infections in The Netherlands in 2010. Virology 423:49-57.
48. Kärber G. 1931. Beitrag zur kollektiven Behandlung pharmakologischer Reihenversuche. Naunyn Schmiedebergs Arch Exp Pathol Pharmakol 162:480-483.
49. Nikolay B, Weidmann M, Dupressoir A, Faye O, Boye CS, Diallo M, Sall AA. 2014. Development of a Usutu virus specific real-time reverse transcription PCR assay based on sequenced strains from Africa and Europe. J Virol Methods 197:51-4.

50. B.Bushnell. 2019. BBMap download, on SourceForge.net. https://sourceforge.net/projects/bbmap/. Accessed 8.9.18.
51. Bankevich A, Nurk S, Antipov D, Gurevich AA, Dvorkin M, Kulikov AS, Lesin VM, Nikolenko SI, Pham S, Prjibelski AD, Pyshkin AV, Sirotkin AV, Vyahhi N, Tesler G, Alekseyev MA, Pevzner PA. 2012. SPAdes: a new genome assembly algorithm and its applications to single-cell sequencing. J Comput Biol 19:455-77.
52. Li H. 2018. Minimap2: pairwise alignment for nucleotide sequences. Bioinformatics 34:3094-3100.
53. Kearse M, Moir R, Wilson A, Stones-Havas S, Cheung M, Sturrock S, Buxton S, Cooper A, Markowitz S, Duran C, Thierer T, Ashton B, Meintjes P, Drummond A. 2012. Geneious Basic: an integrated and extendable desktop software platform for the organization and analysis of sequence data. Bioinformatics 28:1647-9.
54. Tamura K, Peterson, D., Peterson, N., Stecher, G., Nei, M. & Kumar, S. 2011. MEGA5: molecular evolutionary genetics analysis using maximum likelihood, evolutionary distance, and maximum parsimony methods. Mol Biol Evol 28:2731–2739.

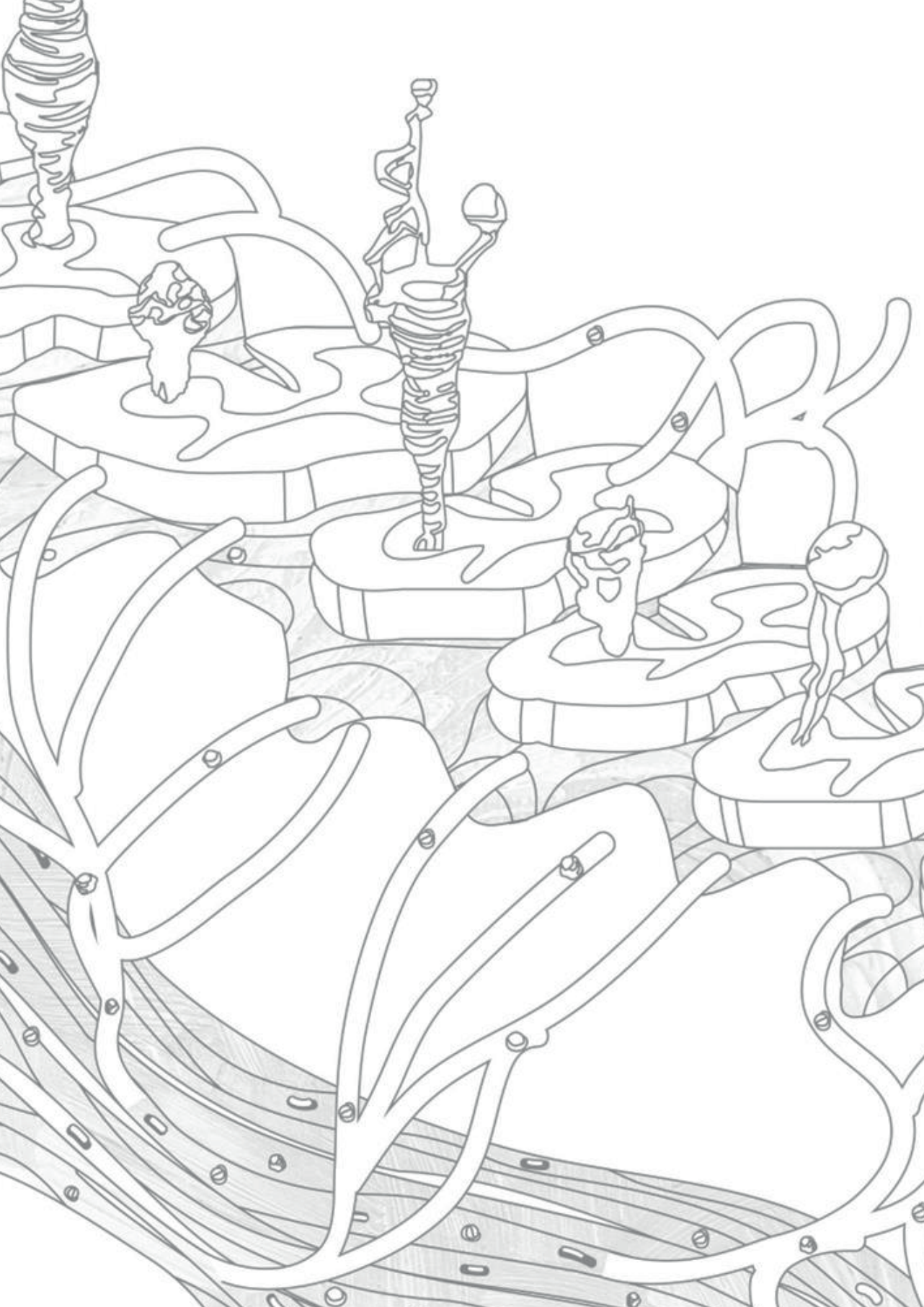

Chapter

4

Comparative analysis of EV-D68 clinical isolates from before and after 2014 in human pluripotent stem cell-derived neural models

Syriam Sooksawasdi Na Ayudhya, Lisa Bauer, Kristina Lanko, Debby van Riel

Manuscript in preparation

Abstract

Enterovirus D68 (EV-D68) primarily causes mild respiratory disease. However, since 2014, outbreaks have been linked to the emergence of severe respiratory illness, occasionally associated with neurological complications. Acute flaccid myelitis is the most common neurological complication, while other brain related neurological diseases, such as meningitis, meningioencephalitis and encephalitis are less frequently reported. In vivo studies have shown that EV-D68 infects motor neurons in the spinal cord, with rare virus detection in other cells or parts of the central nervous system (CNS). Although multiple clades have been circulating since 2014, it remains unclear whether viruses from different clades, or those circulating before 2014 and after 2014, differ in their infection or replication efficiency in cells of the CNS as well as the associated cellular responses. Here, we compared the infection and replication kinetics of EV-D68 isolates from before and after 2014 on human pluripotent stem cell (hPSC)-derived spinal motor neurons (sMNs) and Ngn2 cortical neurons co-cultured with astrocytes. Our findings demonstrate that EV-D68 isolates did not exhibit a specific tropism for sMNs in vitro. All EV-D68 isolates, except one, replicated in both neural models but the efficiency varied among isolates. No differences in replication and infection efficiency were observed between isolates from before and after 2014. One isolate replicated in both cultures without the release of detectable progeny virus within the supernatants, suggesting different routes of cell-to-cell transmission among EV-D68 isolates. EV-D68 infection in hPSC-derived sMNs reduced expression of choline acetyltransferase and initiated cell death independent of apoptosis. Together, our findings suggest that the high susceptibility of motor neurons to EV-D68 infection and the associated cellular changes contribute to the neuropathogenesis.

Introduction

Enterovirus D68 (EV-D68), belonging to genus Enterovirus within the family of *Picornaviridae*, is associated with mild or subclinical respiratory disease and rarely with severe disease (1). However, in 2014, EV-D68 emerged in the United States and caused an outbreak of severe respiratory illness which coincided with an upsurge of acute flaccid myelitis (AFM) in children (2, 3). Since then, EV-D68 outbreaks have been documented worldwide in a biennial pattern in 2016 and 2018 (4, 5). Since the COVID-19 pandemic, there has not been an increase of severe disease associated with EV-D68 infection, despite detectable circulation of the virus in different geographical location (6, 7).

Enterovirus D68 has been diversified into clades A-D, in which clade B is subdivided into subclades B1–B3 (8). Some studies classify A as A1 and D1 as A2 (9, 10). During the outbreak in 2014, subclade B1 was the most prevalent and directly associated with neurological complications (2, 3, 11). Later, epidemiological and clinical observations suggested that other clades, including B3 and A2, were also associated with neurological complications supporting the hypothesis that EV-D68 infection in the central nervous system (CNS) is not a clade-specific feature (12-14).

Enterovirus D68 infection in the CNS has been associated with neurological complications including meningitis, meningoencephalitis, encephalitis and AFM. Among these neurological diseases, AFM is the most commonly reported. Clinical manifestation of AFM is in line with specific lesions in the anterior horn of the spinal cord and presence of EV-D68 antigen and viral RNA in the spinal cord from a fatal AFM case (15, 16). In experimentally inoculated mice, EV-D68 isolates from different clades show strong tropism towards motor neurons in the spinal cord but very limited in the brain (17, 18). In addition, other neurological complications with brain related diseases like encephalitis and meningoencephalitis are less frequently reported (19). In contrast to the in vivo observations that EV-D68 has a strong tropism for motor neurons. In vitro studies suggest that EV-D68 isolates from different clades can infect and replicate in various cell types of the CNS, including cortical neurons found in the cerebral cortex (20-25). However, the exact neurotropism of EV-D68 isolates from before and after 2014 have not been studied comprehensively.

The mechanisms through which an EV-D68 infection in cells of the CNS leads to neuronal dysfunction and clinical disease remain poorly understood. Majority of patients with EV-D68 neurological complication developed limb paralysis with persist motor deficits at 1 year after diagnosis (26, 27). In experimentally inoculated mice, EV-D68 infection in the spinal cord resulted in motor neurons death, and loss of choline acetyltransferase (ChAT), an enzyme responsible for the biosynthesis of neurotransmitter acetylcholine which is important for signalling between neural synapses (17, 18, 28).

To investigate whether EV-D68 has a specific tropism towards motor neurons compared to other types of neurons, we infected human pluripotent stem cell (hPSC)-derived spinal motor neurons (sMNs) and Ngn2 cortical neurons co-cultured with astrocytes. We directly compared the cell tropism and replication efficiency of EV-D68 isolates from different clades from before and after 2014. In addition, we investigated the cellular effects of EV-D68 replication on sMNs.

Materials and methods

Cell lines, compounds and recombinant proteins

Rhabdomyosarcoma cells (RD cells) (ATCC) were cultured in Dulbecco's modified Eagle's medium (DMEM; Lonza, Switzerland) supplemented with 10% (vol/vol) fetal calf serum (FCS; Sigma-Aldrich), 100 IU/ml penicillin (Lonza), 100 IU/ml streptomycin (Lonza), and 2 mM L-Glutamine (Lonza), at 37°C with 5% CO_2. Compounds and recombinant proteins were reconstituted according to the manufacturer's protocol.

Human pluripotent stem cells

Human pluripotent stem cells WTC-11 (Coriell no. GM25256, obtained from the Gladstone Institute, San Francisco, CA, USA), were used to generate cortical neurons, astrocytes and sMNs. WTC-11 hPSCs were maintained in hPSCs medium (Table 1), released with Accutase (Life Technologies), and grown on a Matrigel (Corning) -coated 6-wells. Medium was refreshed every other day, and cells were cultured at 37°C and 5% CO_2.

Differentiation of hPSCs to cortical neurons co-cultured with astrocytes

Protocol for the differentiation of hPSCs to cerebral cortex cortical neurons was adapted combining several protocols (29-31). Briefly, hPSCs were directly differentiated into excitatory cortical neurons by forcibly overexpressing the neuronal determinant Ngn-2 (30, 31). Later, hPSC-derived astrocytes were added to the culture in a 1:1 ratio to support neuronal maturation. At day 3, the medium was changed to Ngn2 medium (Table 1). Differentiation of astrocytes was performed as described previously (32). From day 6 onward, half of the medium was refreshed every other day. Cultures were maintained at 37°C and 5% CO_2 throughout the differentiation process.

Differentiation of hPSCs to sMNs

Human pluripotent stem cells were differentiated into sMNs as previously described with slight modification (33, 34). Human pluripotent stem cells were dissociated with Collagenase type IV (ThermoFisher Scientific) to allow formation of small clusters of embryoid bodies. The basic medium for all following steps is referred to as sMNs basic medium (Table 1). The embryoid bodies were cultured in sMNs basic medium supplemented with reagents for promoting sMNs differentitation including Y-27632 (5 µM; Merck Millipore; 688001), SB431542 (40 µM; Tocris Bioscience; 1614), LDN-193189 (0.2 µM; Stemgent; 04-0074-02), and CHIR99021 (3 µM; Tocris Bioscience; 4423). From day 2 medium was changed to sMNs basic medium supplemented with retinoic acid (0.1 µM; Sigma; R2625) and Smoothened Agonist (SAG) (500 nM; Merck Millipore; 566660). From day 7 on sMNs basic medium supplemented with retinoic acid (0.1 µM; Sigma; R2625) and SAG (500 nM; Merck Millipore; 566660) Brain-Derived Neurotrophic Factor (BDNF) (10 ng/ml; Peprotech; CYT-207) and Glial Cell Line-Derived Neurotrophic Factor (GDNF) (10 ng/ml; Peprotech; 450-10B). On day 9, embryoid bodies were dissociated into single cells with 0.05% trypsin (GibcoTM, 25300054). Motor neuron progenitors were subsequently plated on pre-coated Poly-L-Ornithine (Sigma; P2533) and Matrigel-coated glass coverslips or Matrigel (10 ul/ml in KO-DMEM)-coated 24-well plates at 65,000 cells per well in the medium from day 9. From day 14 on sMNs basic medium was supplemented with 10ng/ml BDNF, 10ng/ml GDNF, 20µM N-[N-(3,5-difluorophenacetyl)-l-alanyl]-S-phenylglycine t-butyl ester (DAPT) (20 µM; Tocris Bioscience; 2634). On day 16, Ciliary Neurotrophic Factor (CNTF) (10 ng/ml; Peprotech; 450-13B) was additionally added to sMN basic medium supplemented with 10ng/ml BDNF, 10ng/ml GDNF, 20µM DAPT. From day 17 onwards, the medium was switched to sMNs basic medium supplemented with BDNF, GDNF, and CNTF (each 10 ng/ml, Peprotech) to maintain maturation and long-term culture.

Table 1. List of differentiation media

Name	Reagents with final concentration	Manufacturer
hPSCs medium	Stemflex medium	ThermoFisher Scientific
	100 IU/ml penicillin	Lonza
	100 µg/ml streptomycin	Lonza
	1X RevitaCell	ThermoFisher Scientific
Ngn2 cortical neurons co-cultured with astrocytes medium	Neurobasal medium	ThermoFisher Scientific
	100 IU/ml penicillin	Lonza
	100 µg/ml streptomycin	Lonza
	2 mM glutamine	Lonza
	2% B27 minus RA supplement	ThermoFisher Scientific
	10ng/ml Human Recombinant Neurotrophin-3 (NT3)	Stemcell Technologies
	10 ng/ml brain-derived neurotrophic factor (BDNF)	Prospecbio
	4 µg/ml Doxycycline (DOX)	Sigma
sMNs basic medium	DMEM: Ham's F12	Lonza
	Neurobasal medium	ThermoFisher Scientific
	100 IU/ml penicillin	Lonza
	100 µg/ml streptomycin	Lonza
	1X N2 supplement	ThermoFisher Scientific
	1X B27 minus RA supplement	ThermoFisher Scientific
	1 ul/ml 2-Mercaptoethanol	ThermoFisher Scientific
	0.5 uM ascorbic Acid	Sigma

Viruses

Enterovirus-D68 included in this study were isolated from clinical specimens at the National Institute of Public Health and the Environment (RIVM), Bilthoven, The Netherlands. The clinical specimens were isolated from respiratory samples and were isolated and propagated on RD cells at 33°C in 5% CO_2. The viruses from different clades included in this study, year of isolation, virus reference number and accession number are as follow; clade A (or A1) (2012; 4311200821; MN954536) (21, 35), subclade B2 (2012; 4311201039; MN954539) (21, 35), subclade B1 (2013; 4311300117; MN954538) (21, 35), subclade A2 (or D1) (2018; 4311801122; MN726791), subclade B3 (2019; 3101900710; MN726799) (36). All virus stocks were sequenced to exclude cell culture adaptive mutations.

Virus titration

Virus titers were determined by endpoint dilution on a subconfluent layer of RD cells. Briefly, 10-fold serial dilutions of samples were titrated on RD cells and incubated at 33°C in 5% CO_2. At day 5, virus titers were determined by visual inspection of cytopathic effect. Viral titers were calculated according to the method of Spearman-Kärber and expressed as 50% tissue culture infective dose (TCID50) (37).

Replication kinetics and virus infection

Virus infections were performed by incubating hPSC-derived cultures with virus at a multiplicity of infection (MOI) of 0.1 or 1 at 37°C in 5% CO_2 for 1 hour. Subsequently, the inoculum was removed, after which half fresh and half old medium was added to the hPSCs cultures. Supernatants were collected at the indicated time points.

Immunofluorescent staining

At indicated time points, cells were fixed with 10% formalin for 15 minutes and permeabilized with 1% triton (Sigma; T8787) in PBS for 15 minutes. Cells were blocked with 5% bovine serum albumin (BSA; Aurion) for 30 minutes after which cells were incubated with primary antibodies overnight at 4°C. Cells were washed twice with washing buffer (PBS with 0.1% BSA (Aurion) and incubated with secondary antibodies for 1 hour at room temperature. Primary antibodies and secondary antibodies with used concentrations can be found in Table 2. For apoptosis staining, cells were first incubated overnight with the primary antibodies against cleaved caspase-3 (CC3) at 4°C. Subsequently, cells were incubated with secondary antibodies for 1 hour at room temperature. Then, cells were incubated with rabbit anti-EV-D68 VP1 which was pre-conjugated overnight with Zenon™ Rabbit IgG Labeling Kits Alexa-647 (Invitrogen, z25308) at 4°C. Nuclei were stained by Hoechst (1:1000, Invitrogen, H3570) for 10 minutes at room temperature. Samples were processed using a Zeiss LSM 700 laser scanning microscope. All images were processed using Zen 2010 software and Image J.

Flow cytometry

Spinal motor neuron cultures derived from hPSCs were washed with PBS, released with 0.25% trypsin-EDTA (Gibco) and collected in a V-bottom plate. Live/dead staining was performed (Invitrogen) for 15 minutes at 4°C, after which cells were permeabilized using cytofix/cytoperm (BD Biosciences) for 20 minutes at 4°C and blocked with 10% normal donkey serum for 30 minutes at 4°C. Cells were incubated at 4°C an anti-EV-D68 VP1 antibody and an antibody to detect ChAT (Table1) followed by an incubation with secondary antibodies for 30 minutes. After 3 washing steps, cells were measured on a flow cytometer (BD FACS Lyrics). Data were analyzed using FlowJo 10 software (Ashland, OR, USA).

Table 2. List of antibodies for immunofluorescence and flow cytometry

Antibody	Antibody	Concentration	Manufacturer	Catalogue no.
Primary	Rabbit anti-EV-D68 VP1	10 ug/ml	GeneTex	132313
	Goat anti-ChAT	25 ug/ml	Sigma Aldrich	AB144P
	Guinea pig anti-MAP2	2% v/v	Synaptic Systems	188004
	Rabbit anti-cleaved caspase 3	10 ug/ml	Cell Signalling	9661
Secondary	Donkey anti-rabbit AF488	20 ug/ml	Invitrogen	A21206
	Donkey anti-goat AF555	10 ug/ml	Invitrogen	A21432
	Donkey anti-guinea pig AF647	2.5 ug/ml	Jackson Immuno research	706-605-148

RNA isolation

Samples were lysed in 200 µl Magnapure 96 external lysis buffer (Roche, 63749130031). Next, Agencourt AMPure XP (Berckman Coulter, A63880) beads were added into a 96-well plate. Mixture of lysis buffer and samples were transferred into the AM Pure beads and mixed thoroughly by pipetting up and down followed by an incubation step at room temperature for 15 minutes. Subsequently, the plate containing the beads was placed on a magnetic 96-well block for 3 minutes and the supernatant was removed from the plate. Then 70% ethanol was added and samples were washed three times on the magnetic plate for 30 seconds at room temperature. After the last washing step, the plate was air-dried for 3 minutes. Then, the plate with beads was taken off from the magnetic 96-well block and the beads were resuspended with elution buffer (Roche).

Real-time quantitative PCR to determine viral RNA

Viral RNA was isolated from spinal motor neuron cultures using Magnapure 96 external lysis buffer (Roche, 63749130031). For viral RNA quantification, a real-time TaqMan assay was performed using the Applied Biosystems 7500 real-time PCR system (Thermo Fisher Scientific). The experiments were performed by adding forward and reverse EV-D68 primers (75 pmol/µl) and the probes (10 pmol/µl). Sequences including EV-D68 specific primer and probe used in the study were shown in Table 3. The following reaction conditions were applied for all PCR experiments: 5 minutes at 50°C and 20 seconds at 95°C, followed by 45 cycles at 95°C for 3 seconds, and 60°C for 31 seconds.

Reverse transcriptase quantitative PCR to determined gene expression of host genes

RNA was isolated from the spinal motor neuron cultures using Magnapure 96 external lysis buffer (Roche, 63749130031). RNA was reverse transcribed into cDNA using superscript IV reverse transcriptase (Invitrogen) according to the manufacturer's protocol. Gene expression was determined with gene specific primers (Table 4) using SYBR® Green PCR Master Mix (Life technologies). Gene of interests were normalized to the house-keeping gene beta-Actin.

Table 3. Sequences of EV-D68 primers and probes

Primer/probe	Sequence (5'-3')
Forward primer	TGTTCCCACGGTTGAAAACAA
Reverse Primer	TGTCTAGCGTCTCATGGTTTTCAC
Probe 1	TCCGCTATAGTACTTCG
Probe 2	ACCGCTATAGTACTTCG

Table 4. Gene-specific primers for PCR

Species	Gene	Sequence (5'>3')
human	OCT4	GATGGCGTACTGTGGGCCC
human	OCT4	TGGGACTCCTCCGGGTTTTG
human	SOX2	GGGAAATGGGAGGGGTGCAAAAGAGG
human	SOX2	TTGCGTGAGTGTGGATGGGATTGGTG
human	NANOG	CAGCCCTGATTCTTCCACCAGTCCC
human	NANOG	TGGAAGGTTCCCAGTCGGGTTCACC
human	HB9	GCACCAGTTCAAGCTCAACA
human	HB9	TTTGCTGCGTTTCCATTTC
human	ISL1	TGTTTGAAATGTGCGGAGTG
human	ISL1	GCATTTGATCCCGTACAACC
human	CHAT	TGAGTACTGGCTGAATGACATG
human	CHAT	AGTACACCAGAGATGAGGCT
human	PAX6	GCCCTCACAAACACCTACAG
human	PAX6	TCATAACTCCGCCCATTCAC
human	b-ACTIN	CCCTGGACTTCGAGCAAGAG
human	b-ACTIN	ACTCCATGCCCAGGAAGGAA

Results

No difference in replication efficiency between EV-D68 clinical isolates from before and after 2014 in hPSC-derived sMNs and Ngn2 cortical neuron co-cultures

We investigated the replication efficiency of different EV-D68 isolates in hPSC-derived sMNs and Ngn2 cortical neuron co-cultures (Fig1A, Fig S1). Viruses from before 2014 included A/2012, B2/2012 and B1/2013, and after 2014 included A2/2018 and B3/2019. All virus stocks were sequenced to exclude cell-culture adaptive mutations (21). All EV-D68 isolates except B3/2019 replicated in both hPSC-derived sMNs and Ngn2 cortical neuron co-cultures (Fig 1B and C). Virus titers in the supernatants increased overtime up to 72 hours post infection (hpi) with differences in the replication efficiency among isolates. In hPSC-derived sMNs, although not significant, A2/2018 and B1/2013 replicated more efficiently than A/2012 and B2/2012 (Fig 1B and D). In contrast, in Ngn2 cortical neuron co-cultures, isolate A/2012 replicated more efficiently than A2/2018, B2/2012 and B1/2013, respectively (Fig 1C and E). Altogether, there is no difference in replication efficiency between viruses from before and after 2014 in hPSC-derived sMNs and Ngn2 cortical neuron co-cultures, but the replication efficiency varies among isolates.

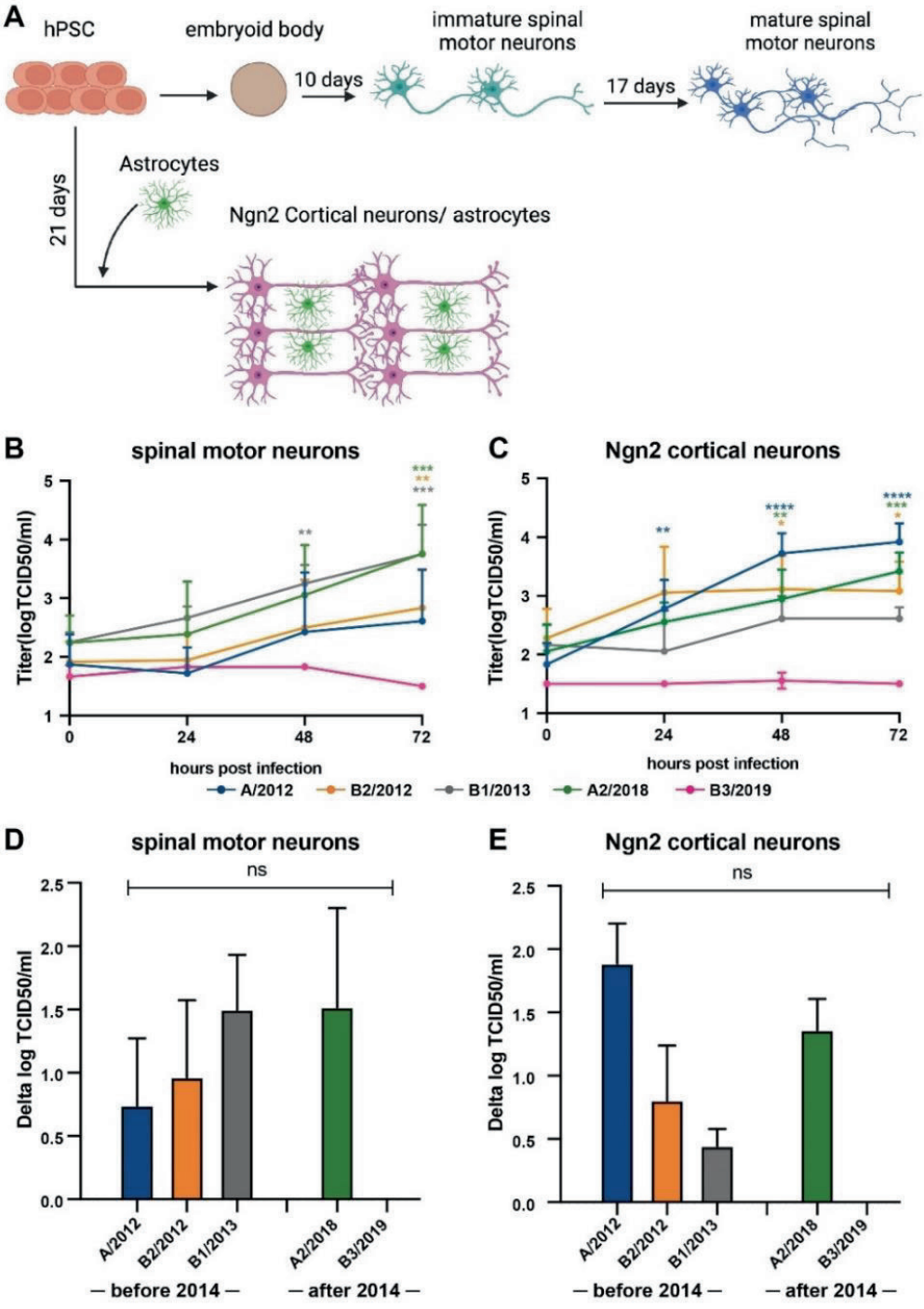
A
hPSC
embryoid body
10 days
immature spinal motor neurons
17 days
mature spinal motor neurons
Astrocytes
21 days
Ngn2 Cortical neurons/ astrocytes
B
spinal motor neurons
Titer(logTCID50/ml)
hours post infection
C
Ngn2 cortical neurons
Titer(logTCID50/ml)
hours post infection
A/2012
B2/2012
B1/2013
A2/2018
B3/2019
D
spinal motor neurons
Delta log TCID50/ml
ns
A/2012
B2/2012
B1/2013
A2/2018
B3/2019
— before 2014 —
— after 2014 —
E
Ngn2 cortical neurons
Delta log TCID50/ml
ns
A/2012
B2/2012
B1/2013
A2/2018
B3/2019
— before 2014 —
— after 2014 —

Fig 1. Replication kinetics of EV-D68 isolates in hPSC-derived sMNs and Ngn2 cortical neuron co-cultures. (A) Schematic illustration of neuronal differentiation. (B) Growth kinetics of EV-D68 isolates in hPSC-derived sMNs and (C) Ngn2 cortical neuron co-cultures at an MOI of 0.1. Statistical analysis was performed using One-Way ANOVA with Dunnett's test, and virus infected samples were compared to input. (D) Differences in logTCID50 virus titer at 72 hpi compared to input in sMNs and (E) Ngn2 cortical neuron co-cultures. Statistical analysis was performed using One-Way ANOVA with Turkey's multiple comparison test. Data represent mean ±SD from at least 3 independent experiments. *, $P \leq 0.05$; **, $P \leq 0.01$; ***, $P \leq 0.001$; ****, $P \leq 0.0001$; ns, not significant; ANOVA, analysis of variance; SD, standard deviation.

EV-D68 isolates infect hPSC-derived sMNs and Ngn2 cortical neuron co-cultures

To investigate the cell tropism of EV-D68 isolates, infected hPSC-derived sMNs and Ngn2 cortical neuron co-cultures were stained for virus antigen VP1 and neuron specific markers at 24 and 72 hpi. All EV-D68 isolates were able to infect $ChAT^+$ motor neurons (Fig 2). In Ngn2 cortical neuron co-cultures, all EV-D68 infected preferentially $MAP2^+$ cortical neurons, and rarely $GFAP^+$ astrocytes (Fig 3A and B). $VP1^+$ cells were observed in sMNs as well as Ngn2 cortical neuron co-cultures infected with B3/2019, even though progeny virus could not be detected in the supernatants of infected cultures (Fig 1B and C). The number of infected cells in both hPSC-derived neural cultures seemed to increased up to 72 hpi (Fig S2, Fig S3).

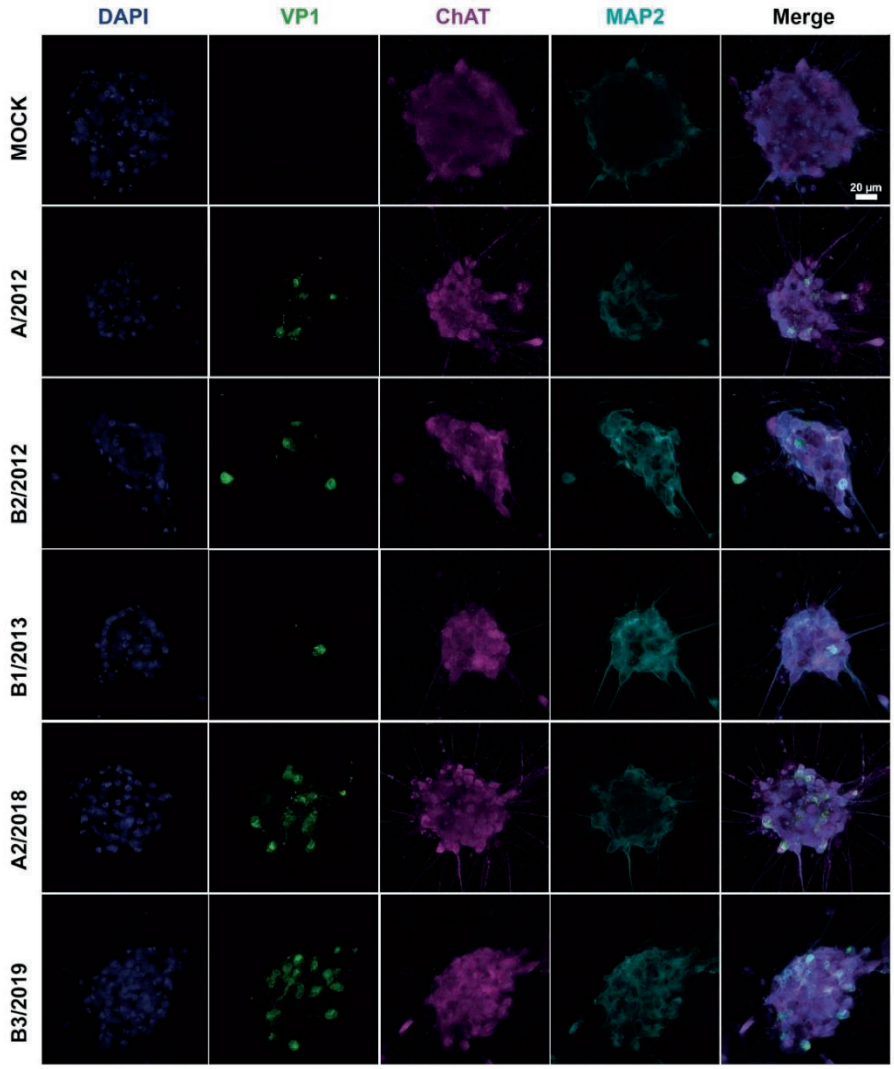

Fig 2. Infection of EV-D68 in hPSC-derived sMNs. Infection of hPSC-derived sMNs with EV-D68 isolates at an MOI of 0.1 at 24 hpi. Motor neurons were fixed and staining for ChAT (magenta), MAP2 (cyan) and EV-D68 VP1 antigen (green). Cells were counterstained with HOECHST (blue) to visualize nuclei. VP1, viral protein 1; ChAT, choline acetyltransferase; MAP2, microtubule-associated protein.

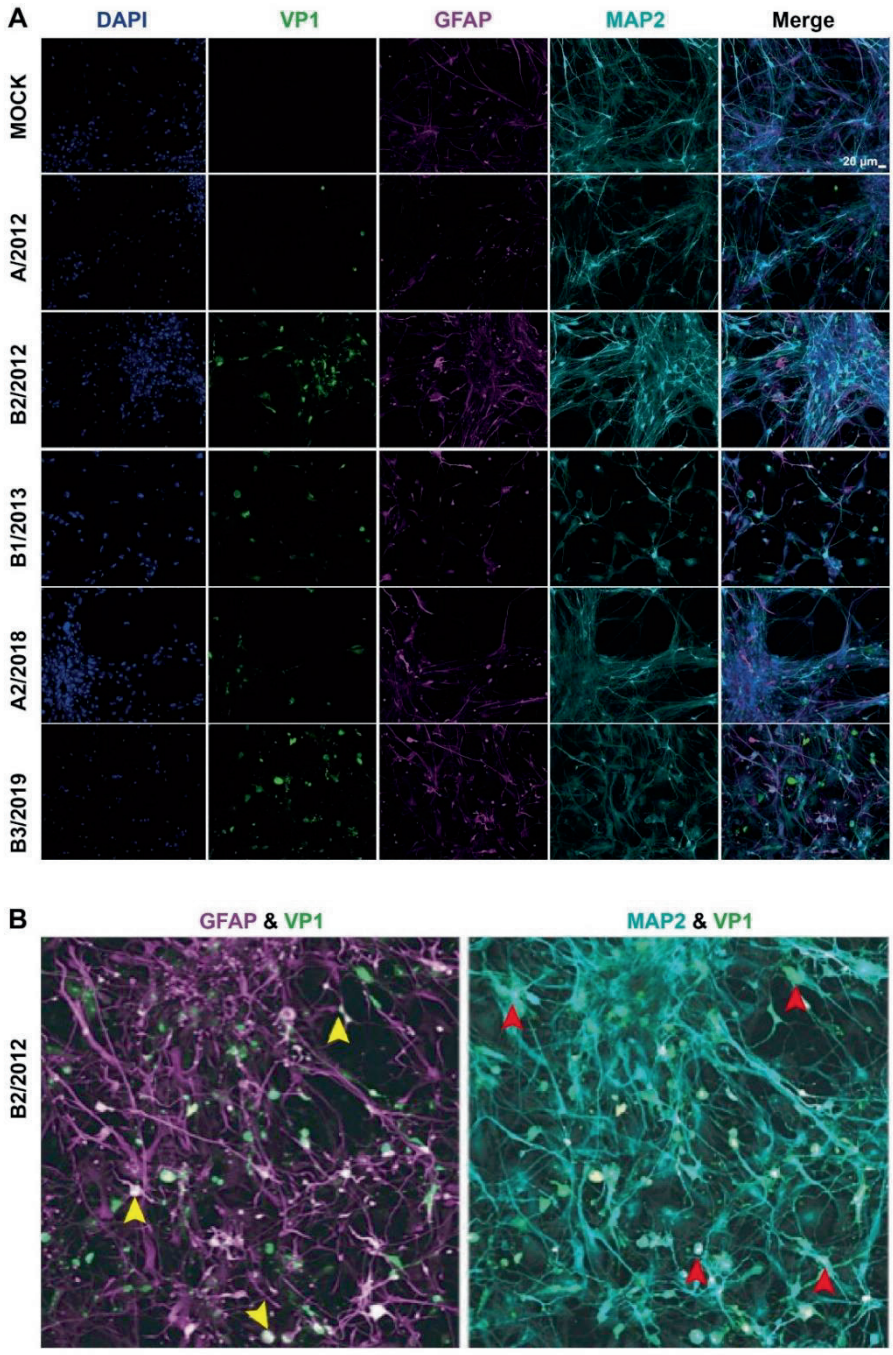

Fig 3. Infection of EV-D68 in hSPC-derived Ngn2 cortical neuron co-cultures. (A) Infection of hPSC-derived Ngn2 cortical neuron co-cultures with EV-D68 isolates at an MOI of 0.1. At 24 hpi, cultures

were fixed and stained for neural marker MAP2 (cyan), astrocytes marker GFAP (magenta) and for EV-D68 VP1 antigen (green). Cells were counterstained with HOECHST (blue) to visualize the nuclei. (B) Left panel, double staining for EV-D68 VP1 and GFAP cells shows infected astrocytes (yellow arrow). Right panel: double staining for EV-D68 VP1 and MAP2 shows infected neurons (red arrow). VP1, viral protein 1; GFAP, glial fibrillary acidic protein; MAP2, microtubule-associated protein.

Infection and replication of subclade B3/2019 in hPSC-derived sMNs

Enterovirus D68 subclade B3/2019 spread through the cultures without an increase of infectious virus in the cultures (Fig 2, S Fig2). To investigate this in more detail, we quantified intracellular RNA at 0, 6, 8, and 24 hpi in hSPC-derived sMNs infected with an MOI 0.1. We included A2/2018 isolate, which replicated to high titers, as a positive control (Fig 1B). An increase of intracellular viral RNA was detected for both isolates, although the replication seemed less efficient after inoculation with B3/2019 compared to A2/2018 (Fig 4A). Next, to understand whether infectious virus particles were formed intracellular, infected sMNs were frozen-thawed 3 times. We determined the virus titers in the supernatants and compared them to the frozen and thawed lysates. A significant increase of infectious virus was observed in the frozen and thawed lysates compared supernatants for both A2/2018 and B3/2019 (Fig 4B). Furthermore, the percentage of infected VP1^{+} cells increased from 24 to 72 hpi (MOI of 1) for both viruses. The percentage of VP1+ increased from 21.6% to 42% for A2/2018 and 12.5% to 27% for B3/2019 at 72 hpi (Fig 4C). Together, these findings suggested that isolate B3/2019 replicates and spreads in the hPSC-derived sMNs, despite a lack of detectable infectious virus in the supernatants.

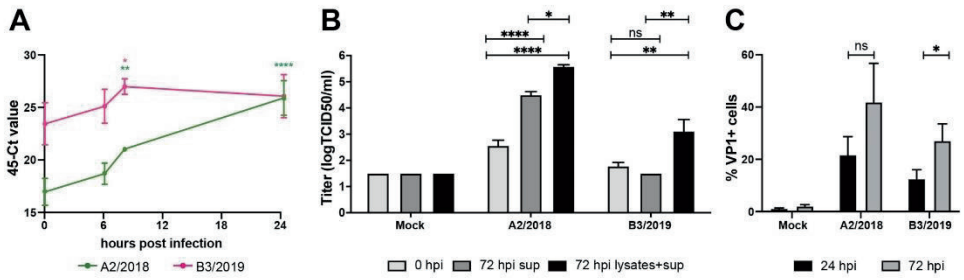

Fig 4. Infection and replication efficiency of A2/2018 and B3/2019 in hPSC-derived sMNs. (A) Intracellular RNA replication of A2/2018 and B3/2019 after infection with an MOI of 0.1. Statistical analysis was performed using One-Way ANOVA with Dunnett's test, compared to 0 hpi. (B) Quantification of intracellular and extracellular virus from A2/2018 and B3/2019 infected (MOI 0.1) sMNs at 72 hpi. (C) Percentage of VP1^{+} cells sMNs infected with A2/2018 and B3/2019 (MOI 1) at 24 and 72 hpi quantified by flow cytometry. Statistical analysis was performed using the One-Way ANOVA with Turkey's multiple comparison test. Data represent mean ± SD from at least 3 independent experiments. *, $P \leq 0.05$; **, $P \leq 0.01$; ****, $P \leq 0.0001$; ns, not significant; ANOVA, analysis of variance; SD, standard deviation; hpi, hours post infection.

EV-D68 infection causes cell death in hPSC-derived sMNs but does not induce CC3.

To investigate whether EV-D68 replication induces cell death in sMNs, the viability of A2/2018 and B3/2019 infected (MOI 1) hPSC-derived sMNs was determined using a live/death staining. At 24 hpi, infection with A2/2018 or B3/2019 resulted in ~60% of death cells compared to 20% in the mock inoculated cultures (Fig 5A). To determine if apoptosis plays a role in virus induced cell death, hPSC-derived sMNs were infected with A2/2018 and B3/2019 (MOI 1) and stained for the apoptosis marker CC3 and VP1 virus antigen at 72 hpi. Cleaved-caspase 3^{+} cells were detected in all cultures, but they did not co-localize with VP1+ in motor neurons (Fig 5B). Together, the findings suggest that EV-D68 infection of hPSC-derived sMNs results in neuronal cell death, independent of apoptosis.

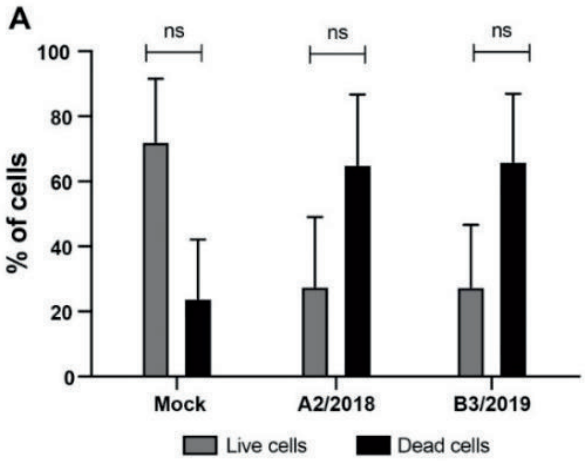

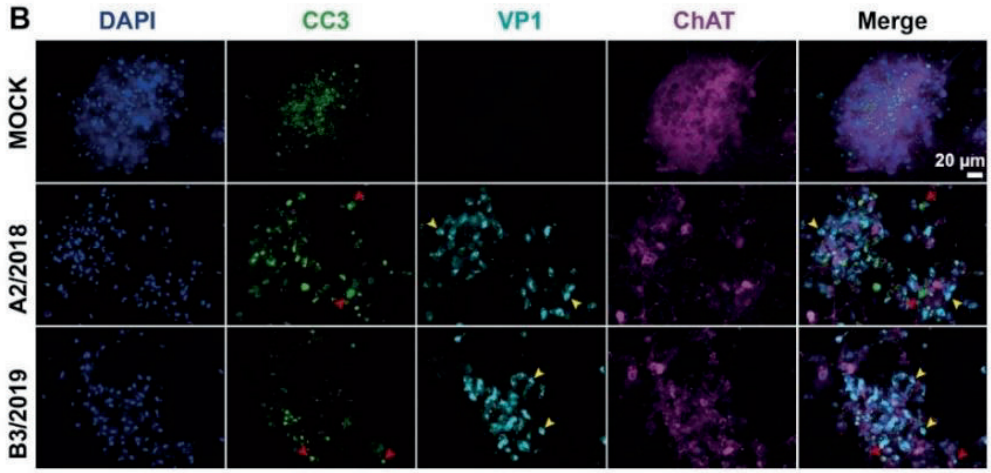

Fig 5. Percentage of live and dead cells, and immunofluorescence staining of CC3 and VP1 virus antigen in EV-D68 inoculated hPSC-derived sMNs. (A) Percentage of live and dead cells after inoculation with A2/2018 and B3/2019 on hPSC-derived sMNs with an MOI of 1 at 72 hpi. (B) Human PSC-derived sMNs were inoculated with A2/2018 and B3/2019 with an MOI of 1. At 72 hpi, the cells were stained for apoptotic marker CC3 (green), VP1 conjugated with ZenonTM rabbit IgG labelling kit Alexa-647 (cyan) and motor neuron marker ChAT (magenta). CC3 staining (red arrow) and VP1 (yellow arrow) did not co-localise. Data shown as a representative from 3 independent experiments. ns, not statistic significant; CC3, cleaved caspase-3; VP1, viral protein 1; ChAT, choline acetyltransferase.

Effect of EV-D68 infection on ChAT mRNA and protein expression

Based on previous findings in EV-D68 inoculated mice show that ChAT expression was lost in the anterior horn of the spinal cord (17, 18), we explored this further in our hPSC-derived sMNs model. To investigate whether the ChAT mRNA expression changes after EV-D68 infection, we performed RT-qPCR. Choline acetyltransferase mRNA expression did not change after inoculation with A2/2018 or B3/2019 (MOI 1, 24 hpi) compared to mock treated cells (Fig 6A). However, ChAT expression on live cells in the cultures, measured by mean fluorescent intensity (MFI), was significantly decreased after inoculation with A2/2018 or B3/2019 compared to mock treated sMNs (Fig 6B and C). The results showed that EV-D68 infection reduces ChAT expression on protein level but not on RNA level in hPSC-derived sMNs at 24 hpi.

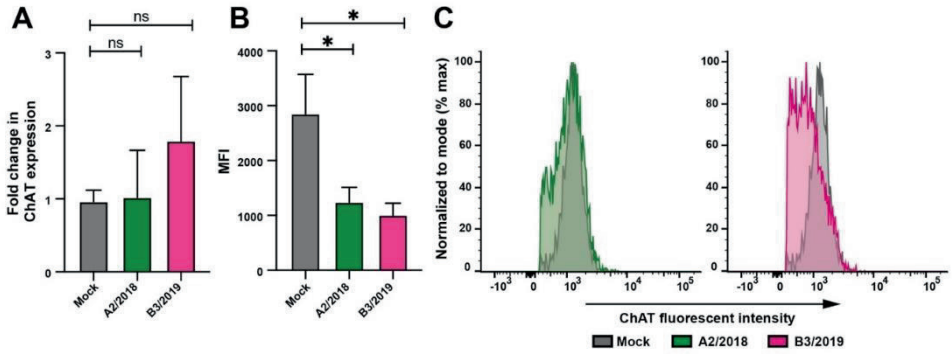

Fig 6. Expression of ChAT in EV-D68 infected inoculated hPSC-derived sMNs. Human PSC-derived sMNs were infected with A2/2018 and B3/2019 at an MOI of 1. (A) mRNA levels of ChAT (fold change over mock). (B) Mean fluorescent intensity of ChAT on live cells after infection with A2/2018 or B3/2019 was measured (10,000 events) by flow cytometry. (C) Histogram of MFI of ChAt expression on infected cells compared to mock treated cells. Statistical analysis was performed using One-Way ANOVA with Turkey's multiple comparison test. Data represent mean ± SD from at least 3 independent experiments. *, $P \leq 0.05$; ns, not statistic significant; MFI, mean fluorescent intensity; ChAT, choline acetyltransferase; ANOVA, analysis of variance; SD, standard deviation.

Discussion

Our study comprehensively compares the neurotropism of EV-D68 isolates from before and after 2014 in relevant hPSC-derived neural models. We did not observe that EV-D68 has a strong preference for motor neurons compared to cortical neurons. Furthermore, our results suggest that there are no differences in the neurotropism between clades or isolates from before and after 2014, but that infection and replication varied among virus isolates. Finally, we showed that EV-D68 infection in hPSC-derived sMNs resulted in decreased expression of ChAT and triggered cell death in sMNs.

In vitro and in vivo data show that EV-D68 has a neurotropic potential when it enters the CNS. Our study shows that EV-D68 infects and replicates both in motor and cortical neurons, which is in line with previous in vitro studies (22, 24, 38). However, in vivo in experimentally inoculated mice and from a human case, EV-D68 targets predominantly motor neurons (16, 17). Our in vitro data suggest that the preferential motor tropism observed in vivo is likely associated with the route of neuroinvasion. It has been suggested that EV-D68 enters the CNS via retrograde axonal transport in peripheral nerves, which would result in direct exposure of motor neurons in the spinal cord (24). In addition, we observed that EV-D68 is able to infect astrocytes co-cultured with cortical neurons. In vivo, EV-D68 viral RNA was detected in non-neuronal cells in the spinal cord of an AFM case which could represent glial cells (16). These findings suggest that non-neuronal cell types might also be susceptible for EV-D68 infection besides neurons.

Enterovirus D68 associated neurological disease does not seem to be clade specific, nor a recently acquired feature since the 2014 outbreak. EV-D68-associated cases of AFM have been reported before 2014, and linked to viruses from different clades (2, 16). This is in line with in vitro findings from others and us that do not report differences in the replication efficiency among EV-D68 clades, or viruses from before and after 2014 in neuronal cells models (17, 21, 22, 24). However, replication and infection efficiency in neural cultures differs among isolates suggesting a role for currently unknown viral factors. For example, one isolate used in this study, B3/2019, was not able to release progeny virus into the supernatant despite virus spread throughout the culture. This suggested that B3/2019 isolate might use a different mechanism to spread from cell to cell compared to other EV-D68 viruses. How and if these differences among isolates affect the (neuro)pathogenesis in vivo as well as the role of individual viral proteins is unclear.

In vivo, EV-D68 infection in sMNs leads to the loss of ChAT expression and subsequent cell death (17, 18). These direct effects of EV-D68 replication in sMNs can contribute to the development of paralysis in vivo. In this study, we showed a decreased in protein levels of ChAT in EV-D68 infected hPSC-derived sMNs already at 24 hpi. Dysregulation of ChAT protein, which is important for the synthesis of neurotransmitter acetylcholine,

might result in neuronal dysfunction and muscle weakness (39, 40). Moreover, we have shown that EV-D68 infection caused sMNs death which was independent of apoptosis. A similar cell death mechanism has been reported in EV-D68 infected primary rat cortical neurons (38). EV-D68 infection resulted in lytic sMNs death when inoculated with a high MOI, but a low MOI did not result in clear cell death despite efficient virus replication within the cultures (24). These observations suggest that release of EV-D68 is not necessarily via a lytic infection, but might also progress through a non-lytic exit pathway, for instance, via extracellular vesicles as observed for other enteroviruses (41-44). Further studies should reveal when and how an EV-D68 infection results in cell death in motor neurons.

Overall, our findings suggest that EV-D68 isolates can infect and replicate in hPSC-derived sMNs and Ngn2 cortical neuron co-cultures in vitro regardless of clade or year of isolation. Furthermore, we show that EV-D68 does not have a specific tropism towards motor neurons in vitro, and that infection of motor neurons can result in reduced expression of ChAT and cell death. This susceptibility of motor neurons for EV-D68, and the associated cellular changes likely contribute to the neuropathogenesis.

Supplementary figures

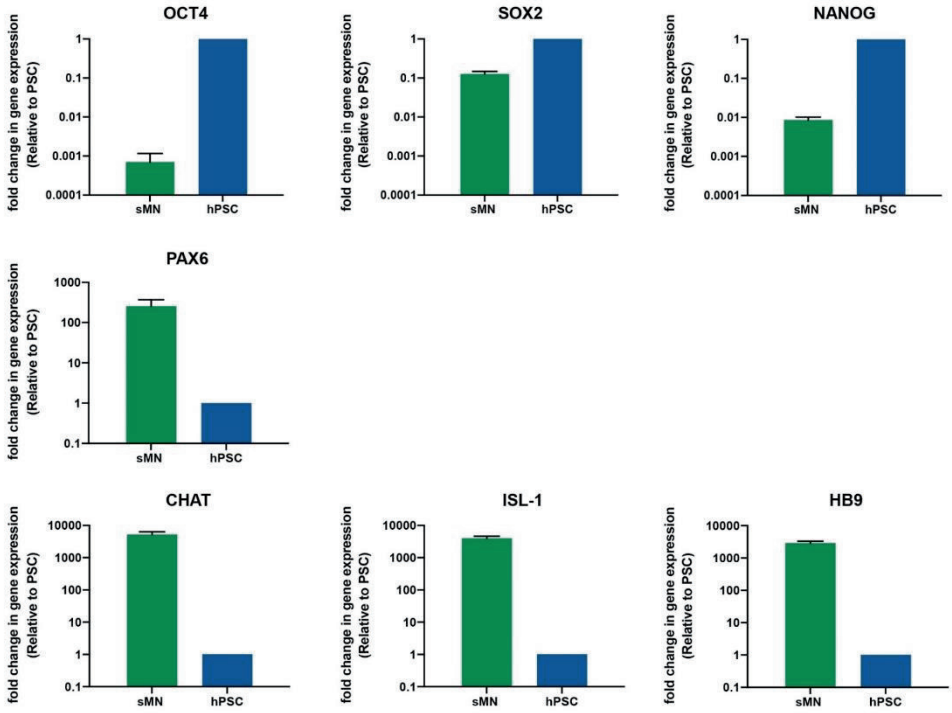

Fig S1. Characterization of hPSC-derived sMNs differentiation by qPCR. Gene expression of sMNs compared to hPSCs was determined by qRT-PCR from. Stem cell markers included OCT4, SOX2, NANOG, differentiation marker included PAX6 and neuron specific markers included choline acetyltransferase (ChAT), ISL-1, HB9.

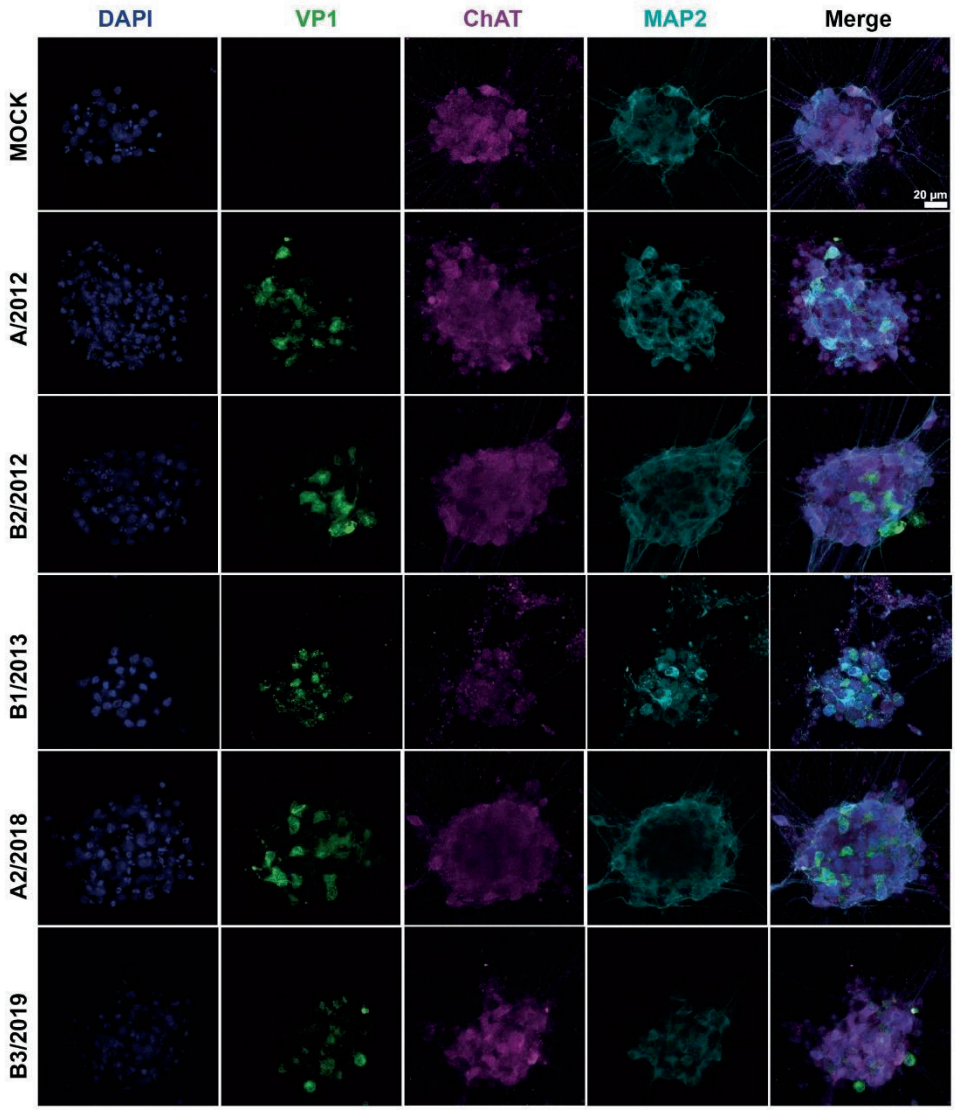

Fig S2. EV-D68 infection of hPSC-derived sMNs at 72hpi. Infection of hPSC-derived sMNs with EV-D68 at an MOI of 0.1, at 72 hours post infection. Infected cells were stained for EV-D68 VP1 antigen (green), Motor neurons were stained for ChAT (magenta) and MAP2 (cyan). Cells were counterstained with HOECHST (blue) to visualize the nuclei. VP1; viral protein 1; ChAT, choline acetyltransferase; MAP2, microtubule-associated protein.

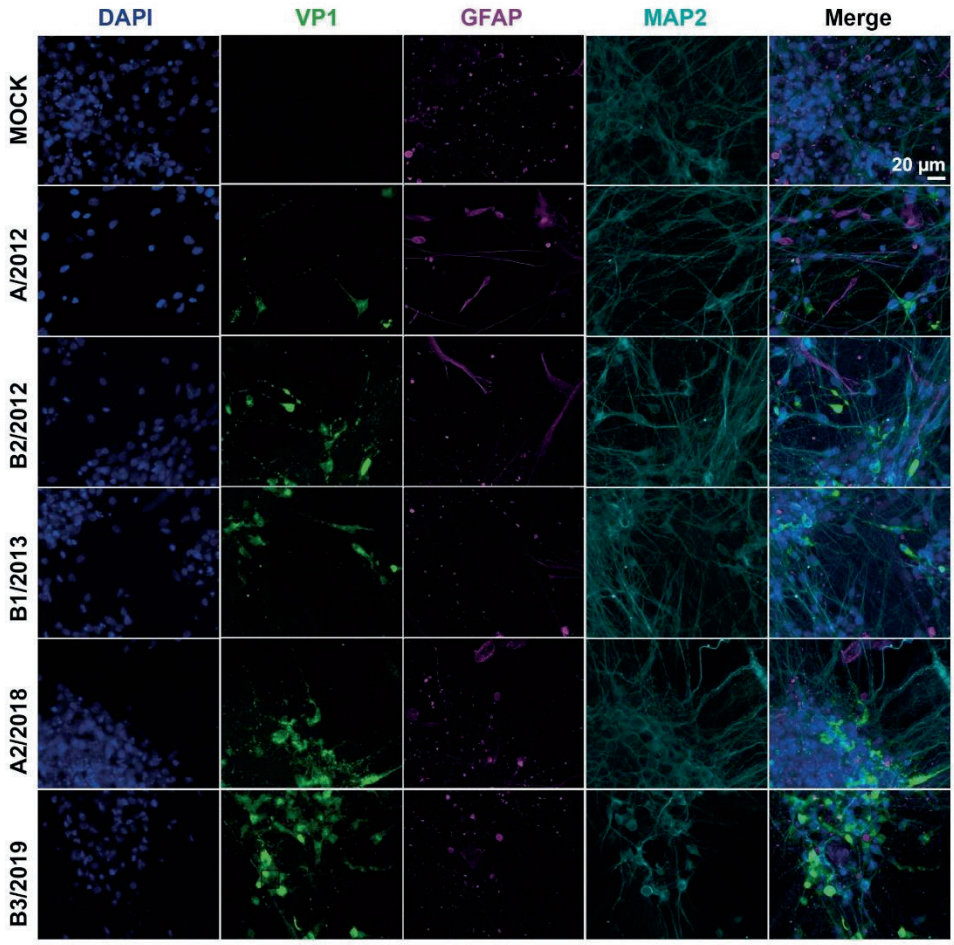

Fig S3. EV-D68 infection of hSPC-derived Ngn2 cortical neuron co-cultures at 72 hpi. Infection of hPSC-derived Ngn2 cortical neuron co-cultured with EV-D68 at an MOI of 0.1, 72 hpi. Infected cells were stained for EV-D68 VP1 antigen (green), neuronal marker MAP2 (cyan), astrocyte marker GFAP (magenta) Cells were counterstained with HOECHST (blue) to visualized the nuclei. VP1, viral protein 1; GFAP, glial fibrillary acidic protein; MAP2, microtubule-associated protein.

References

1. Nino Khetsuriani, Ashley LaMonte-Fowlkes, M. Steven Oberste, Pallansch MA. Enterovirus Surveillance --- United States, 1970--2005. MMWR CDC Surveillance Summaries. 2006;15(55(SS08)):1-20.
2. Greninger AL, Naccache SN, Messacar K, Clayton A, Yu G, Somasekar S, et al. A novel outbreak enterovirus D68 strain associated with acute flaccid myelitis cases in the USA (2012-14): a retrospective cohort study. Lancet Infect Dis. 2015;15(6):671-82.
3. Messacar K, Abzug MJ, Dominguez SR. 2014 outbreak of enterovirus D68 in North America. J Med Virol. 2016;88(5):739-45.
4. Kramer R, Sabatier M, Wirth T, Pichon M, Lina B, Schuffenecker I, et al. Molecular diversity and biennial circulation of enterovirus D68: a systematic screening study in Lyon, France, 2010 to 2016. Euro Surveill. 2018;23(37).
5. Messacar K, Pretty K, Reno S, Dominguez SR. Continued biennial circulation of enterovirus D68 in Colorado. J Clin Virol. 2019;113:24-6.
6. Fall A, Han L, Abdullah O, Norton JM, Eldesouki RE, Forman M, et al. An increase in enterovirus D68 circulation and viral evolution during a period of increased influenza like illness, The Johns Hopkins Health System, USA, 2022. J Clin Virol. 2023;160:105379.
7. Benschop KS, Albert J, Anton A, Andres C, Aranzamendi M, Armannsdottir B, et al. Re-emergence of enterovirus D68 in Europe after easing the COVID-19 lockdown, September 2021. Euro Surveill. 2021;26(45).
8. Yip CCY LJ, Sridhar S, Lung DC, Luk S, Chan KH et al. First Report of a Fatal Case Associated with EV-D68 Infection in Hong Kong and Emergence of an Interclade Recombinant in China Revealed by Genome Analysis. Int J Mol Sci. 2017;16(18).
9. Midgley SE, Benschop K, Dyrdak R, Mirand A, Bailly JL, Bierbaum S, et al. Co-circulation of multiple enterovirus D68 subclades, including a novel B3 cluster, across Europe in a season of expected low prevalence, 2019/20. Euro Surveill. 2020;25(2).
10. Bal A, Sabatier M, Wirth T, Coste-Burel M, Lazrek M, Stefic K, et al. Emergence of enterovirus D68 clade D1, France, August to November 2018. Euro Surveill. 2019;24(3).
11. Messacar K, Schreiner TL, Maloney JA, Wallace A, Ludke J, Oberste MS, et al. A cluster of acute flaccid paralysis and cranial nerve dysfunction temporally associated with an outbreak of enterovirus D68 in children in Colorado, USA. Lancet. 2015;385(9978):1662-71.
12. Pellegrinelli L, Giardina F, Lunghi G, Uceda Renteria SC, Greco L, Fratini A, et al. Emergence of divergent enterovirus (EV) D68 sub-clade D1 strains, northern Italy, September to October 2018. Euro Surveill. 2019;24(7).
13. Wang G, Zhuge J, Huang W, Nolan SM, Gilrane VL, Yin C, et al. Enterovirus D68 Subclade B3 Strain Circulating and Causing an Outbreak in the United States in 2016. Sci Rep. 2017;7(1):1242.
14. Dyrdak R, Grabbe M, Hammas B, Ekwall J, Hansson KE, Luthander J, et al. Outbreak of enterovirus D68 of the new B3 lineage in Stockholm, Sweden, August to September 2016. Euro Surveill. 2016;21(46).
15. Messacar K, Schreiner TL, Van Haren K, Yang M, Glaser CA, Tyler KL, et al. Acute flaccid myelitis: A clinical review of US cases 2012-2015. Ann Neurol. 2016;80(3):326-38.

16. Vogt MR, Wright PF, Hickey WF, De Buysscher T, Boyd KL, Crowe JE. Enterovirus D68 in the Anterior Horn Cells of a Child with Acute Flaccid Myelitis. N Engl J Med. 2022;386(21):2059-60.
17. Hixon AM, Yu G, Leser JS, Yagi S, Clarke P, Chiu CY, et al. A mouse model of paralytic myelitis caused by enterovirus D68. PLoS Pathog. 2017;13(2):e1006199.
18. Morrey JD, Wang H, Hurst BL, Zukor K, Siddharthan V, Van Wettere AJ, et al. Causation of Acute Flaccid Paralysis by Myelitis and Myositis in Enterovirus-D68 Infected Mice Deficient in Interferon alphabeta/gamma Receptor Deficient Mice. Viruses. 2018;10(1).
19. Maloney JA, Mirsky DM, Messacar K, Dominguez SR, Schreiner T, Stence NV. MRI findings in children with acute flaccid paralysis and cranial nerve dysfunction occurring during the 2014 enterovirus D68 outbreak. AJNR Am J Neuroradiol. 2015;36(2):245-50.
20. Brown DM, Hixon AM, Oldfield LM, Zhang Y, Novotny M, Wang W, et al. Contemporary Circulating Enterovirus D68 Strains Have Acquired the Capacity for Viral Entry and Replication in Human Neuronal Cells. mBio. 2018;9(5).
21. Sooksawasdi Na Ayudhya S, Meijer A, Bauer L, Oude Munnink B, Embregts C, Leijten L, et al. Enhanced Enterovirus D68 Replication in Neuroblastoma Cells Is Associated with a Cell Culture-Adaptive Amino Acid Substitution in VP1. mSphere. 2020;5(6).
22. Rosenfeld AB, Warren AL, Racaniello VR. Neurotropism of Enterovirus D68 Isolates Is Independent of Sialic Acid and Is Not a Recently Acquired Phenotype. MBio. 2019;10(5).
23. Sridhar A, Depla JA, Mulder LA, Karelehto E, Brouwer L, Kruiswijk L, et al. Enterovirus D68 Infection in Human Primary Airway and Brain Organoids: No Additional Role for Heparan Sulfate Binding for Neurotropism. Microbiol Spectr. 2022;10(5):e0169422.
24. Hixon AM, Clarke P, Tyler KL. Contemporary Circulating Enterovirus D68 Strains Infect and Undergo Retrograde Axonal Transport in Spinal Motor Neurons Independent of Sialic Acid. J Virol. 2019;93(16).
25. Campbell K. Cortical neuron specification: it has its time and place. Neuron. 2005;46(3):373-6.
26. Martin JA, Messacar K, Yang ML, Maloney JA, Lindwall J, Carry T, et al. Outcomes of Colorado children with acute flaccid myelitis at 1 year. Neurology. 2017;89(2):129-37.
27. Elrick MJ, Pekosz A, Duggal P. Enterovirus D68 molecular and cellular biology and pathogenesis. J Biol Chem. 2021;296:100317.
28. Oda Y. Choline acetyltransferase: the structure, distribution and pathologic changes in the central nervous system. Pathol Int. 1999;49(11):921-37.
29. Bauer L, Lendemeijer B, Leijten L, Embregts CWE, Rockx B, Kushner SA, et al. Replication Kinetics, Cell Tropism, and Associated Immune Responses in SARS-CoV-2- and H5N1 Virus-Infected Human Induced Pluripotent Stem Cell-Derived Neural Models. mSphere. 2021;6(3):e0027021.
30. Frega M, van Gestel SH, Linda K, van der Raadt J, Keller J, Van Rhijn JR, et al. Rapid Neuronal Differentiation of Induced Pluripotent Stem Cells for Measuring Network Activity on Micro-electrode Arrays. J Vis Exp. 2017(119).
31. Zhang Y, Pak C, Han Y, Ahlenius H, Zhang Z, Chanda S, et al. Rapid single-step induction of functional neurons from human pluripotent stem cells. Neuron. 2013;78(5):785-98.
32. Lendemeijer B, Unkel M, Mossink B, Hijazi S, Sampedro SG, Shpak G, et al. Rapid specification of human pluripotent stem cells to functional astrocytes. bioRxiv 2022.08.25.5051662022.

33. Maury Y, Côme J, Piskorowski RA, Salah-Mohellibi N, Chevaleyre V, Peschanski M, et al. Combinatorial analysis of developmental cues efficiently converts human pluripotent stem cells into multiple neuronal subtypes. Nat Biotechnol. 2015;33(1):89-96.
34. Guo W, Naujock M, Fumagalli L, Vandoorne T, Baatsen P, Boon R, et al. HDAC6 inhibition reverses axonal transport defects in motor neurons derived from FUS-ALS patients. Nat Commun. 2017;8(1):861.
35. Meijer A, Benschop KS, Donker GA, van der Avoort HG. Continued seasonal circulation of enterovirus D68 in the Netherlands, 2011-2014. Euro Surveill. 2014;19(42).
36. Midgley SE, Benschop K, Dyrdak R, Mirand A, Bailly JL, Bierbaum S, et al. Co-circulation of multiple enterovirus D68 subclades, including a novel B3 cluster, across Europe in a season of expected low prevalence, 2019/20. Euro Surveill. 2020;25(2).
37. Atkinson GF. The Spearman-Karber Method of Estimating 50% Endpoints. Cornell University. Dept. of Biometrics.: Biometrics Unit Technical Reports;; 1961. Contract No.: BU-141-M.
38. Poelaert KCK, van Kleef RGDM, Liu M, van Vliet A, Lyoo H, Gerber LS, et al. Enterovirus D-68 Infection of Primary Rat Cortical Neurons: Entry, Replication, and Functional Consequences. mBio. 2023:e0024523.
39. Takamori M. Myasthenia Gravis: From the Viewpoint of Pathogenicity Focusing on Acetylcholine Receptor Clustering, Trans-Synaptic Homeostasis and Synaptic Stability. Front Mol Neurosci. 2020;13:86.
40. Rodríguez Cruz PM, Cossins J, Beeson D, Vincent A. The Neuromuscular Junction in Health and Disease: Molecular Mechanisms Governing Synaptic Formation and Homeostasis. Front Mol Neurosci. 2020;13:610964.
41. Gu J, Wu J, Fang D, Qiu Y, Zou X, Jia X, et al. Exosomes cloak the virion to transmit Enterovirus 71 non-lytically. Virulence. 2020;11(1):32-8.
42. Lai JK, Sam IC, Chan YF. The Autophagic Machinery in Enterovirus Infection. Viruses. 2016;8(2).
43. Bird SW, Maynard ND, Covert MW, Kirkegaard K. Nonlytic viral spread enhanced by autophagy components. Proc Natl Acad Sci U S A. 2014;111(36):13081-6.
44. Rudy MJ, Coughlan C, Hixon AM, Clarke P, Tyler KL. Density Analysis of Enterovirus D68 Shows Viral Particles Can Associate with Exosomes. Microbiol Spectr. 2022;10(1):e0245221.

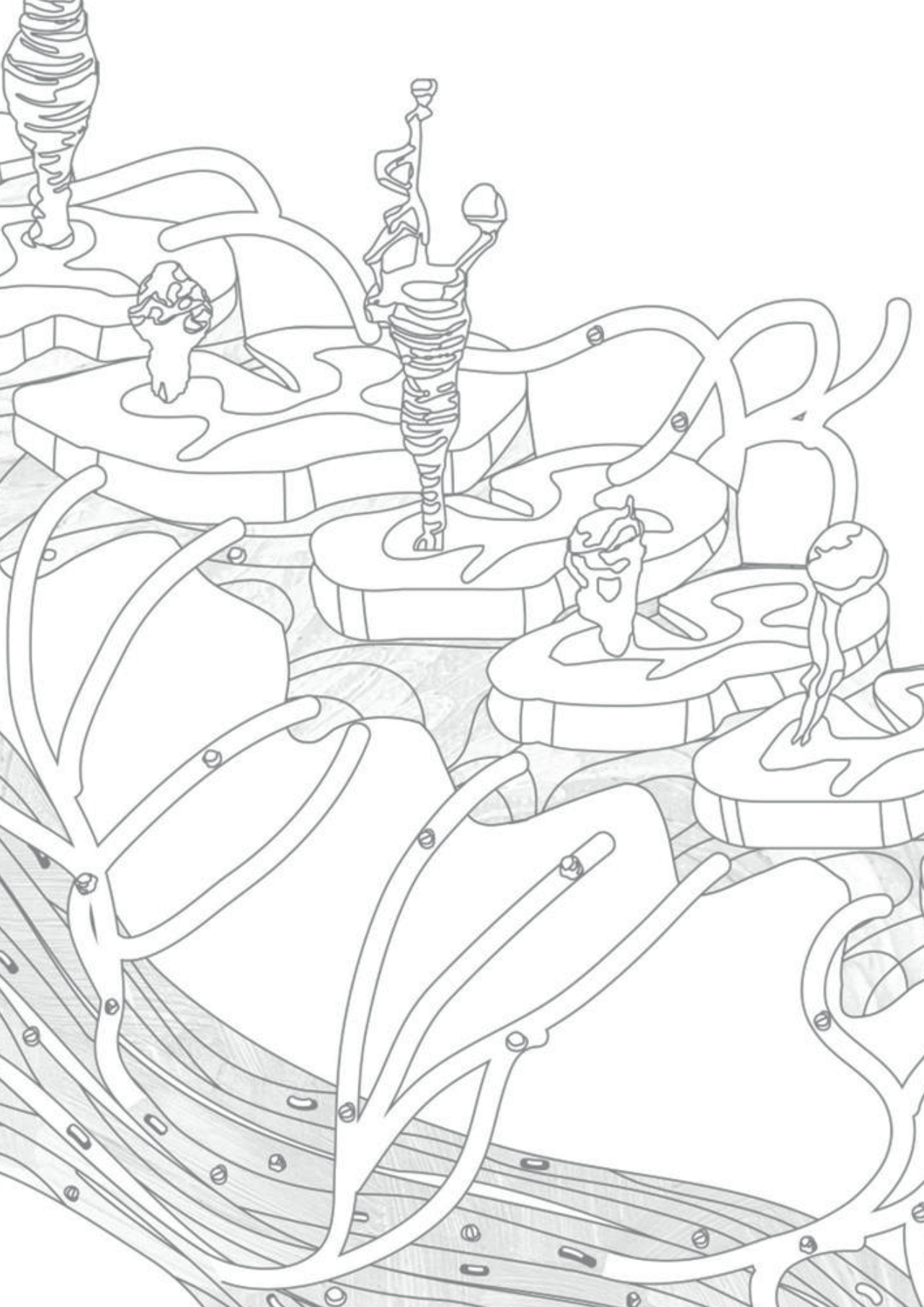

Chapter

5

Detection of intrathecal antibodies to diagnose enterovirus infections of the central nervous system

Syriam Sooksawasdi Na Ayudhya*, Gregorius J. Sips*, Susanne Bogers, Lonneke M.E. Leijten, Brigitta M. Laksono, Leonard C. Smeets, Andrea Bruning, Kimberley Benschop, Katja Wolthers, Debby van Riel, Corine H. GeurtsvanKessel

* These authors contributed equally to this work

J Clin Virol. 2022 Jul; 152:105190.

Abstract

Background

Enterovirus-D68 (EV-D68) predominantly causes respiratory disease. However, EV-D68 infections also have been associated with central nervous system (CNS) complications, most specifically acute flaccid myelitis (AFM). Diagnosing EV-D68-associated CNS disease is challenging since viral RNA is rarely detected in cerebrospinal fluid (CSF).

Objective

In order to determine an EV antibody index (AI), we evaluated the value of a commercially available quantitative ELISA to detect EV-specific antibodies in paired CSF and blood.

Study design

Nine paired CSF and blood samples were obtained from patients with EV-D68-associated AFM or from patients with a confirmed EV-associated CNS disease. EV-specific antibodies were detected using a quantitative ELISA. A Reiber diagram analysis was performed, by which the AI was calculated. Subsequently, EV ELISA results were compared with an EV-D68 virus neutralization test.

Results

ELISA detected EV-specific antibodies in 1 out of the 3 patients with EV-D68-associated AFM and in 3 out of the 6 patients with confirmed EV-associated CNS disease. In these patients, the AI was indicative for intrathecal antibody production against enterovirus. Assay comparison showed that EV-D68 neutralizing antibody detection increased the sensitivity of EV-D68 antibody detection.

Conclusions

A quantitative EV IgG ELISA in combination with Reiber diagram analysis and AI-calculation can be used as a diagnostic tool for EV-associated CNS disease, including EV-D68. An EV-D68 specific ELISA will improve the sensitivity of the tool. With the growing awareness that the detection of non-polio enteroviruses needs to be improved, diagnostic laboratories should consider implementation of EV serology.

Keywords: Enteroviruses; Enterovirus D68; Antibody index; Reiber diagram; Acute Flaccid Myelitis; Serology

Abbreviations

AI: Antibody index
EV: Enteroviruses
Acute Flaccid Myelitis: AFM
Cerebrospinal fluid: CSF
HHV6: Human herpesvirus type 6
HSV1: Herpes simplex virus type 1
HSV2: Herpes simplex virus type 2
JC virus: John Cunningham virus
VZV: Varicella zoster virus
EBV: Epstein-Barr virus
CMV: Cytomegalovirus

Formatting of funding sources

DvR is supported by a fellowship from the Netherlands Organization for Scientific Research (VIDI contract 91718308).

Background

Several enteroviruses (EVs), e.g., Coxsackievirus, Echovirus, EV-A71 and EV-D68, have been associated with central nervous system (CNS) diseases [1]. In 2014, EV-D68 caused outbreaks which were associated with respiratory diseases and neurological complications, including acute flaccid myelitis (AFM) [2, 3]. Since then, EV-D68 causes biennial outbreaks, to a minimal extent in 2020, probably related to COVID-19-related measures [4, 5]. Diagnostics to confirm EV-D68-associated CNS complications are challenging, since viral RNA is rarely detected in cerebrospinal fluid (CSF) [6]. In contrast, EV-D68-specific antibodies have been detected in the CSF of patients with EV-D68-associated CNS complications, which suggests viral invasion. Therefore, the European Non-Polio Enterovirus Network (ENPEN) has recommended to explore reliable detection of intrathecal antibodies against EVs. For this purpose, it is of relevance to study the widely available diagnostic tools [7-12].

When measuring virus-specific antibodies in CSF, it is essential to discriminate between those that are blood-derived and those that are synthesized locally in the CNS [13-15]. During CNS inflammation, the blood-CSF barrier function may be impaired, resulting in leakage of systemic antibodies into the CSF. In addition, decreased CSF flow, or polyclonal antibody expansion in the CNS, can affect the interpretation of CSF serology [16, 17]. By using a Reiber diagram these potential influences can be corrected, increasing the reliability of the antibody index (AI) (Figure 1) [15-18].

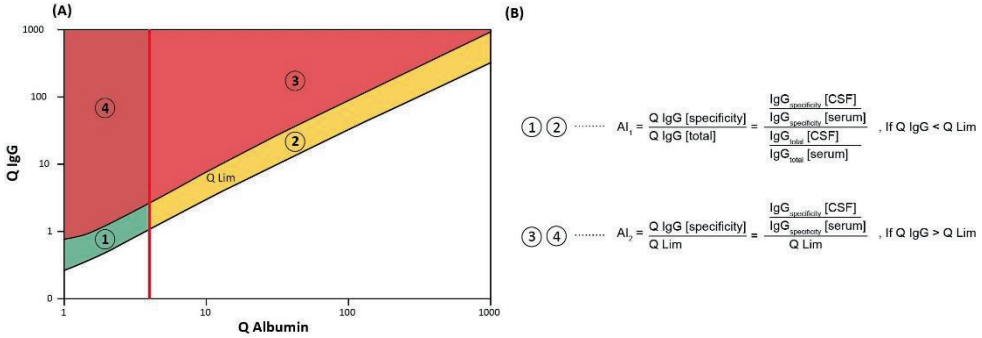

Figure 1. Reiber diagram and antibody index. (A) Reiber diagram illustrates intrathecal IgG synthesis by presenting the IgG CSF-serum quotient (Q IgG) in relation to the albumin CSF-serum quotient (Q albumin), and showing the hyperbolic function with discrimination line (Q Lim) that indicates the upper reference range of Q IgG. The age-dependency for Q Albumin and CSF protein concentration is indicated by the vertical red line [16, 17]. The diagram depicts 4 ranges: 1) Normal IgG, normal blood-CSF barrier; 2) Normal IgG, blood-CSF barrier dysfunction; 3) Intrathecal IgG synthesis, blood-CSF barrier dysfunction; 4) Intrathecal IgG synthesis, normal blood-CSF barrier. (B) Formula to determine the antibody index (AI) depends on the location of Q IgG within the diagram.

Objective

In paired CSF and blood samples from patients with EV-D68-associated AFM, a commercially available, quantitative EV ELISA was evaluated for its value to detect intrathecal antibodies against EVs. To assess the sensitivity of the EV ELISA in detecting EV-D68 specific antibodies, blood samples were tested both with ELISA and an EV-D68 virus neutralization test (VNT).

Study design

Specimen

Paired CSF and blood samples were collected from 3 patients with clinical signs of AFM. EV-D68 RNA was detected in their respiratory samples (EV-D68-AFM-#1-3). Based on clinical signs, patient history and the detection of EV-D68 RNA, these patients were considered as confirmed EV-D68 AFM. In comparison, paired CSF and blood (serum or plasma) samples from 6 patients with confirmed EV-associated CNS disease (EV-CNS-#1-6) were included. To determine the EV-ELISA specificity, 9 paired CSF and blood samples from patients with confirmed non-EV viral encephalitis (NON-EV-CNS) were included (HHV6, HSV1, HSV2, JC virus, parechovirus, VZV, EBV, CMV). Furthermore, blood samples from 4 patients with EV-D68 respiratory diseases were included (EV-D68-RTI-#1-4). Diagnostic specimens were provided by Erasmus MC, Rotterdam and Reinier Haga Medisch Diagnostisch Centrum, Delft, both in the Netherlands.

Serology

EV-specific antibodies were detected with a quantitative ELISA (SERION classic EV IgA, IgG and IgM) according to the manufacturer's protocol (Viron/Serion; Wurzburg, Germany). This CE marked, quantitative ELISA EV IgG has been validated for the detection of intrathecal antibodies in CSF. To assess the EV ELISA sensitivity, we compared the results with those of an EV-D68 specific VNT using blood samples from patients EV-D68-AFM-#2-3 and EV-D68-RTI-#1-4. The micro-neutralization assay was performed with two-fold sample dilution series which were incubated with EV-D68 subclade B3 (Genbank reference MN954541) (100 CCID50/ 60 ul per well) at 37 oC for 1 hour. Next, rhabdomyosarcroma cells (ATCC) in Dulbecco MEM Eagle Medium (Lonza, Basel, Switzerland) supplemented with 1% (V/V) penicillin/streptomycin (Lonza), 1% (V/V) L-Glutamine (Lonza) and 10% (V/V) fetal bovine serum (Lonza) were added to the serum/virus-mix, and incubated at 33 ^{o}C with 5% CO_2. The cytopathic effect was scored at day 5 post-inoculation. Based on assay validation, the cut-off value for positive VNT titer was >1/24.

Reiber diagram analysis and AI calculation

Albumin and total IgG in blood and CSF were measured by nephelometry. The age-dependent albumin CSF-blood quotient and CSF-blood immunoglobulin quotient were determined and analyzed using a Reiber diagram to correct for local synthesis of polyclonal IgG in the CNS. The AI is the ratio between CSF-blood quotient of the virus-specific IgG and total IgG, following Reiber's formula's (Figure 1), with a cut-off value of 1.5 [15-19].

Ethical approval

Ethical approval was obtained from the Erasmus MC Medical Ethics Committee (MEC-2015-306) to anonymously analyze samples of included patients.

Results

In 1 out of the 3 patients with EV-D68-associated AFM, antibodies above the assay cut-off were detected in CSF, and the EV IgG-AI was indicative for intrathecal antibody production against EV (EV-D68-AFM-#1). In patient EV-D68-AFM-#3, EV-specific antibodies were below the assay cut-off, while in patient EV-D68-AFM-#2 EV-specific antibodies were not detected (Table 1); therefore, an AI was not calculated. In patients with EV-confirmed CNS disease, a positive IgG-AI was determined in 3 out of the 6 patients (EV-CNS-#3-5). Altogether, 4 out of the 9 patients with confirmed or suspected EV-associated CNS disease had an AI above 1.5, which is suggestive for EV-specific intrathecal antibody production. The Reiber diagram analysis from all AI-positive patients supported intrathecal antibody production. Use of a corrected formula (depicted in Figure 1, for range 3 and 4) was required based on evidence for polyclonal antibody production in 3 patients (range 4; EV-CNS-#3-5) (Table 1). Non-EV viral encephalitis CSF and blood samples all tested negative in the EV ELISA (Supplementary table 1).

To determine the sensitivity of the EV ELISA, blood samples from patients EV-D68-AFM-#2-3 and patients EV-D68-RTI-#1-4 were tested by an in-house VNT. Overall, EV-D68 neutralizing antibodies were detected more frequently than were EV-specific IgG, IgA or IgM detected by ELISA. In patients EV-D68-AFM-#2-3 and EV-D68-RTI-#2, EV-specific Ig were not detected by the EV ELISA assay, while EV-D68 neutralization antibodies were. In patients EV-D68-RTI-#2 and #4, EV-D68 neutralizing titers increased in time, but this trend was not observed in EV IgA, IgM or IgG titers measured by ELISA (Table 2).

Patient No.	Age	Diagnosis	Clinical specimen for diagnostic EV-PCR	Genotype	Blood sampling (days post diagnostic PCR)	EV ELISA blood	Blood		EV ELISA CSF	CSF		Antibody Index	Reiber diagram area
						IgG (U/ml)	Total IgG (g/ml)	Albumin (g/ml)	IgG(U/ml)	Total IgG (g/ml)	Albumin (g/ml)		
EV-D68-AFM-#1	2y	AFM	nasal wash	EV-D68	0	71.2	7.6	38.8	103.1	0.03	0.2	2.6	2
EV-D68-AFM-#2	1y	AFM	nasal wash	EV-D68	0	<5	n.d	n.d	<5	n.d	n.d	n.d	n.d
EV-D68-AFM-#3	4y	AFM	nasal wash	EV-D68	n.d.	8.8	n.d	n.d	<5	n.d	n.d	n.d	n.d
EV-CNS-#1	2mo	meningitis	CSF	CV-B5	0	<5	n.d.	n.d.	<5	n.d.	n.d	n.d	n.d
EV-CNS-#2	37y	meningitis	CSF	CV-B5	0	41.6	12.3	46.1	46.8	0.05	0.5	0.9	2
EV-CNS-#3	30y	meningitis	CSF	E-5	1	20.4	10.8	47	6.7	0.03	0.2	1.5	4
EV-CNS-#4	30y	meningitis	CSF	E-6#	0	55.7	13.9	64	n.d.	0.03	0.2	2.7	4
EV-CNS-#5	42y	CSF tumor	CSF	n.d.	2	16	7.3	49	12.8	0.03	0.3	2.8	4
EV-CNS-#6	34y	meningitis	CSF	E-9	0	42.7	10.8	53.1	49.2	<0.003*	<0.09*	n.d	n.d

Table 1. Antibody Index (AI) determination in patients with confirmed EV-associated CNS infection or AFM and EV-D68 infections using SERION ELISA classic EV IgG.

Positive (Pos) IgG cut-off is >15.0 U/ml. Equivalent (Eq) IgG is 11.0-15.0 U/ml. Negative (Neg) IgG cut-off is <11.0 U/ml. Y, years old; Mo, months old; CV, Coxsackievirus; E, Echovirus; EV-D68, Enterovirus D68; CSF, cerebrospinal fluid; AFM, acute flaccid myelitis; n.d, not detectable; # determined on feces

Patient No.	Age	Diagnosis	Clinical specimen for diagnostic EV-PCR	Blood sampling (days post diagnostic PCR)	EV ELISA blood						VNT titer
					IgA	IgA (U/ml)	IgM	IgM (U/ml)	IgG	IgG (U/ml)	
EV-D68-AFM-#2	1y	AFM	nasal wash	0	Neg	<4	Neg	<5	Neg	<5	240
EV-D68-AFM-#3	4y	AFM	nasal wash	0	Neg	5.9	Neg	<5	Neg	8.8	768
EV-D68-RTI-#1	50y	RTI	BAL	0	Neg	<5	Pos	22.2	Neg	5.5	768
EV-D68-RTI-#2	61y	RTI	throat swab	0	Neg	<4	Neg	<5	Neg	<5	48
				14	Neg	<4	Neg	<5	Neg	<5	48
				28	Neg	<4	Neg	<5	Neg	<5	96
				41	Neg	<4	Neg	<5	Neg	<5	192
				98	Neg	<4	Neg	<5	Neg	<5	288
EV-D68-RTI-#3	30y	RTI	throat swab	0	Pos	39.5	Pos	15.3	Eq	14.9	288
EV-D68-RTI-#4	61y	RTI	throat swab	6	Neg	4.8	Neg	<5	Neg	5.2	768
				38	Pos	15.1	Neg	<5	Pos	15.7	≥49152
				76	Neg	7.8	Neg	<5	Pos	17.7	≥49152
				93	Eq	10.3	Neg	<5	Eq	14.7	≥49152
				99	Neg	7.7	Neg	<5	Pos	18.1	36864

Table 2. Comparison of SERION ELISA classic EV IgA, IgM, IgG and virus neutralization test (VNT) in blood samples from patients with EV-D68-positive respiratory samples

Positive (Pos) IgG cut-off is >15.0 U/ml. Equivalent (Eq) IgG is 11.0-15.0 U/ml. Negative (Neg) IgG cut-off is <11.0 U/ml. Y, years old; AFM, acute flaccid myelitis; RTI, respiratory tract infection; BAL, bronchoalveolar lavage; EV, enterovirus; VNT, virus neutralization test

Discussion

This study demonstrated that a quantitative EV IgG ELISA combined with a Reiber diagram analysis and AI-calculation can be a useful addition to the diagnostic toolbox when studying EV-D68 associated CNS disease. To increase the sensitivity of EV-D68 specific antibody detection, a specific EV-D68 IgG ELISA should be developed.

Diagnostics for virus-associated CNS complications are challenging, as viral RNA is rarely detected in CSF. Specifically, EV-D68 viral RNA is detected in the CSF of only 3% of AFM cases, which proportion is low compared to other EVs [20]. The detection of intrathecal production of virus-specific antibodies provides indirect evidence for EV infection in CNS [13-15], and is therefore a useful addition to diagnostics. In previous studies, EV-specific antibodies in the CSF of patients with AFM were detected with the use of a peptide microarray [13] or VirScan technique [14], but supporting analyses of blood-CSF barrier function were not included. The lack of such analyses makes it difficult to distinguish virus-specific antibodies found in CSF from, for example, aspecific antibodies derived from polyclonal B cell stimulation in the brain. A Reiber diagram can increase the reliability of the results, but does always require collection of paired CSF and blood samples.

Serum EV IgG, IgM and IgA detection can be used for diagnostics of a respiratory EV infection [21], although samples ideally need to be collected before the start of intravenous immunoglobulin treatment. At the same time, levels of IgG will increase during the course of disease. In this study, all specimens were collected at the moment of initial diagnosis (with still detectable viral RNA), which may explain the relatively low IgG and AI levels. Although IgM and IgA AI can be determined as well, these are considered less sensitive [8, 17].

To our knowledge, there is currently no commercially available EV-D68 specific ELISA. The commercial ELISA that we used contains recombinant antigens from conserved and subtype-specific epitopes of the VP1 of CV-B1, CV-B3 and CV-B5 and E-6 and E-9. According to the manufacturer's information, these epitopes cross-react with other EVs, including EV-D68. However, these VP1-specific epitopes might not be the most immunodominant epitope of EV-D68, resulting in lower detection rates compared to detection of virus neutralizing antibodies. In this study, we have used the assay cut-off recommended by the manufacturer to determine positivity of antibody detection.

Altogether, we show that a quantitative EV ELISA in combination with Reiber diagram analysis and EV AI calculation can be used to detect virus-specific intrathecal antibodies in patients with EV-D68-associated CNS disease. To improve the sensitivity of detection, an EV-D68-specific ELISA with minimal cross-reactivity against other EVs should be developed. Diagnostic laboratories should consider implementing CSF EV serology to support the increasing demand of tools to identify CNS complications caused by non-polio EVs [12].

Supplementary

Supplementary table 1. Antibody Index (AI) determination in PCR confirmed patients with non-EV viral encephalitis (NON-EV-CNS) using SERION ELISA classic EV IgG.

Diagnostic PCR on CSF	IgG CSF	IgG Blood	AI
JC	Neg	Neg	n.d
VZV	Neg	Neg	n.d
HSV2	Neg	22.54	n.d
HSV1	Neg	Neg	n.d
CMV	Neg	Neg	n.d
HHV6	49.88	54.57	1.43
VZV	Neg	Eq	n.d
Parecho	Neg	Eq	n.d
EBV	Neg	Neg	n.d

Positive (Pos) IgG cut-off is >15.0 U/ml. Equivalent (Eq) IgG is 11.0-15.0 U/ml. Negative (Neg) IgG cut-off is <11.0 U/ml.; n.d., not-detectable; AI, Antibody index; Cut-off value of AI > 1.5

References

1. Huang HI, Shih SR. Neurotropic Enterovirus Infections in the Central Nervous System. Viruses. 2015;7:6051-66.
2. Messacar K, Abzug MJ, Dominguez SR. 2014 outbreak of enterovirus D68 in North America. J Med Virol. 2016;88:739-45.
3. Sooksawasdi Na Ayudhya S, Laksono BM, van Riel D. The pathogenesis and virulence of enterovirus-D68 infection. Virulence. 2021;12:2060-72.
4. Messacar K, Pretty K, Reno S, Dominguez SR. Continued biennial circulation of enterovirus D68 in Colorado. J Clin Virol. 2019;113:24-6.
5. [Shah MM, Perez A, Lively JY, Avadhanula V, Boom JA, Chappell J, et al. Enterovirus D68-Associated Acute Respiratory Illness – New Vaccine Surveillance Network,

United States, July-November 2018-2020. MMWR Morb Mortal Wkly Rep. 2021;70:1623-8.
6. [Hopkins SE, Desai J, Benson L. Acute Flaccid Myelitis: A Call for Vigilance and an Update on Management. Pediatr Neurol. 2021;114:26-8.
7. Harvala H, Broberg E, Benschop K, Berginc N, Ladhani S, Susi P, et al. Recommendations for enterovirus diagnostics and characterisation within and beyond Europe. J Clin Virol. 2018;101:11-7.
8. Dorta Contreras AJ. Intrathecal synthesis of immunoglobulins in Neisseria meningitidis and echovirus 6 meningoencephalitis. J Mol Neurosci. 1999;12:81-7.
9. Kaiser R, Dörries R, Martin R, Fuhrmeister U, Leonhardt KF, ter Meulen V. Intrathecal synthesis of virus-specific oligoclonal antibodies in patients with enterovirus infection of the central nervous system. J Neurol. 1989;236:395-9.
10. Roivainen M, Agboatwalla M, Stenvik M, Rysä T, Akram DS, Hovi T. Intrathecal immune response and virus-specific immunoglobulin M antibodies in laboratory diagnosis of acute poliomyelitis. J Clin Microbiol. 1993;31:2427-32.
11. Sojka M, Wsolova L, Petrovičova A. Coxsackieviral infections involved in aseptic meningitis: a study in Slovakia from 2005 to 2009. Euro Surveill. 2011;16.
12. Fischer TK, Simmonds P, Harvala H. The importance of enterovirus surveillance in a post-polio world. Lancet Infect Dis. 2021.
13. Mishra N, Ng TFF, Marine RL, Jain K, Ng J, Thakkar R, et al. Antibodies to Enteroviruses in Cerebrospinal Fluid of Patients with Acute Flaccid Myelitis. mBio. 2019;10.
14. Schubert RD, Hawes IA, Ramachandran PS, Ramesh A, Crawford ED, Pak JE, et al. Pan-viral serology implicates enteroviruses in acute flaccid myelitis. Nat Med. 2019;25:1748-52.
15. Shamier MC, Bogers S, Yusuf E, van Splunter M, Ten Berge J, Titulaer M, et al. The role of antibody indexes in clinical virology. Clin Microbiol Infect. 2021.
16. Reiber H, Peter JB. Cerebrospinal fluid analysis: disease-related data patterns and evaluation programs. J Neurol Sci. 2001;184:101-22.
17. Reiber H, Lange P. Quantification of virus-specific antibodies in cerebrospinal fluid and serum: sensitive and specific detection of antibody synthesis in brain. Clin Chem. 1991;37:1153-60.
18. Reusken C, Boonstra M, Rugebregt S, Scherbeijn S, Chandler F, Avšič-Županc T, et al. An evaluation of serological methods to diagnose tick-borne encephalitis from serum and cerebrospinal fluid. J Clin Virol. 2019;120:78-83.
19. Schwenkenbecher P, Skripuletz T, Lange P, Dürr M, Konen FF, Möhn N, et al. Intrathecal Antibody Production Against Epstein-Barr, Herpes Simplex, and Other Neurotropic Viruses in Autoimmune Encephalitis. Neurol Neuroimmunol Neuroinflamm. 2021;8.
20. Lopez A, Lee A, Guo A, Konopka-Anstadt JL, Nisler A, Rogers SL, et al. Vital Signs: Surveillance for Acute Flaccid Myelitis - United States, 2018. MMWR Morb Mortal Wkly Rep. 2019;68:608-14.
21. Boman J, Nilsson B, Juto P. Serum IgA, IgG, and IgM responses to different enteroviruses as measured by a coxsackie B5-based indirect ELISA. J Med Virol. 1992;38:32-5.

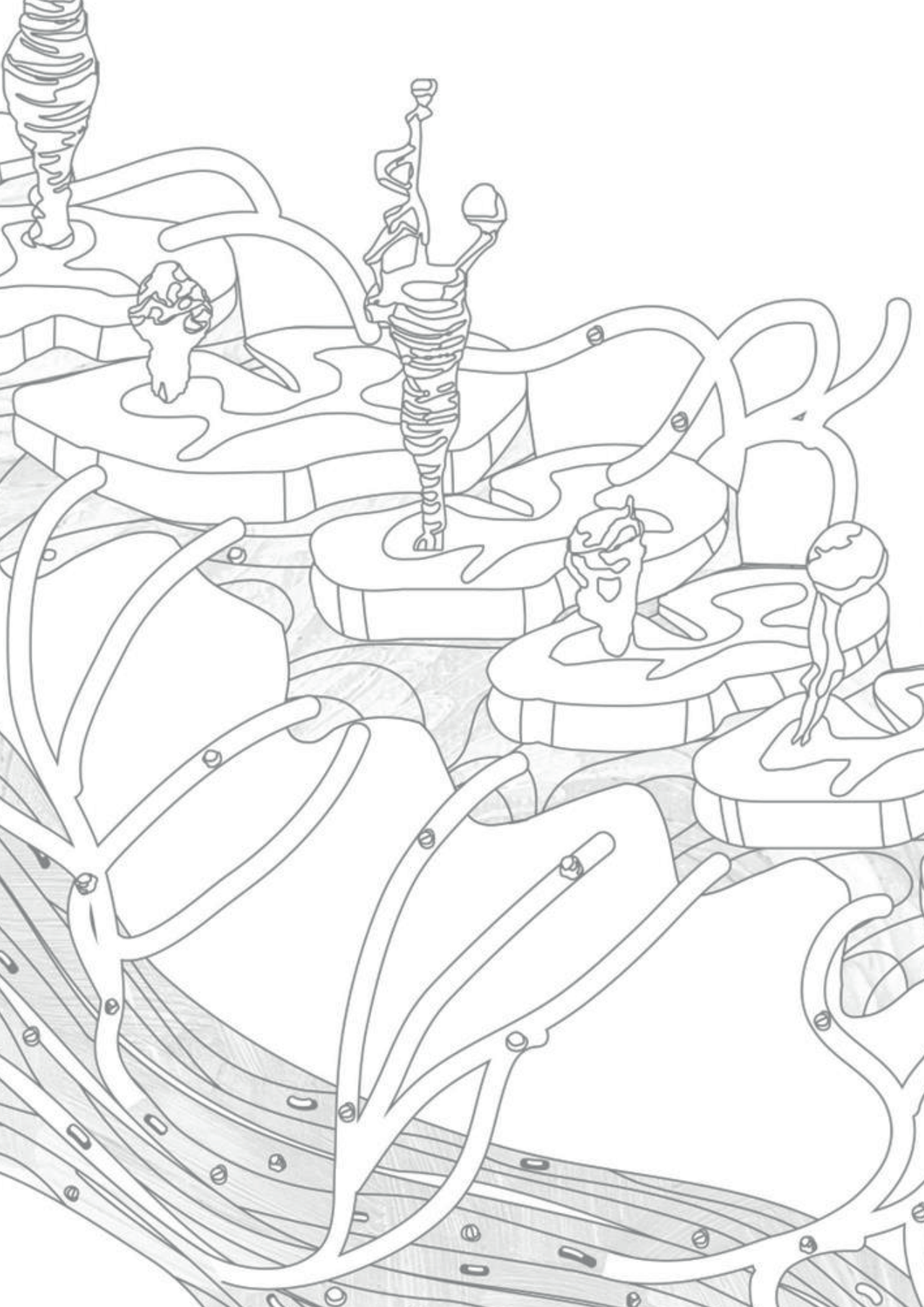

Chapter

6

General discussion

Historically, Enterovirus D68 (EV-D68) infections were primarily associated with mild respiratory diseases and rarely resulted in severe respiratory complications. However, since 2014, EV-D68 has caused worldwide outbreaks with clinical manifestations of severe respiratory disease and occasional neurological complications. These outbreaks raised significant concerns, particularly due to the emergence of acute flaccid myelitis (AFM), a neurological complication resembling polio-like myelitis. This thesis aims to provide fundamental insights into the systemic pathogenesis of EV-D68 by utilizing various in vitro models. Additionally, the thesis evaluates diagnostic techniques for detecting EV-D68 infection in the central nervous system (CNS).

Systemic dissemination of EV-D68

Although the respiratory tract serves as the primary replication site of EV-D68, the development of extra-respiratory complications, including AFM, relies on the systemic spread of the virus into the circulation (viremia). This is similar for other EVs, such as poliovirus and EV-A71, where the development of viremia is critical for virus spread to other tissues, including the brain and spinal cord (1, 2).

The mechanism of which EV-D68 spreads from its primary replication site, the respiratory tract, into the circulation remains unclear. EV-D68 might disseminate into the blood directly from the respiratory tract by disrupting the respiratory epithelial-endothelial barrier, via basolateral release of virus from respiratory epithelial cells, or through direct infection of pulmonary endothelial cells (3). Enterovirus D68 is known to cause destruction of ciliated respiratory epithelial cells of the upper airway in a human primary epithelial cell model, suggesting that the integrity of the epithelial-endothelial barrier could be damaged during EV-D68 infection (4). However, it has not been studied whether EV-D68 can be released from the basolateral side of epithelial cells, or if it can infect endothelial cells, thereby releasing progeny virus from pulmonary endothelial cells directly into the circulation.

In addition to direct virus spill over from the respiratory tract into the circulation, I hypothesized that immune cells might play a role in the development of an EV-D68 viremia. In **chapter 2**, I have shown that B cells are permissive for EV-D68. The data suggest that activated B cells, which are located in lymphoid tissues, facilitate EV-D68 replication and subsequently release into the circulation. This finding aligns with the detection of EV-D68 viral RNA in the lymph nodes of experimentally EV-D68-inoculated ferrets and cotton rats (5, 6). Moreover, a previous study revealed the susceptibility and permissiveness of splenic B cells in the marginal zone of the white pulp to another EV, coxsackievirus B3 (7). Overall, the findings suggest that activated B cells in lymphoid tissues are involved in facilitating the replication of EVs, and potentially contributing to the development of viremia.

Enterovirus D68 could reach activated B cells within lymphoid tissues either cell-free or cell-associated. Once the virus has disseminated from the respiratory tract into the

circulation, it enters lymphoid tissues, where it encounters activated B cells. In addition to direct dissemination, I have shown that immature dendritic cells can pick up and transmit EV-D68 to B cells resulting in virus infection in autologous B cells **(Chapter 2)**. Previous in vitro and in vivo studies have revealed that dendritic cells can carry and transmit EV-A71 to target cells or tissues through the lymph nodes and peripheral blood (8, 9). Further research should investigate the role of immune cells and specifically B cells and dendritic cells in contributing to the systemic dissemination of EV-D68.

Neuroinvasion and neurotropism of EV-D68

Acute flaccid myelitis is the most frequently reported neurological complication associated with EV-D68 infection (10, 11). In line with this clinical manifestation, EV-D68 exhibits a strong tropism for spinal motor neurons in vivo which results in loss of motor neurons in the spinal cord (12-14). The loss of motor neurons corresponds to a distinct pattern of limb paralysis observed in mice intramuscularly inoculated with EV-D68, starting in the lumbar region within the ipsilateral anterior horn adjacent to the injection site, followed by involvement of the contralateral anterior horn, and eventually extending to the cervical spinal cord (15). In mouse models, different routes of EV-D68 inoculation (intracerebral, intraperitoneal, intramuscular, and intranasal) resulted in the infection in the spinal cord without evidence of efficient virus infection and replication in other parts of the CNS (12, 14). Although less frequently, there have also been reports on non-AFM neurological complications and related neurological diseases in the brain caused by EV-D68 in humans, including encephalitis, meningoencephalitis and meningitis (16-19). Therefore, I investigated whether EV-D68 has a specific tropism for motor neurons and how this leads to loss of function. I conducted a side-by-side comparison of the replication and infection efficiency of EV-D68 isolates in human pluripotent stem cell (hPSC)-derived spinal motor neurons and cortical neurons co-cultured with astrocytes (Chapter 4). The study revealed that both hPSC-derived spinal motor neurons and cortical neurons are both susceptible and permissive to EV-D68 infection independent of virus isolates **(Chapter 4)** (12, 20). This suggests that EV-D68 does not have a specific tropism towards motor neurons in vitro, but that other factors determine tropism for motor neurons in vivo.

The route of neuroinvasion could determine the in vivo cell tropism in the CNS and thereby most commonly associated neurological disease, AFM. It is likely that EV-D68, like poliovirus, enters the CNS via spinal nerves. For this, EV-D68 would first have to spread systemically, and subsequently infect skeletal muscle cells from where EV-D68 could be transmitted to motor neurons via the neuromuscular junction. Inside the nerve endings of the motor neurons, virus will spread to the soma of the motor neurons in the spinal cord via retrograde axonal transport (21, 22). As such, the detection of EV-D68 primarily in spinal motor neurons in vivo may be correlated to the route of neuroinvasion rather than a specific tropism for spinal motor neurons.

The functional receptor(s) for EV-D68 on cells of the CNS remains inconclusive. Although sialic acids have been identified as a functional receptor for EV-D68 in vitro, research has shown that EV-D68 can enter CNS cells independent of sialic acids (20, 21, 23). However, sialic acids on N-glycans or glycosphingolipids facilitate infection in primary rat cortical neurons (24). This finding aligns with my study in **chapter 3**, where sialic acids facilitate EV-D68 infection of neuroblastoma cells. In addition to sialic acids, the neuron-specific intercellular adhesion molecule 5 (ICAM-5), which belongs to the immunoglobulin superfamily, has also been identified as a functional receptor for EV-D68 in vitro (25). However, ICAM-5 is not expressed on cells in the spinal cord or on axon termini of motor neurons, indicating that ICAM-5 cannot function as a receptor for EV-D68 on motor neurons (21). As multiple enteroviruses, including poliovirus, rhinovirus, and coxsackie B virus, bind to members of the immunoglobulin superfamily (26), it cannot be excluded that other members of the immunoglobulin superfamily with a structure similar to ICAM-5 might play a role as functional receptor for EV-D68 infection on neurons.

Neurovirulence of EV-D68

The neurovirulent potential of EV-D68 has been investigated in postmortem spinal cord tissue, in vivo animal models, and by imaging. The most prominent pathological change of EV-D68 infection in the CNS is the loss of motor neurons in the anterior horn of the spinal cord (11, 14). Similar to lesions reported from postmortem and in vivo models, magnetic resonance imaging showed lesions in the anterior horn of the spinal cord, particularly in cervical regions and upper thoracic regions, and electrodiagnostic studies showed a motor neuropathy and functional deficit (11). Here, I will discuss mechanisms associated with neuronal dysfunction and death in motor neurons, and dysregulated immune response that might contribute to the neurovirulence of EV-D68.

Mechanisms underlying virus-induced neuronal dysfunction and cell death

Although it is well described that EV-D68 targets motor neurons and predominantly results in the development of AFM, little is known about the underlying mechanisms inducing neuronal dysfunction and degeneration. In general, several mechanisms have been identified to contribute to virus-associated neuronal dysfunction, although it has not been studied comprehensively for EV-D68.

Virus-induced cell death, either via lysis of infected cells or activation of apoptotic cell death, are likely contributors to the development of clinical disease. Apoptosis in CNS cells is triggered by several neurotropic viruses, such as poliovirus, West Nile virus, and human immunodeficiency virus (HIV) (27-29). However, in vitro, EV-D68-associated cell death in motor neurons and primary rat cortical neurons is independent of the apoptosis pathway **(Chapter 4)** (24). This is consistent with the negative staining of caspase-3 in the anterior horn of the spinal cord of a fatal AFM patient (16). These findings suggest a potential role for non-apoptotic cell death, including necroptosis, autophagic cell death, and pyroptosis, in exacerbating neuronal dysfunction (24, 30, 31).

Virus infection in the nervous system can change the synaptic function. For example, simian immunodeficiency virus infection in the brain of rhesus monkeys reduces choline acetyltransferase (ChAT) in the synapses leading to synaptic dysfunction and neuronal dysfunction. This could explain HIV-associated dementia in humans (32, 33). In this thesis, I have shown that EV-D68 infection results in a decrease of ChAT expression in motor neurons **(Chapter 4)** (12, 14). The underlying mechanism on how EV-D68 reduces ChAT expression and possibly dysregulates synaptic and neuronal functioning, and eventually contribute to clinical disease, remains inconclusive.

Alterations in axonal transport could be another potential mechanism that can lead to neuronal dysfunction. Neurotropic viruses, including poliovirus, can dysregulate the activity of protein kinases and phosphatases which are important for the activity of kinesin and dynein, microtubule proteins responsible for axonal transport in neural cells (34, 35). In vitro, EV-D68 utilized retrograde axonal transport in motor neurons (21), however, whether and how the virus dysregulates axonal transport has yet to be investigated.

Overall, future studies should focus on the mechanism of cell death as well as how EV-D68 triggers neuronal dysfunction possibly via decreased ChAT expression or disrupted axonal transport in the acute and post-acute phase. This knowledge will also enhance the understanding on the long-term consequences of AFM, where people suffer from motor deficits, despite functional improvement.

Virus-induced immunopathogenesis

The neuroinflammatory response in EV-D68 infection in the CNS, including the role of glial cells like microglia and astrocytes, remains largely unknown. An autopsy of a patient with EV-D68 found positive staining of EV-D68 antigen in non-neuronal cells, which could represent glial cells (36). Whether glial cells are susceptible to EV-D68 and/or able to trigger neuroinflammatory response remains elusive.

Another autopsy report of an AFM patient revealed that EV-D68-infected motor neurons in the anterior horn of the spinal cord were surrounded by immune cells such as CD68+ macrophages and CD8+ cytotoxic T cells and also showed perforin staining in the neurons. Furthermore, genes associated with the antigen presentation MHC-I pathway were upregulated in inflamed areas compared to non-inflamed areas. These findings indicate the role of the immune response in causing death of motor neurons, and eventually leading to paralysis (36). Together, in vivo cell death of motor neurons could be the direct result from an EV-D68 infection and/or the associated immune response.

Comparison of the neuropathogenesis among EV-D68 clades

Prior to 2014, multiple clades of EV-D68 were endemic in different countries and mainly caused mild respiratory diseases (37-39). During that period, EV-D68 infection caused by different clades, including clade A, B1 and C, only very rarely were associated with

neurological complications (10, 36, 40). In the 2014 outbreak in the United States, subclade B1 was the most prevalent and associated with severe respiratory diseases and AFM (10, 41). It was initially thought that neuropathogenesis of EV-D68 is a recent acquired feature and correspondent to subclade B1. However, other subclades, namely A2 (or D1) and B3, were also associated with neurological complications, including AFM, during EV-D68 outbreaks in 2016 and 2018 (10, 17, 42-45).

Similar to clinical and epidemiological findings, several virological studies including those described in **Chapters 3 and 4** have shown that the ability of EV-D68 isolates to infect CNS cells in vitro or to cause CNS disease in vivo is not a clade-specific feature (12, 20, 21). During the 2014 outbreak, the investigation examining the relationship between genetic analysis and clinical diseases revealed no significant correlation between EV-D68 genetic variation (including clades or individual mutations) and clinical outcomes (46). In addition, I have shown that viruses from before and after 2014 do not differ in their tropism in motor neurons and cortical neurons **(Chapter 4)**. Interestingly, discrepancies in the infection and replication efficiency were observed among EV-D68 isolates which were independent of clade or year of isolation **(Chapter 3 and 4)**, suggesting that viral factors might contribute to EV-D68 infection in the CNS.

Viral factors associated with neuropathogenesis of EV-D68

Genetic changes in different parts of the enterovirus genome have been shown to contribute to the neurovirulence. For example, genetic changes in the internal ribosomal entry site (IRES) in 5'UTR region, which is important for virus replication and translation, is associated with the neurovirulence of poliovirus and EV-A71 in vivo (47, 48). Several in vitro and in vivo studies of amino acid substitutions in the non-structural proteins, such as the 2A or 3C protein were shown to play a key role for virulence determination of EV-A71, and structural capsid protein VP1 affected receptor usage for virus binding to cell surface receptor which contribute to the neurovirulence of EV-A71 (49-54).

The role of genetic changes in emergence of neurotropic potential of EV-D68 remains inconclusive. Several studies have suggested a role for specific viral proteins or locations in these proteins. These include specific amino acid substitutions in VP1, VP2, and VP3 capsid proteins, the 3D RNA-dependent RNA polymerase, or nucleotide substitutions in the IRES which are present in viruses from subclade B1 of the 2014 outbreak in which some of those are also present in other neurotropic enteroviruses, like poliovirus and EV-A71 (10, 42). Furthermore, amino acid substitutions in non-structural proteins are present that affect the protease cleavage efficiency and thereby increase virus replication and transmission (55). However, these amino acid substitutions are not consistently associated with EV-D68 isolates from AFM cases. For example, specific amino acid substitutions in subclade B1 isolated from AFM patients, were not found in subclade B3 viruses which also were associated with cases of AFM (56). Furthermore, the amino acid substitutions observed in isolates from subclade B1

in 2014, which coincided with those in other neurotropic EVs, were not found in isolates from subclade B3 in 2016 and 2018 (57). Comparative in vitro and in vivo analyses using reverse genetic viruses that contain specific amino acid substitutions should unravel which viral factors are associated with neuropathogenesis of EV-D68.

5'UTR region of EV-D68 genome has been suggested to play a role in neurovirulence of EV-D68 infection. Sequencing of 2014 outbreak isolates showed variations in the 5' UTR region of the genome compared to the historical Fermon strain (58, 59). Genetic and structure changes in the IRES in 5'UTR region of contemporary EV-D68 isolates results in increased IRES activities in neuronal and lung cell lines. It could be that the changes in 5'UTR might increase neurovirulence in contemporary isolates of EV-D68 by improving the efficiency of translation and/or replication in neural tissues as previously shown by other enteroviruses. However, the genetic change in the IRES region did not affect the viral growth in neuronal cell line (60). Future research should be determined the effect of mutation in IRES and IRES activity in contributing to neurovirulence in vivo.

Among various proteins, EV-D68 2A protein has been identified as a viral factor contributing to neurovirulence in vivo. A recent study conducted on mice intramuscularly inoculated with EV-D68 highlighted the significance of the EV-D68 2A protein in causing paralysis. The neurovirulence induced by the EV-D68 2A protein was effectively inhibited through prophylactic treatment with Telaprevir, a 2A protease inhibitor. Collectively, this treatment led to a decrease in viral titers and apoptotic activity in both the muscles and spinal cord, and eventually to improvement of paralysis outcomes (15).

Cell-culture-adaptive mutation & EV-D68 pathogenesis studies

One of the challenges in studying the pathogenesis of EV-D68 is that EV-D68 acquire mutations within a few cell-culture passages **(Chapter 3)**. In general, RNA viruses including EV-D68 have low-fidelity RNA-dependent RNA polymerases resulting in replication errors in the viral RNA (61). This rapid mutation could result in an increased number of basic residues on their surface protein, enabling the virus to interact with negatively charged glycosaminoglycan (GAG) chains comprised of heparan sulfate, which abundantly expresses in numerous tissues, as an attachment receptor. As a consequence, the virus becomes fitter and thereby gains advantage over heparan-sulfate-independent variants (62). This phenomenon has also been described for other EVs like EV-A71, foot-and-mouth disease virus, and human rhinovirus-87 (52, 63-65).

Similar to other EVs, EV-D68 with cell-culture-adaptive amino acid substitutions binds to heparan sulfate, which is abundantly expressed on the cell surface of many cell lines. The adaptation thus results in the recognition of heparan sulfate as an additional receptor besides sialic acids **(Chapter 3)** (66). The interaction with heparan sulfate allows EV-D68 to circumvent PLA2G16, which is a common host factor for EVs that facilitates viral genomes release from virus-containing endocytic vesicles (66). This

suggests that the utilization of distinct receptors by various strains of EV-D68 can lead to different infection pathways, and might lead to phenotypic changes.

In general, EV-D68 stocks are not reported to be sequenced before they are included in pathogenesis studies (20, 21, 67). Since cell-culture-adaptive amino acid substitutions can cause phenotypic changes in vitro **(Chapter 3)**, sequencing every virus stock is crucial to ensure its alignment with the original clinical isolate. In order to minimize the chance of mutations that result in the recognition of heparan sulfate, cell lines could be established in which heparan sulfate is knocked out and where clinically relevant receptors, for example, sialic acids, are overexpressed.

The utility of antibody index (AI) serology in the diagnosis of virus infections in the CNS

The detection of viral RNA or DNA in cerebrospinal fluid (CSF) is a widely used diagnostic tool to diagnose viral infections in the CNS. However, as viruses are not always present in the CSF, it might be challenging to diagnose viral myelopathies. The detection of virus-specific antibodies in the CSF and the calculation of the antibody index (AI), that corrects for leakage of antibodies over the blood-brain barrier, is an alternative, indirect indicator of a virus infection in the CNS **(Chapter 5)**. For EVs, the detection of viral RNA in CSF in cases of meningitis or encephalitis are highly sensitive (>90%), making the AI calculation unnecessary. In contrast, viral RNA in CSF in EV-D68 associated AFM cases is less frequently detected (~31%) (68). The absence of EV-D68 in the CSF might be due to its transient presence in CSF, the lack of virus released into the intrathecal compartment or the timing of specimen collection (41, 69). Therefore, most of the EV-D68 associated neurological disease diagnoses are based on the detection of viral RNA from respiratory samples (70), and in these cases the detection of the AI in CSF would be an important additional diagnostic tool.

The calculation of AI has been utilized to diagnose other viral infections in the CNS, as well as to diagnose autoimmune diseases. An example is the use of the AI in diagnosing flavivirus infections in the CNS, where the rapid virus clearance results in the absence of viral RNA in the CSF in most patients during the course of the disease (71, 72). Another example is the use of the AI for the detection of measles in subacute sclerosing panencephalitis cases, as in these cases there is no extracellular release of virus (73).

While the calculation of the AI is a useful serologic diagnostic tool to identify virus-associated neurological disease, multiple factors should be taken into account when interpreting the results. Firstly, since the measurement of antibody levels in the blood and CSF are important for AI calculation, the sensitivity and specificity of the used IgG/IgM/IgA ELISA should always be determined first (Chapter 5) (71). In case of low sensitivity or specificity, an additional confirmation, such as VNT is needed (71). Secondly, the day on which the sample is collected may affect the levels of virus-specific IgGs and thus influence the AI. In general, samples collected early after disease onset

have lower levels of IgG **(Chapter 5)**. Thirdly, multiple sclerosis and other immune diseases can commonly induce positive AI associated to polyspecific immune responses against measles virus, rubella virus and varicella-zoster virus. Thereby, AI calculation in immune diseases should be performed for several viruses (74, 75). Finally, it should be noted that the reliability of the AI decreases after treatment with intravenous immunoglobulin (68). By considering and understanding these crucial factors, the accuracy in the viral diagnosis can be ensured.

Concluding remarks and future perspectives

The outbreak of EV-D68 in 2014 raised concerns as it was associated with severe respiratory and neurological diseases, notably AFM, a polio-like myelitis. The change in the epidemiology and the surge in severe cases during 2014 and subsequent outbreaks prompted questions about the pathogenesis of EV-D68 infections. This thesis has provided fundamental knowledge on the systemic pathogenesis of EV-D68 using in vitro models and explored the diagnostic utility of intrathecal antibody detection in EV-D68 infection in the CNS. **Chapter 2** revealed that immune cells, in particular B cells, are susceptible and permissive to EV-D68 which might play a role in the development of a viremia and the systemic dissemination. **Chapters 3 and 4** reported that the neurotropism of EV-D68 is dependent on neither the virus's clade nor the year of isolation. **Chapter 4** showed that the tropism of EV-D68 in hPSC-derived neurons in vitro is not specific to motor neurons which contrasts to the neurotropism in vivo. In addition, **Chapter 3** reported that cell culture adaptive mutation alters the in vitro phenotype of EV-D68 infection in neuroblastoma cells and highlighted the importance to sequence virus stock when used in pathogenesis studies. Lastly, **Chapter 5** demonstrated the potential of the detection of virus-specific intrathecal antibody and the use of the AI in diagnosing EV-D68 infections in the CNS.

It remains unclear whether the unusual severity of the EV-D68 outbreak in 2014 was related to higher virulence, increased number of circulating viruses, or a combination of both. Current data showed that there are no clear differences in neurovirulence, either in vitro or in vivo, between EV-D68 isolates from before and after 2014 (12, 20, 23). However, there might still be an increased virulence in other replication sites, such as respiratory tract epithelium. Besides increased virulence, there could also be other factors, such as antigenic evolution, changes in antigenicity and reduction of population immunity, that led to increased number of circulating EV-D68 (56, 76, 77). Several reports did indicate a higher number of circulating EV-D68 starting from 2008 (38, 78, 79). However, this could be a byproduct of increased awareness and screening.

The 2014 outbreak demonstrated the potential of EV-D68 to cause epidemic disease. In fact, after easing the COVID-19 lockdown, there has been an increase in EV-D68 infections associated with respiratory disease (80), although not with neurological disease. The unpredictable nature of EV-D68 requires more insight into the circulation

of this virus. EV-D68 detection in sewage is a good measure of circulation of EV-D68 in the population (81-83). Continued surveillance of EV-D68 in humans and environmental (sewage) samples will provide more information on the circulation of EVs, including EV-D68, which could give early warning of potential outbreaks. Moreover, even though AFM has not been reported frequently after the COVID-19 lockdown, we should be aware that EV-D68 has the potential to cause AFM (80). Development of assays to detect EV-D68 antibodies in the CSF will contribute to the diagnosis of EV-D68 infection associated neurological disease. Although there are currently no licensed vaccines or treatment to prevent EV-D68 associated AFM, previous studies in mouse models have shown that antibodies can protect against AFM and death (12, 84). These findings pave a way for vaccine development which can induce humoral immunity or the development of immunotherapy in protecting against the occurrence of AFM during EV-D68 outbreaks. Enhancing our understanding of the pathogenesis of EV-D68 will offer insights for developing therapeutic interventions and vaccines, as well as improving patient outcomes.

References

1. Racaniello VR. One hundred years of poliovirus pathogenesis. Virology. 2006;344(1):9-16.
2. Cheng HY, Huang YC, Yen TY, Hsia SH, Hsieh YC, Li CC, et al. The correlation between the presence of viremia and clinical severity in patients with enterovirus 71 infection: a multi-center cohort study. BMC Infect Dis. 2014;14:417.
3. Sooksawasdi Na Ayudhya S, Laksono BM, van Riel D. The pathogenesis and virulence of enterovirus-D68 infection. Virulence. 2021;12(1):2060-72.
4. Essaidi-Laziosi M, Brito F, Benaoudia S, Royston L, Cagno V, Fernandes-Rocha M, et al. Propagation of respiratory viruses in human airway epithelia reveals persistent virus-specific signatures. J Allergy Clin Immunol. 2018;141(6):2074-84.
5. Zheng HW, Sun M, Guo L, Wang JJ, Song J, Li JQ, et al. Nasal Infection of Enterovirus D68 Leading to Lower Respiratory Tract Pathogenesis in Ferrets (Mustela putorius furo). Viruses. 2017;9(5).
6. Patel MC, Wang W, Pletneva LM, Rajagopala SV, Tan Y, Hartert TV, et al. Enterovirus D-68 Infection, Prophylaxis, and Vaccination in a Novel Permissive Animal Model, the Cotton Rat (Sigmodon hispidus). PLoS One. 2016;11(11):e0166336.
7. Mena I, Perry CM, Harkins S, Rodriguez F, Gebhard J, Whitton JL. The role of B lymphocytes in coxsackievirus B3 infection. Am J Pathol. 1999;155(4):1205-15.
8. Zhao T, Zhang Z, Zhang Y, Feng M, Fan S, Wang L, et al. Dynamic Interaction of Enterovirus 71 and Dendritic Cells in Infected Neonatal Rhesus Macaques. Front Cell Infect Microbiol. 2017;7:171.
9. Helgers LC, Bhoekhan MS, Pajkrt D, Wolthers KC, Geijtenbeek TBH, Sridhar A. Human Dendritic Cells Transmit Enterovirus A71 via Heparan Sulfates to Target Cells Independent of Viral Replication. Microbiol Spectr. 2022;10(6):e0282222.

10. Greninger AL, Naccache SN, Messacar K, Clayton A, Yu G, Somasekar S, et al. A novel outbreak enterovirus D68 strain associated with acute flaccid myelitis cases in the USA (2012-14): a retrospective cohort study. Lancet Infect Dis. 2015;15(6):671-82.
11. Messacar K, Schreiner TL, Van Haren K, Yang M, Glaser CA, Tyler KL, et al. Acute flaccid myelitis: A clinical review of US cases 2012-2015. Ann Neurol. 2016;80(3):326-38.
12. Hixon AM, Yu G, Leser JS, Yagi S, Clarke P, Chiu CY, et al. A mouse model of paralytic myelitis caused by enterovirus D68. PLoS Pathog. 2017;13(2):e1006199.
13. Sun S, Bian L, Gao F, Du R, Hu Y, Fu Y, et al. A neonatal mouse model of Enterovirus D68 infection induces both interstitial pneumonia and acute flaccid myelitis. Antiviral Res. 2019;161:108-15.
14. Morrey JD, Wang H, Hurst BL, Zukor K, Siddharthan V, Van Wettere AJ, et al. Causation of Acute Flaccid Paralysis by Myelitis and Myositis in Enterovirus-D68 Infected Mice Deficient in Interferon alphabeta/gamma Receptor Deficient Mice. Viruses. 2018;10(1).
15. Frost J, Rudy MJ, Leser JS, Tan H, Hu Y, Wang J, et al. Telaprevir Treatment Reduces Paralysis in a Mouse Model of Enterovirus D68 Acute Flaccid Myelitis. J Virol. 2023:e0015623.
16. Kreuter JD, Barnes A, McCarthy JE, Schwartzman JD, Oberste MS, Rhodes CH, et al. A fatal central nervous system enterovirus 68 infection. Arch Pathol Lab Med. 2011;135(6):793-6.
17. Esposito S, Chidini G, Cinnante C, Napolitano L, Giannini A, Terranova L, et al. Acute flaccid myelitis associated with enterovirus-D68 infection in an otherwise healthy child. Virol J. 2017;14(1):4.
18. Giombini E, Rueca M, Barberi W, Iori AP, Castilletti C, Scognamiglio P, et al. Enterovirus D68-Associated Acute Flaccid Myelitis in Immunocompromised Woman, Italy. Emerg Infect Dis. 2017;23(10):1690-3.
19. Yogo N, Imamura T, Muto Y, Hirai K. Cardiopulmonary failure as a result of brainstem encephalitis caused by enterovirus D68. BMJ Case Rep. 2019;12(11).
20. Rosenfeld AB, Warren AL, Racaniello VR. Neurotropism of Enterovirus D68 Isolates Is Independent of Sialic Acid and Is Not a Recently Acquired Phenotype. MBio. 2019;10(5).
21. Hixon AM, Clarke P, Tyler KL. Contemporary Circulating Enterovirus D68 Strains Infect and Undergo Retrograde Axonal Transport in Spinal Motor Neurons Independent of Sialic Acid. J Virol. 2019;93(16).
22. Ohka S, Hao Tan S, Kaneda S, Fujii T, Schiavo G. Retrograde axonal transport of poliovirus and EV71 in motor neurons. Biochem Biophys Res Commun. 2022;626:72-8.
23. Sooksawasdi Na Ayudhya S, Meijer A, Bauer L, Oude Munnink B, Embregts C, Leijten L, et al. Enhanced Enterovirus D68 Replication in Neuroblastoma Cells Is Associated with a Cell Culture-Adaptive Amino Acid Substitution in VP1. mSphere. 2020;5(6).
24. Poelaert KCK, van Kleef RGDM, Liu M, van Vliet A, Lyoo H, Gerber LS, et al. Enterovirus D-68 Infection of Primary Rat Cortical Neurons: Entry, Replication, and Functional Consequences. mBio. 2023:e0024523.
25. Wei W, Guo H, Chang J, Yu Y, Liu G, Zhang N, et al. ICAM-5/Telencephalin Is a Functional Entry Receptor for Enterovirus D68. Cell Host Microbe. 2016;20(5):631-41.
26. Peters CE, Carette JE. Return of the Neurotropic Enteroviruses: Co-Opting Cellular Pathways for Infection. Viruses. 2021;13(2).

27. Blondel B, Colbère-Garapin F, Couderc T, Wirotius A, Guivel-Benhassine F. Poliovirus, pathogenesis of poliomyelitis, and apoptosis. Curr Top Microbiol Immunol. 2005;289:25-56.
28. Chu JJH, Ng ML. The mechanism of cell death during West Nile virus infection is dependent on initial infectious dose. J Gen Virol. 2003;84(Pt 12):3305-14.
29. Petito CK, Roberts B. Evidence of apoptotic cell death in HIV encephalitis. Am J Pathol. 1995;146(5):1121-30.
30. Lin JY, Huang HI. Autophagy is induced and supports virus replication in Enterovirus A71-infected human primary neuronal cells. Sci Rep. 2020;10(1):15234.
31. Zhu X, Wu T, Chi Y, Ge Y, Wu B, Zhou M, et al. Pyroptosis induced by enterovirus A71 infection in cultured human neuroblastoma cells. Virology. 2018;521:69-76.
32. Spencer DC, Price RW. Human immunodeficiency virus and the central nervous system. Annu Rev Microbiol. 1992;46:655-93.
33. Koutsilieri E, Czub S, Scheller C, Sopper S, Tatschner T, Stahl-Hennig C, et al. Brain choline acetyltransferase reduction in SIV infection. An index of early dementia? Neuroreport. 2000;11(11):2391-3.
34. Autret A, Martin-Latil S, Mousson L, Wirotius A, Petit F, Arnoult D, et al. Poliovirus induces Bax-dependent cell death mediated by c-Jun NH2-terminal kinase. J Virol. 2007;81(14):7504-16.
35. Nüesch JP, Rommelaere J. NS1 interaction with CKII alpha: novel protein complex mediating parvovirus-induced cytotoxicity. J Virol. 2006;80(10):4729-39.
36. Vogt MR, Wright PF, Hickey WF, De Buysscher T, Boyd KL, Crowe JE. Enterovirus D68 in the Anterior Horn Cells of a Child with Acute Flaccid Myelitis. N Engl J Med. 2022;386(21):2059-60.
37. Linsuwanon P, Puenpa J, Suwannakarn K, Auksornkitti V, Vichiwattana P, Korkong S, et al. Molecular epidemiology and evolution of human enterovirus serotype 68 in Thailand, 2006-2011. PLoS One. 2012;7(5):e35190.
38. Meijer A, van der Sanden S, Snijders BE, Jaramillo-Gutierrez G, Bont L, van der Ent CK, et al. Emergence and epidemic occurrence of enterovirus 68 respiratory infections in The Netherlands in 2010. Virology. 2012;423(1):49-57.
39. Kaida A, Kubo H, Sekiguchi J, Kohdera U, Togawa M, Shiomi M, et al. Enterovirus 68 in children with acute respiratory tract infections, Osaka, Japan. Emerg Infect Dis. 2011;17(8):1494-7.
40. Opanda SM WF, Khamadi S, Coldren R, Bulimo WD. Genetic diversity of human enterovirus 68 strains isolated in Kenya using the hypervariable 3=-end of VP1 gene. PLoS One. 2014;9:e102866.
41. Sejvar JJ, Lopez AS, Cortese MM, Leshem E, Pastula DM, Miller L, et al. Acute Flaccid Myelitis in the United States, August-December 2014: Results of Nationwide Surveillance. Clin Infect Dis. 2016;63(6):737-45.
42. Zhang Y, Cao J, Zhang S, Lee AJ, Sun G, Larsen CN, et al. Genetic changes found in a distinct clade of Enterovirus D68 associated with paralysis during the 2014 outbreak. Virus Evol. 2016;2(1):vew015.
43. Dyrdak R, Grabbe M, Hammas B, Ekwall J, Hansson KE, Luthander J, et al. Outbreak of enterovirus D68 of the new B3 lineage in Stockholm, Sweden, August to September 2016. Euro Surveill. 2016;21(46).

44. Knoester M, Helfferich J, Poelman R, Van Leer-Buter C, Brouwer OF, Niesters HGM, et al. Twenty-nine Cases of Enterovirus-D68-associated Acute Flaccid Myelitis in Europe 2016: A Case Series and Epidemiologic Overview. Pediatr Infect Dis J. 2019;38(1):16-21.
45. Bal A, Sabatier M, Wirth T, Coste-Burel M, Lazrek M, Stefic K, et al. Emergence of enterovirus D68 clade D1, France, August to November 2018. Euro Surveill. 2019;24(3).
46. Tan Y, Hassan F, Schuster JE, Simenauer A, Selvarangan R, Halpin RA, et al. Molecular Evolution and Intraclade Recombination of Enterovirus D68 during the 2014 Outbreak in the United States. J Virol. 2015;90(4):1997-2007.
47. Wu GH, Lee KM, Kao CY, Shih SR. The internal ribosome entry site determines the neurotropic potential of enterovirus A71. Microbes Infect. 2023:105107.
48. Ren RB, Moss EG, Racaniello VR. Identification of two determinants that attenuate vaccine-related type 2 poliovirus. J Virol. 1991;65(3):1377-82.
49. Li B, Yue Y, Zhang Y, Yuan Z, Li P, Song N, et al. A Novel Enterovirus 71 (EV71) Virulence Determinant: The 69th Residue of 3C Protease Modulates Pathogenicity. Front Cell Infect Microbiol. 2017;7:26.
50. Li R, Zou Q, Chen L, Zhang H, Wang Y. Molecular analysis of virulent determinants of enterovirus 71. PLoS One. 2011;6(10):e26237.
51. Yeh MT, Wang SW, Yu CK, Lin KH, Lei HY, Su IJ, et al. A single nucleotide in stem loop II of 5'-untranslated region contributes to virulence of enterovirus 71 in mice. PLoS One. 2011;6(11):e27082.
52. Tan CW, Sam IC, Lee VS, Wong HV, Chan YF. VP1 residues around the five-fold axis of enterovirus A71 mediate heparan sulfate interaction. Virology. 2017;501:79-87.
53. Nishimura Y, Lee H, Hafenstein S, Kataoka C, Wakita T, Bergelson JM, et al. Enterovirus 71 binding to PSGL-1 on leukocytes: VP1-145 acts as a molecular switch to control receptor interaction. PLoS Pathog. 2013;9(7):e1003511.
54. Chua BH, Phuektes P, Sanders SA, Nicholls PK, McMinn PC. The molecular basis of mouse adaptation by human enterovirus 71. J Gen Virol. 2008;89(Pt 7):1622-32.
55. Huang W, Wang G, Zhuge J, Nolan SM, Dimitrova N, Fallon JT. Whole-Genome Sequence Analysis Reveals the Enterovirus D68 Isolates during the United States 2014 Outbreak Mainly Belong to a Novel Clade. Sci Rep. 2015;5:15223.
56. Hodcroft EB, Dyrdak R, Andrés C, Egli A, Reist J, García Martínez de Artola D, et al. Evolution, geographic spreading, and demographic distribution of Enterovirus D68. PLoS Pathog. 2022;18(5):e1010515.
57. Uprety P, Curtis D, Elkan M, Fink J, Rajagopalan R, Zhao C, et al. Association of Enterovirus D68 with Acute Flaccid Myelitis, Philadelphia, Pennsylvania, USA, 2009-2018. Emerg Infect Dis. 2019;25(9):1676-82.
58. Eastman C, Tapprich WE. RNA Structure in the 5' Untranslated Region of Enterovirus D68 Strains with Differing Neurovirulence Phenotypes. Viruses. 2023;15(2).
59. Filipe IC, Guedes MS, Zdobnov EM, Tapparel C. Enterovirus D: A Small but Versatile Species. Microorganisms. 2021;9(8).
60. Furuse Y, Chaimongkol N, Okamoto M, Oshitani H. Evolutionary and Functional Diversity of the 5' Untranslated Region of Enterovirus D68: Increased Activity of the Internal Ribosome Entry Site of Viral Strains during the 2010s. Viruses. 2019;11(7).

61. Vignuzzi M, Stone JK, Arnold JJ, Cameron CE, Andino R. Quasispecies diversity determines pathogenesis through cooperative interactions in a viral population. Nature. 2006;439(7074):344-8.
62. Cagno V, Tseligka ED, Jones ST, Tapparel C. Heparan Sulfate Proteoglycans and Viral Attachment: True Receptors or Adaptation Bias? Viruses. 2019;11(7).
63. Chang CK, Wu SR, Chen YC, Lee KJ, Chung NH, Lu YJ, et al. Mutations in VP1 and 5'-UTR affect enterovirus 71 virulence. Sci Rep. 2018;8(1):6688.
64. Sa-Carvalho D, Rieder E, Baxt B, Rodarte R, Tanuri A, Mason PW. Tissue culture adaptation of foot-and-mouth disease virus selects viruses that bind to heparin and are attenuated in cattle. J Virol. 1997;71(7):5115-23.
65. Vlasak M, Goesler I, Blaas D. Human rhinovirus type 89 variants use heparan sulfate proteoglycan for cell attachment. J Virol. 2005;79(10):5963-70.
66. Baggen J, Liu Y, Lyoo H, van Vliet ALW, Wahedi M, de Bruin JW, et al. Bypassing pan-enterovirus host factor PLA2G16. Nat Commun. 2019;10(1):3171.
67. Brown DM, Hixon AM, Oldfield LM, Zhang Y, Novotny M, Wang W, et al. Contemporary Circulating Enterovirus D68 Strains Have Acquired the Capacity for Viral Entry and Replication in Human Neuronal Cells. mBio. 2018;9(5).
68. Shamier MC, Bogers S, Yusuf E, van Splunter M, Ten Berge JCEM, Titulaer M, et al. The role of antibody indexes in clinical virology. Clin Microbiol Infect. 2021;27(9):1207-11.
69. Mishra N, Ng TFF, Marine RL, Jain K, Ng J, Thakkar R, et al. Antibodies to Enteroviruses in Cerebrospinal Fluid of Patients with Acute Flaccid Myelitis. mBio. 2019;10(4).
70. Harvala H, Broberg E, Benschop K, Berginc N, Ladhani S, Susi P, et al. Recommendations for enterovirus diagnostics and characterisation within and beyond Europe. J Clin Virol. 2018;101:11-7.
71. Reusken C, Boonstra M, Rugebregt S, Scherbeijn S, Chandler F, Avšič-Županc T, et al. An evaluation of serological methods to diagnose tick-borne encephalitis from serum and cerebrospinal fluid. J Clin Virol. 2019;120:78-83.
72. Granerod J, Cunningham R, Zuckerman M, Mutton K, Davies NW, Walsh AL, et al. Causality in acute encephalitis: defining aetiologies. Epidemiol Infect. 2010;138(6):783-800.
73. Wendorf KA, Winter K, Zipprich J, Schechter R, Hacker JK, Preas C, et al. Subacute Sclerosing Panencephalitis: The Devastating Measles Complication That Might Be More Common Than Previously Estimated. Clin Infect Dis. 2017;65(2):226-32.
74. Felgenhauer K, Reiber H. The diagnostic significance of antibody specificity indices in multiple sclerosis and herpes virus induced diseases of the nervous system. Clin Investig. 1992;70(1):28-37.
75. Feki S, Gargouri S, Mejdoub S, Dammak M, Hachicha H, Hadiji O, et al. The intrathecal polyspecific antiviral immune response (MRZ reaction): A potential cerebrospinal fluid marker for multiple sclerosis diagnosis. J Neuroimmunol. 2018;321:66-71.
76. Dyrdak R, Mastafa M, Hodcroft EB, Neher RA, Albert J. Intra- and interpatient evolution of enterovirus D68 analyzed by whole-genome deep sequencing. Virus Evol. 2019;5(1):vez007.
77. Brown DM, Zhang Y, Scheuermann RH. Epidemiology and Sequence-Based Evolutionary Analysis of Circulating Non-Polio Enteroviruses. Microorganisms. 2020;8(12).

78. Rahamat-Langendoen J, Riezebos-Brilman A, Borger R, van der Heide R, Brandenburg A, Schölvinck E, et al. Upsurge of human enterovirus 68 infections in patients with severe respiratory tract infections. J Clin Virol. 2011;52(2):103-6.
79. (CDC) CfDCaP. Clusters of acute respiratory illness associated with human enterovirus 68--Asia, Europe, and United States, 2008-2010. MMWR Morb Mortal Wkly Rep. 2011;60(38):1301-4.
80. Benschop KS, Albert J, Anton A, Andres C, Aranzamendi M, Armannsdottir B, et al. Re-emergence of enterovirus D68 in Europe after easing the COVID-19 lockdown, September 2021. Euro Surveill. 2021;26(45).
81. Tedcastle A, Wilton T, Pegg E, Klapsa D, Bujaki E, Mate R, et al. Detection of Enterovirus D68 in Wastewater Samples from the UK between July and November 2021. Viruses. 2022;14(1).
82. Weil M, Mandelboim M, Mendelson E, Manor Y, Shulman L, Ram D, et al. Human enterovirus D68 in clinical and sewage samples in Israel. J Clin Virol. 2017;86:52-5.
83. Majumdar M, Sharif S, Klapsa D, Wilton T, Alam MM, Fernandez-Garcia MD, et al. Environmental Surveillance Reveals Complex Enterovirus Circulation Patterns in Human Populations. Open Forum Infect Dis. 2018;5(10):ofy250.
84. Vogt MR, Fu J, Kose N, Williamson LE, Bombardi R, Setliff I, et al. Human antibodies neutralize enterovirus D68 and protect against infection and paralytic disease. Sci Immunol. 2020;5(49).

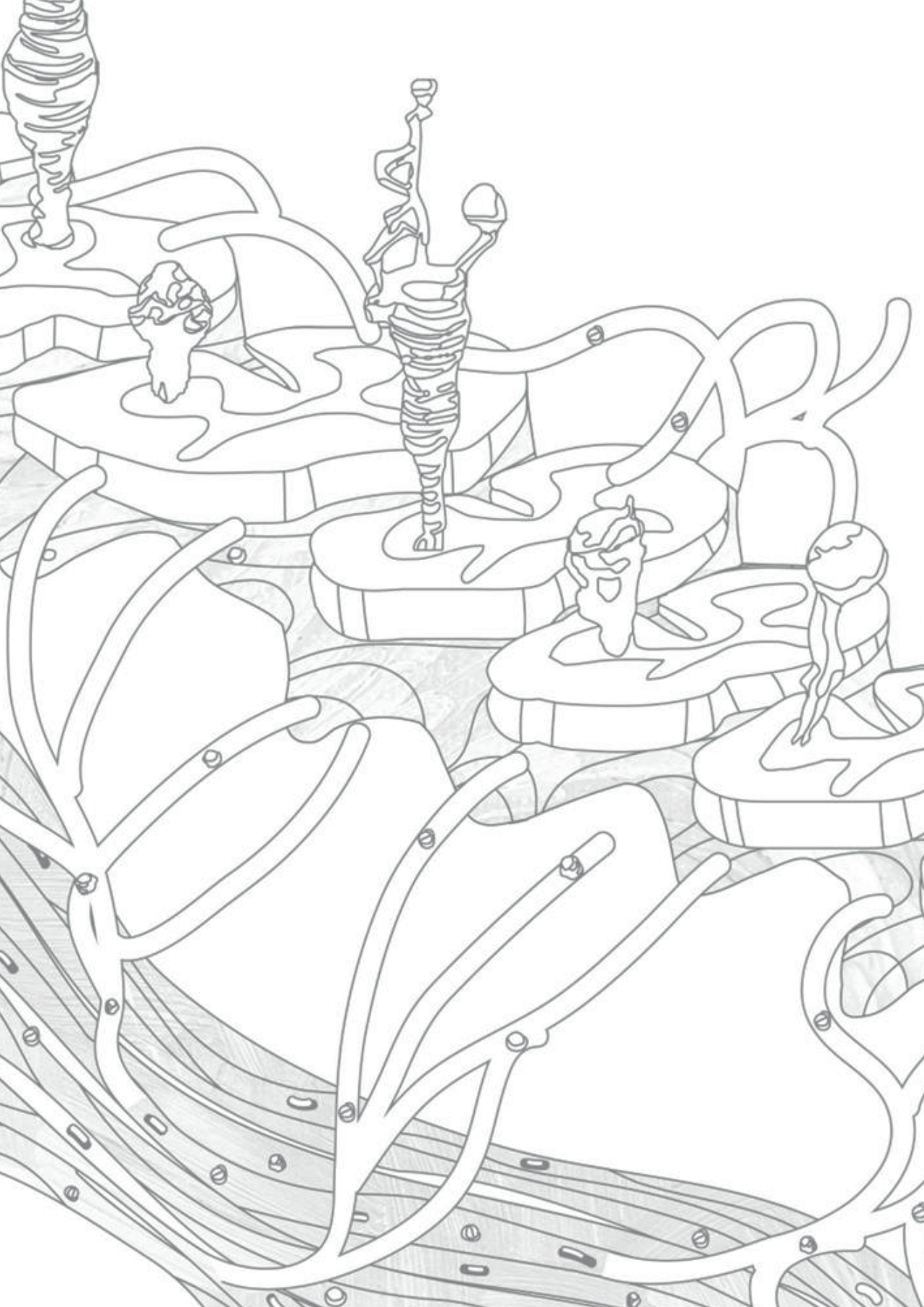

Chapter

7

Summary / Samenvatting

Summary

Unlike other Enteroviruses (EVs), EV-D68 is a respiratory virus that typically causes mild respiratory diseases, and occasionally severe respiratory diseases. However, during the 2014 outbreak in the United States, it became clear that EV-D68 infections are also associated with neurological complications, particularly acute flaccid myelitis (AFM). This thesis focused on the systemic dissemination and neuropathogenesis of EV-D68, as well as evaluating the diagnostics for EV-D68-associated neurological diseases.

Systemic dissemination of enteroviruses including EV-D68 is essential for the development of extra-respiratory diseases. While rarely reported and studied, EV-D68 has been found to cause viremia in EV-D68-infected patients. However, how the EV-D68 disseminates from the respiratory tract into the circulation was never studied. In **Chapter 2**, I investigated the role of human immune cells in the systemic dissemination of EV-D68. I showed that human B cells, but not T cells, are susceptible for EV-D68 infection, and that B cells with a more activated phenotype (germinal center B cells) support EV-D68 replication. We also found that monocytic derived-dendritic cells, especially immature dendritic cells, are susceptible and permissive to EV-D68 infection. Furthermore, immature dendritic cells inoculated with EV-D68 can transferred the virus to autologous B cells. These findings provide fundamental knowledge on the potential role of immune cells that may contribute to systemic dissemination.

Since 2014, there is an increased genetic diversity of EV-D68, and several new subclades emerged. However, whether the ability to cause central nervous system (CNS) complication including AFM is a clade-specific feature remains inconclusive. However, I observed no differences between clinical isolates or clades from before and after 2014 in their replication efficiency in neuroblastoma cell lines (**Chapter 3**), or human pluripotent stem cells (hPSC) derived-spinal motor neurons (**Chapter 4**), although I did observed variations among isolates. The findings suggest that the ability to cause CNS disease is not a recent acquired feature. In fact, in **Chapter 3**, we observed that and cell culture adaptive amino acid substitutions (E271K), increased virus attachment, internalization, and replication in neuroblastoma cells. This E271K amino acid substitution resulted in the recognition of heparan sulfate as an additional receptor besides sialic acids, which highlights the necessity of sequencing the original virus isolate and virus stocks in pathogenesis studies.

Acute flaccid myelitis is the most common neurological complication in infected patients, and in vivo studies show that this is associated with lesions in the anterior horn of the spinal cord. In **Chapter 4**, I investigated the infection and replication efficiency of EV-D68 isolates in hPSC-derived spinal motor neurons which were compared side-by-side with infection and replication in Ngn2 cortical neurons co-cultured with astrocytes. Different EV-D68 isolates replicated in relatively equal efficiency in both neural models. The findings indicate that EV-D68 isolates did not show a specific tropism for hPSC-derived spinal motor neurons over cortical neurons in

vitro. This suggests that the preferential motor tropism of EV-D68 observed *in vivo* is likely related to the route of neuroinvasion. Furthermore, we found that EV-D68 induces cell death in spinal motor neurons, which is independent of apoptosis. Thus, the susceptibility of spinal motor neurons to EV-D68 and the related cellular changes could contribute to the neuropathogenesis and the development of AFM.

Detection of viral RNA or virus antigen in cerebrospinal fluid (CSF) to diagnose EV-D68 infection is challenging. Therefore, the detection of virus-specific antibodies in the CSF and the calculation of the antibody index (AI), which corrects for leakage of antibodies over the blood-brain barrier, is an indirect indicator of a virus infection in the CNS. I found that a quantitative EV ELISA can be used to calculate the AI and can be implemented to diagnose EV-specific intrathecal antibodies in patients with EV associated CNS disease. I further suggest that a more sensitivity ELISA to detect EV-D68 intrathecal antibodies could improve this diagnostic tool (**Chapter 5**).

In conclusion, the work in this thesis has advanced our understanding of the systemic pathogenesis of EV-D68 infections. Our data emphasizes the necessity to further investigate viral factors and biological mechanisms associated with the development of neurological diseases, and improve diagnostics for EV-D68 associated CNS complications.

Summary in Dutch / Samenvatting

Enterovirus D68 (EV-D68) is, in tegenstelling tot andere enterovirussen, een respiratoir virus dat normaliter milde respiratoire aandoeningen veroorzaakt, maar soms komen er toch ook ernstige respiratoire aandoeningen voor. Tijdens een uitbraak in 2014 in de Verenigde Staten werd duidelijk dat EV-D68-infecties ook worden geassocieerd met neurologische complicaties, met in het bijzonder acute flaccid myelitis (AFM). Het hierover verschenen proefschrift richtte zich op de systemische verspreiding en neuropathogenese van EV-D68, en daarnaast ook op de evaluatie van de diagnostiek voor EV-D68 geassocieerde neurologische aandoeningen.

Systemische verspreiding van enterovirussen zoals EV-D68 is essentieel voor de ontwikkeling van extra-respiratoire ziekten. Ondanks dat het zelden gerapporteerd en bestudeerd werd, is er vastgesteld dat EV-D68 viremie kan veroorzaken bij patiënten die zijn geïnfecteerd met EV-D68. Hoe EV-D68 zich verspreidt van de luchtwegen naar de circulatie is nooit bestudeerd. In **hoofdstuk 2** van mijn proefschrift onderzocht ik de rol van menselijke immuuncellen tijdens de systemische verspreiding van EV-D68. Ik toonde aan dat menselijke B-cellen, maar geen T-cellen, gevoelig zijn voor EV-D68 infectie en dat B-cellen met een meer geactiveerd fenotype (germinale centrum B-cellen) de EV-D68-replicatie ondersteunen. We vonden ook dat monocytische afgeleide dendritische cellen en dan vooral de onvolgroeide dendritische cellen gevoelig en permissief zijn voor EV-D68-infectie. Bovendien kunnen met EV-D68-geïnfecteerde onvolgroeide dendritische cellen het virus overbrengen naar autologe B-cellen. Deze bevindingen bieden fundamentele kennis over de mogelijke rol van immuuncellen die kunnen bijdragen aan systemische verspreiding van EV-D68.

Sinds 2014 is de genetische diversiteit van EV-D68 toegenomen en zijn er verschillende subclades ontstaan. Het blijft echter onduidelijk of complicaties van het centrale zenuwstelsel (CZS), waaronder AFM, veroorzaakt door EV-D68 een clade-specifieke eigenschap is. Ik heb geen verschillen waargenomen tussen klinische isolaten van clades voor en na 2014 in hun replicatie-efficiëntie in neuroblastoomcellijnen (**hoofdstuk 3**) of van humane pluripotente stamcellen (hPSC) afgeleide spinale motorneuronen (**hoofdstuk 4**), hoewel ik wel variatie heb waargenomen. De bevindingen suggereren dat het vermogen om een ziekte van het CZS te veroorzaken geen recent verworven eigenschap is van EV-D68. We hebben in hoofdstuk 3 waargenomen dat een celcultuur adaptieve aminozuursubstitutie (E271K), de virusbinding, internalisatie en replicatie in neuroblastoomcellen verhoogde. Deze E271K-amino acid-substitutie resulteerde in de herkenning van heperansulfaat als een extra receptor naast siaalzuur hetgeen laat zien hoe belangrijk het is om de virussen te sequencen die worden gebruikt in pathogenese studies.

AFM is de meest voorkomende neurologische complicatie bij geïnfecteerde patiënten en in vivo studies tonen aan dat dit gepaard gaat met laesies in de voorste hoorn van het ruggenmerg. In **hoofdstuk 4** onderzocht ik de infectie- en replicatie-efficiëntie van

EV-D68-isolaten in hPSC-afgeleide spinale motorneuronen. Die werden vergeleken met infectie en replicatie in een co-culture model bestaande uit Ngn2-corticale neuronen gekweekt met astrocyten. Verschillende EV-D68-isolaten repliceerden in relatief gelijke mate in beide neurale modellen. Deze studie laat zien dat EV-D68-isolaten geen specifiek tropisme vertoonden voor hPSC-afgeleide spinale motorneuronen ten opzichte van corticale neuronen in vitro. Dit suggereert dat het in vivo waargenomen preferentiële motorneuronen tropisme van EV-D68 waarschijnlijk is gerelateerd aan de route van CZS-invasie. Bovendien vonden we dat EV-D68 celdood induceert in spinale motorneuronen hetgeen niet werd veroorzaakt door apoptose. De gevoeligheid van spinale motorneuronen voor EV-D68 en de gerelateerde cellulaire veranderingen zouden kunnen bijdragen aan de neuropathogenese en de ontwikkeling van AFM.

Detectie van viraal RNA of virusantigeen in cerebrospinaal vocht (liquor) om EV-D68-infectie te diagnosticeren is een uitdaging. Daarom is de detectie van virusspecifieke antilichamen in de liquor en de berekening van de antilichaamindex (AI), een indirecte indicator van een virusinfectie in het CZS. De AI corrigeert voor lekkage van antilichamen die over de bloed-hersenbarrière heen kunnen komen. Ik heb ontdekt dat een kwantitatieve enterovirus ELISA kan worden gebruikt om de AI te berekenen. Deze kan vervolgens worden toegepast om enterovirus-specifieke intrathecale antilichamen te diagnosticeren bij patiënten met enterovirus-geassocieerde CZS-aandoeningen. Verder geef ik de suggestie dat een gevoeligere ELISA om EV-D68 intrathecale antilichamen te detecteren zou helpen om dit diagnostisch hulpmiddel te verbeteren (**hoofdstuk 5**).

Concluderend kan worden gesteld dat het werk in dit proefschrift ons inzicht in de systemische pathogenese van EV-D68-infecties heeft bevorderd. Onze data benadrukken de noodzaak om virale factoren en biologische mechanismen die geassocieerd worden met de ontwikkeling van neurologische aandoeningen verder te onderzoeken en de diagnostiek voor EV-D68-geassocieerde complicaties van het CZS te verbeteren.

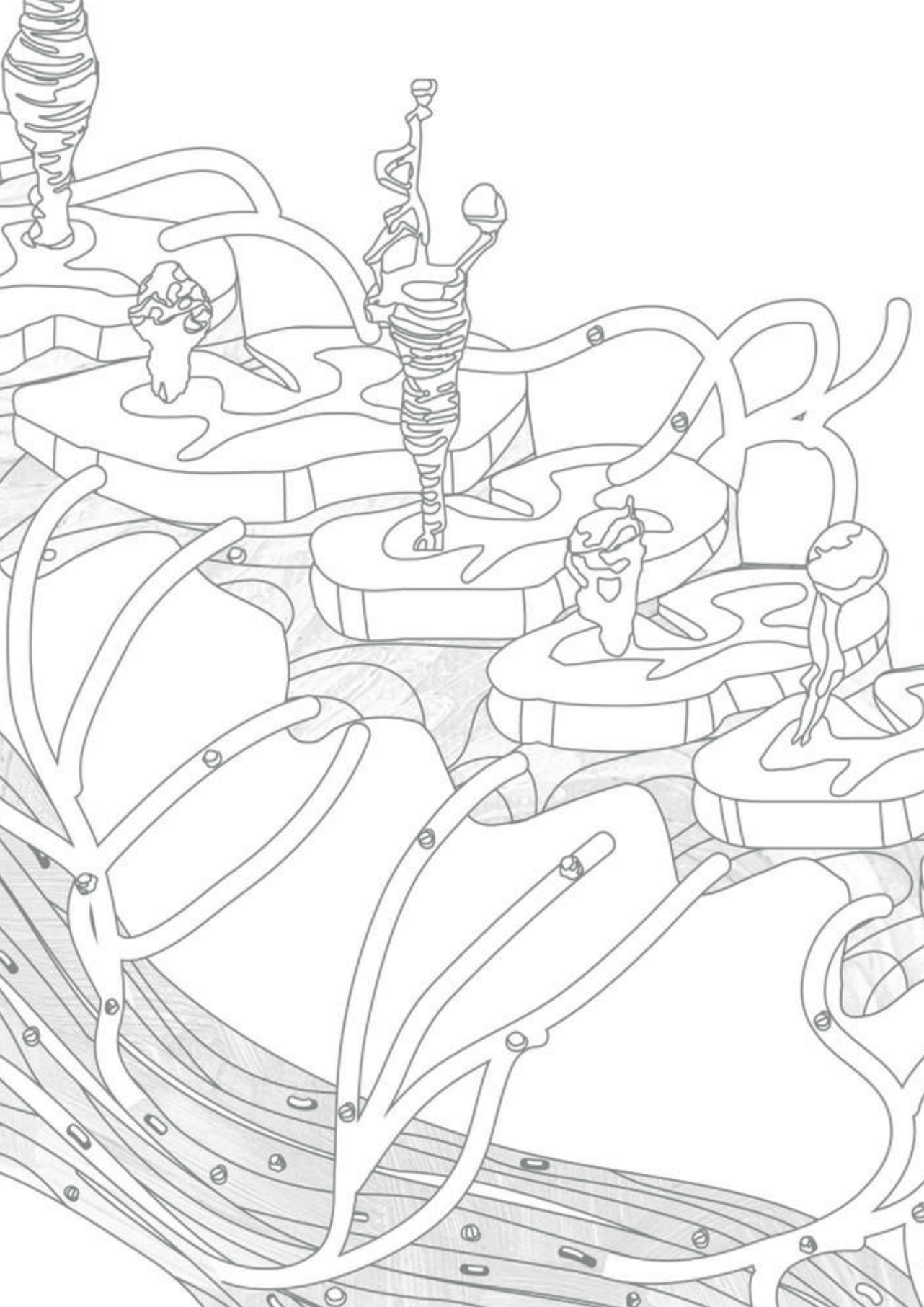

Chapter

8

Appendices

About the author
Portfolio
Publication lists

About the author

Syriam Sooksawasdi Na Ayudhya was born on the 8th March 1990 in Chiang Mai, Thailand. She finished her secondary school education at Demonstration school Chiang Mai University. She obtained her degree in Veterinary Medicine with first class honor from Khon Kaen University, Khon Kaen, Thailand. After working as a clinician in an animal hospital in Chiang Mai for about a year, she awarded a scholarship from Thai Ministry of Higher Education, Science, Research and Innovation to pursue her master's and doctorate's education in biomedical field.

She did her master's in a research master program of Infection and Immunity at Erasmus MC, Erasmus University Rotterdam, Rotterdam, the Netherlands. She performed a research internship at Department of Viroscience, Erasmus MC, Rotterdam, the Netherlands on understanding virus replication efficiency of Enterovirus D68 in cells of the central nervous system under the supervision of Dr. Debby van Riel. She then broadened her interest in the pathogenesis of Enterovirus D68 by enrolling in a doctorate education at Department of Viroscience, Erasmus MC under the supervision of Dr. Debby van Riel and mentorship of Prof. dr. Thijs Kuiken. Her research focuses on the systemic pathogenesis of Enterovirus D68. After this PhD, Syriam will start her career as a lecturer and researcher in Faculty of Veterinary Medicine, Prince Songkhla University, Songkhla, Thailand. She would like to do more research focusing on viral infectious diseases in animals and emerging infectious disease in human-animal interface.

PhD Portfolio

Name PhD student	Syriam Sooksawasdi Na Ayudhya
Erasmus MC department	Viroscience
Research school	Postgraduate School Molecular Medicine
Supervisors	Prof. dr. Thijs Kuiken (Promotor) Dr. Debby van Riel (Co-protmotor)

Awards

	Year
Europic 2022 Travel grant	2022

Courses and workshops

15th HKU-Pasteur Virology Course: Coronaviruses	2019
Erasmus MC graduate school The NGS in DNA diagnostic course	2019
Erasmus MC graduate school The SCORE PhD course	2020
Erasmus MC graduate school Erasmus MC - Scientific Integrity	2021
Erasmus University Rotterdam English Advance C1.1	2021
Erasmus MC graduate school Workshop on Biomedical English Writing	2020

Oral presentation

40th American Society of Virology conference	2021

Poster presentation

KNVM&KVMM 2021 conference	2021
The Dutch Annual Virology Symposium (DAVS 2021)	2021
Europic 2022 conference	2022
8th European Congress of Virology conference Biomedical PhD Day	2022

Teaching

Winter course I for Infection and Immunity MSc program	2019

Publication lists

Sooksawasdi Na Ayudhya S*, Sips GJ*, Bogers S, Leijten LME, Laksono BM, Smeets LC, Bruning A, Benschop K, Wolthers K, van Riel D, GeurtsvanKessel CH. Detection of intrathecal antibodies to diagnose enterovirus infections of the central nervous system. J Clin Virol. 2022 Jul;152:105190. doi: 10.1016/j.jcv.2022.105190. Epub 2022 May 23. PMID: 35640402.

*These authors contributed equally to this work

Sooksawasdi Na Ayudhya S, Laksono BM, van Riel D. The pathogenesis and virulence of enterovirus-D68 infection. Virulence. 2021 Dec;12(1):2060-2072. doi: 10.1080/21505594.2021.1960106. PMID: 34410208; PMCID: PMC8381846.

Sooksawasdi Na Ayudhya S, Meijer A, Bauer L, Oude Munnink B, Embregts C, Leijten L, Siegers JY, Laksono BM, van Kuppeveld F, Kuiken T, Geurts-van Kessel C, van Riel D. Enhanced Enterovirus D68 Replication in Neuroblastoma Cells Is Associated with a Cell Culture-Adaptive Amino Acid Substitution in VP1. mSphere. 2020 Nov 4;5(6):e00941-20. doi: 10.1128/mSphere.00941-20. Erratum in: mSphere. 2020 Dec 9;5(6): PMID: 33148825; PMCID: PMC7643833.

Sooksawasdi Na Ayudhya S, Kuiken T. Reverse Zoonosis of COVID-19: Lessons From the 2009 Influenza Pandemic. Vet Pathol. 2021 Mar;58(2):234-242. doi: 10.1177/0300985820979843. Epub 2020 Dec 9. PMID: 33295843; PMCID: PMC7961641.

Widagdo W, S**ooksawasdi Na Ayudhya S**, Hundie GB, Haagmans BL. Host Determinants of MERS-CoV Transmission and Pathogenesis. Viruses. 2019 Mar 19;11(3):280. doi: 10.3390/v11030280. PMID: 30893947; PMCID: PMC6466079.

Manuscript in the thesis

Laksono BM*, **Sooksawasdi Na Ayudhya S*,** Aguilar-Bretones M, Embregts C, van Nierop GP, van Riel D. Potential role of immune cells in pathogenesis of Enterovirus D68. (submitted)

*These authors contributed equally to this work

Sooksawasdi Na Ayudhya S, Bauer L, Lanko K, Van Riel D. Comparative analysis of EV-D68 clinical isolates from before and after 2014 in human pluripotent stem cell-derived neural models. (manuscript in preparation)

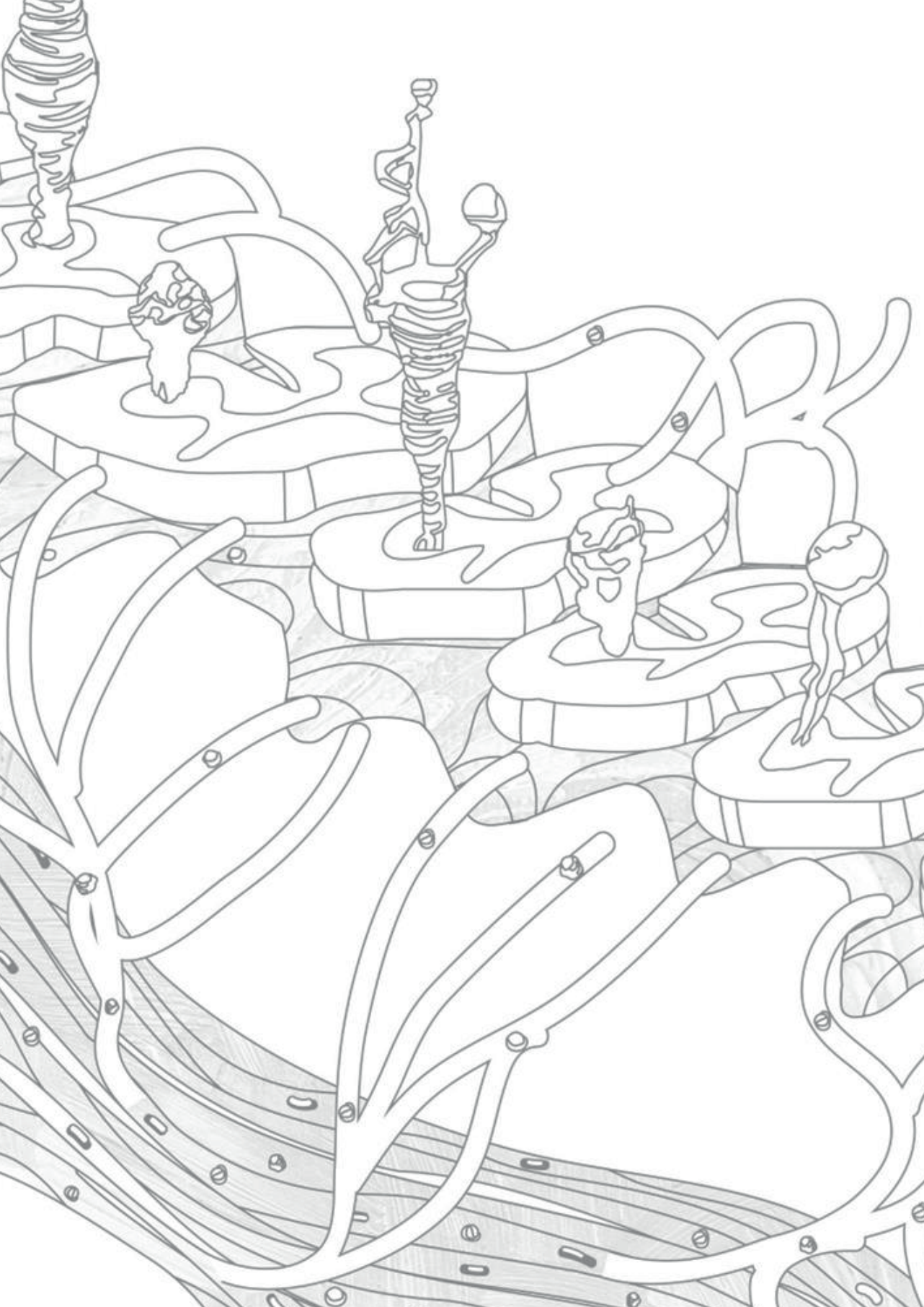

Chapter

9

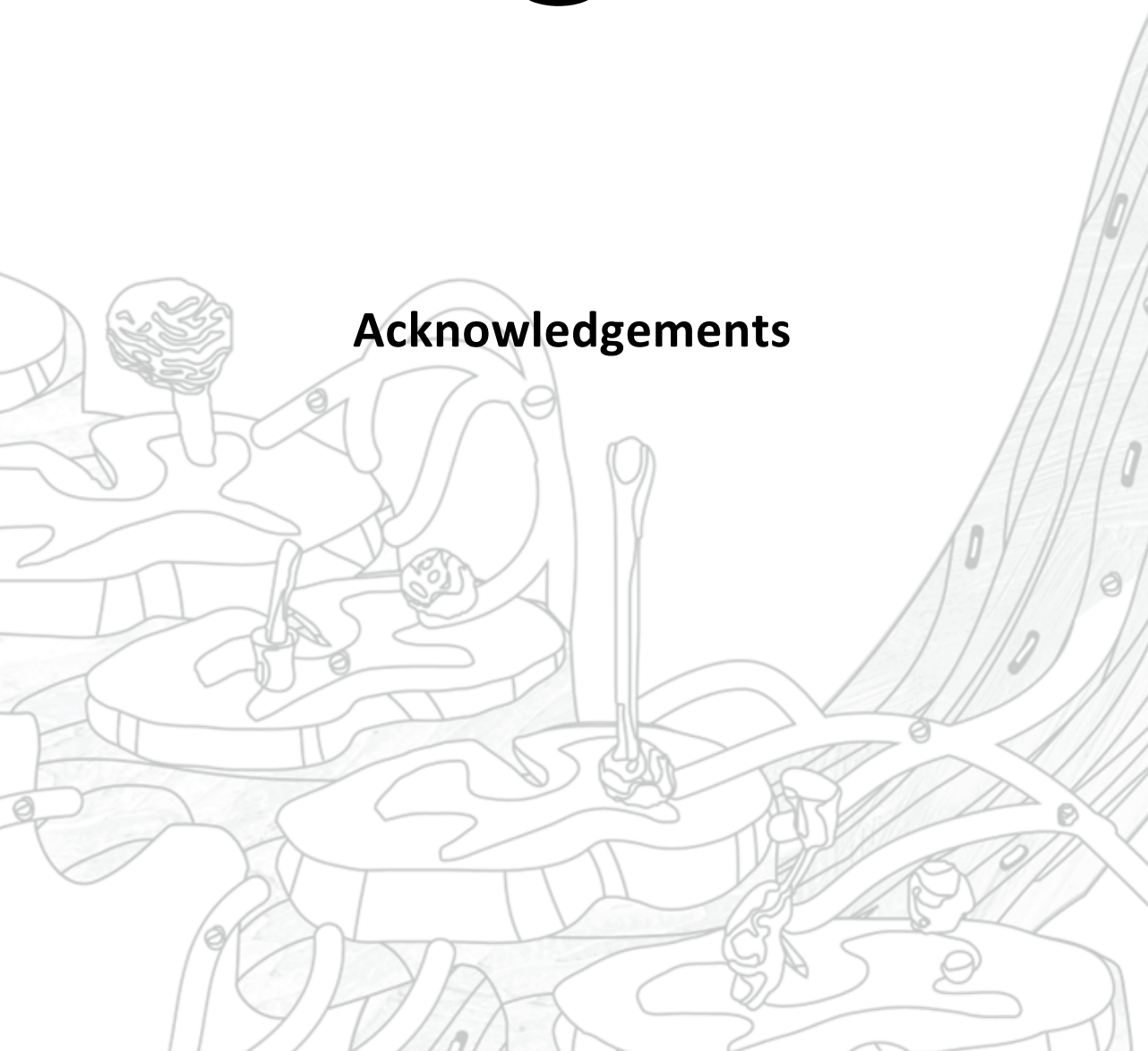

Acknowledgements

This thesis could not be achieved by myself alone but was done with the support, guidance and friendship of several wonderful people surrounding me. This chapter is dedicated to them who were my supporters along the journey of my PhD.

First on the list, is my supervisor/co-promotor, **Debby van Riel**. I am grateful to have you as my supervisor. You give me an opportunity to explore the world of science. I have learned a lot from you. Thank you for all your patience, guidance and support from day 1 until now. I sincerely respect you not only in a profession but also in a person. You embrace equity in many spheres of life. You show me how a group leader who has a ton of work responsibilities still be a care mom of two children and is a supportive supervisor of her advisees. For me who is away from family, having you as my supervisor makes me feel at home. You are one of the most opportunistic person who I know and that is how it can move life forward…I believe. Thank you for showing me the power of a woman who is committed, courageous and never gives up in the face of any obstacles. I will surely miss a Sinterklaas poem and an "S" chocolate (which I originally thought it stands for Syriam) from you.

To my PhD promotor, **Thijs**, it is my pleasure to be under your mentorship and have a chance to work with you. You always give me valuable feedback and ask me brilliant questions about my research. When I struggle with something and need help, you are always there with much-needed support. I learned a lot from you when we wrote the review on reverse zoonosis during the pandemic. Thank you for introducing the book of Philosophy of Science to me, and for your time and enthusiasm in our Philosophy of Science sessions together with Feline, Keshia and Sarah. Our discussion is rich with food for thought. You always emphasize the importance of how to conduct research with a critical view. Thank you for sharing with me knowledge and thoughts on science, nature, wildlife, sustainability, ecology, geography, etc. For me, you are not only an excellent researcher who drives research with curiosity, but also a devoted teacher who loves to teach (totally agree with what Lineke mentioned in her thesis). Your passion for both research and teaching has been a tremendous source of inspiration for me.

Dear **Marion**, thank you for saving me during an unexpected challenge at the beginning of my PhD. Also, thank you **Bart** for accepting me into your group. Although working in the group was not such a long period of time, I learned a lot from you. The concept of a checkerboard in making an experimental setup always works nicely.

I would like to express my gratitude to all collaborators and coauthors of my PhD projects. Special thanks to **Adam, Bas, Gijs, Muriel** and **Kristina**. It was my pleasure to collaborate with you all.

To my favourite Rielscience ladies: **Lisa**, your enthusiasm for science inspires me. Thank you for everything, and for sharing your knowledge on your favourite tiny virus with me. I have learned a lot from you, especially the idea of thinking like a virus thinks. I look forward to witnessing your future scientific endeavours. **Feline**, I have enjoyed

sharing fun stuff with you. I am so glad that you joined our group and I get to know you (and David). I appreciate that you accept to be my paranymph and help me throughout my PhD. Thank you again for your hospitality and kindness. I wish you success and happiness with your family. **Bri**, we have shared many experiences especially when we worked together on the viremia project. I love how you always have a concept for dressing, and it always matches with the makeup every day. Thank you for sharing the spirit of Asia, the support, delightful moments and snacks. I wish you all the best for your future. **Lonneke**, I have always felt comfortable discussing both scientific and non-scientific matters with you. Your guidance in the lab and your kindness have been exceptional. I truly appreciate all the knowledge you've shared. Thank you.

I very much appreciate being a part of the Comparative Pathogenesis (or Wildlife) group. **Corine**, it is always fun talking with you. I am grateful to have an opportunity to work with you. Thank you so much for your supervision and all your support in accomplishing the intrathecal antibody paper. **Carmen**, I missed the time when we had an after-work chat in the office. Thank you for sharing enjoyable moments with me. I wish you success and happiness in your family. **Lineke**, you are the first person in my circle who wholeheartedly embraces sustainability in daily life, and I admire you for that. You are also an awesome vet pathologist who always comes up with good questions. Thank you so much for sharing your knowledge, baby stuff/tips/tricks, and inspiration. **Peter**, it was fun to share experiences in visiting art museums and talk about art with you. Thank you for your support in the lab and for sharing nice stories with me. **Marco**, thank you for guiding me in the lab when I first started joining the group. **Jurre**, sawasdee ka P'Jurre. It was a pleasure working with you during my master's. Thank you for your guidance and enjoyable conversations. I hope we can meet each other in Thailand, Cambodia or Taiwan. **Keshia**, I appreciate getting to know you and discussing the philosophy of science with you. Thank you for accepting to be my paranymph without any hesitation. I wish you all the best for your PhD. **Edwin**, thank you for sharing your knowledge with me. **Valentina**, thank you for letting me take part in your animal experiment and all the good times. **Lars**, I am glad that we met each other again. I wish you all the best in everything you want to pursue and let me know if you have a chance to visit Thailand. **Vera**, I wish you all the best for your Master's and PhD.

Current and former members of EE-17XX (seriously the time I write this, I cannot recall the room number), thank you all for making a pleasant working environment. **Danny**, I appreciate our insightful talks on many topics ranging from PhD life, PhD crisis, and PhD joy to family and relationships. I wish you all the best in wrapping up your PhD and success in your future pursuits. **Eleanor**, it was my pleasure having you as my mate for producing an impressive yield of motor neurons. Thank you for the support, the nice chat and the great teamwork. **Noreen**, thank you for sharing fun stuff, mental support, and PhD slash mom's life. **Melanie**, I appreciate your positive attitude and thanks for sharing it with me. **Imke**, I wish you all the best for your PhD. **Rosanna**, I had a great time in Gdansk with you, thank you for having me.

I would not be able to achieve my PhD without help from several people in the department, especially **Monique, Theo, Willemijn, Mark Sharmier, Laurine, Stefan, Claudia, Jasmine, Nele, Georgina** and **Janet**. Thank you for always sharing your knowledge, materials and time, I very much appreciate it. Also, thanks to **Barry, Miranda, Petra, Tamana, Oanh, David Nieuwenhuijse, David van de Vijver, Emmanuelle, Louella, Ray, Daryl, Diana, Anja** and **Miruna** for sharing many nice talks and experiences. I am happy to know you all and wish you all the best in your careers. I am thankful to **Maria, Simone** and **Peter** for all your helps. Although the time I spent in the Coronavirus group was not very long, I learned a lot from you. **Widagdo, Nisreen, Gadissa, Mart, Debby Schipper, Anna** and **Tim**, thank you for all the nice work discussions.

I am thankful to **Aj. Trasida Ploryngam** and **Aj.Chaiyapat Thamrongyoswittayakul** from the Faculty of Veterinary Medicine, Khon Kaen University for awarding me an exchange scholarship to do an internship at the Faculty of Veterinary Medicine, Utrecht University. That was the beginning of my PhD journey. I also appreciate to have been advised by **Aj. Prasan Tangkawattana** and **Aj. Jaruwan Kampa** during my time in the vet school. I am also grateful for the grant funding from the Ministry of Higher Education, Science, Research and Innovation, Thailand that allows me to do a Master's and PhD in the Netherlands.

Life in Rotterdam would not be this much memorable without these wonderful people. **Juthatip (P'Tarn)** and **Pascal**, thank you for everything. Both of you helped me a lot throughout my seven-year journey in Rotterdam. **Widagdo**, I mention you again here because you have to be mentioned. You were there throughout all the time I was doing my master's until now. I really appreciate that I could always count on you for help. Thank you and cheers to friendship. **Wilson**, your artistic-scientist talent impressed me. Thank you for all the good times. My beloved Thai friends from Erasmus MC, **P'Karn, P'Keng, P'Utt, P'Dew, P'Kade, P'Arm, P'Gift and P'Ply**. It is my pleasure to know you all. I never knew that doctors could be this much fun. We had so many good times together. I truly appreciated our good times and supports from all of you like solving mathematic problem and FACS issue, preparing for PhD defence, having fun trips, joining Friday night dinners, and being a health consultant for my whole family etc. Thank you for everything and hope to catch up with all of you soon in Thailand. **P'Jam, P'Aei, P'Amm, P'Erk, P'Jane, Josse, P'Pump, David, Jinny** and **Grace**, thank you for your helps and all the great time we had together. **Golf, Jan, Bella, Salil, Prae and vet kku gang**, it doesn't matter how far we are, I am grateful to have your support throughout my PhD.

I would not be who I am today without the support of my dear family, **Mom** and **Dad** who are always there with endless support. Your immense unconditional love has kept me forward. I could not be more grateful that you allow your the only one daughter going abroad for several years to pursue her dream. Also, thank you to **Mama** and **Papa** for all the trust and support.

Last but not least, **Yi-Chien** my best buddy and life partner. Besides earning my degree, knowing you has been the best thing about coming to Rotterdam. I really could not imagine how I come this far without you. You are always by my side on both good days and turbulent times. Thank you for being a person who is willing to hear my stories every day and to share your stories with me. Words are never enough to appreciate all the things you do for me. Hold my hands tightly, we are ready to create another wonderful journey in Thailand. Special thanks to **Thun Sian** for joining Mama's PhD life in the last year. It was a special moment carrying you with me to do fun stuff in the lab. Your naughty smile is my source of encouragement. When you grow up, I definitely will share this unforgettable PhD journey with you.